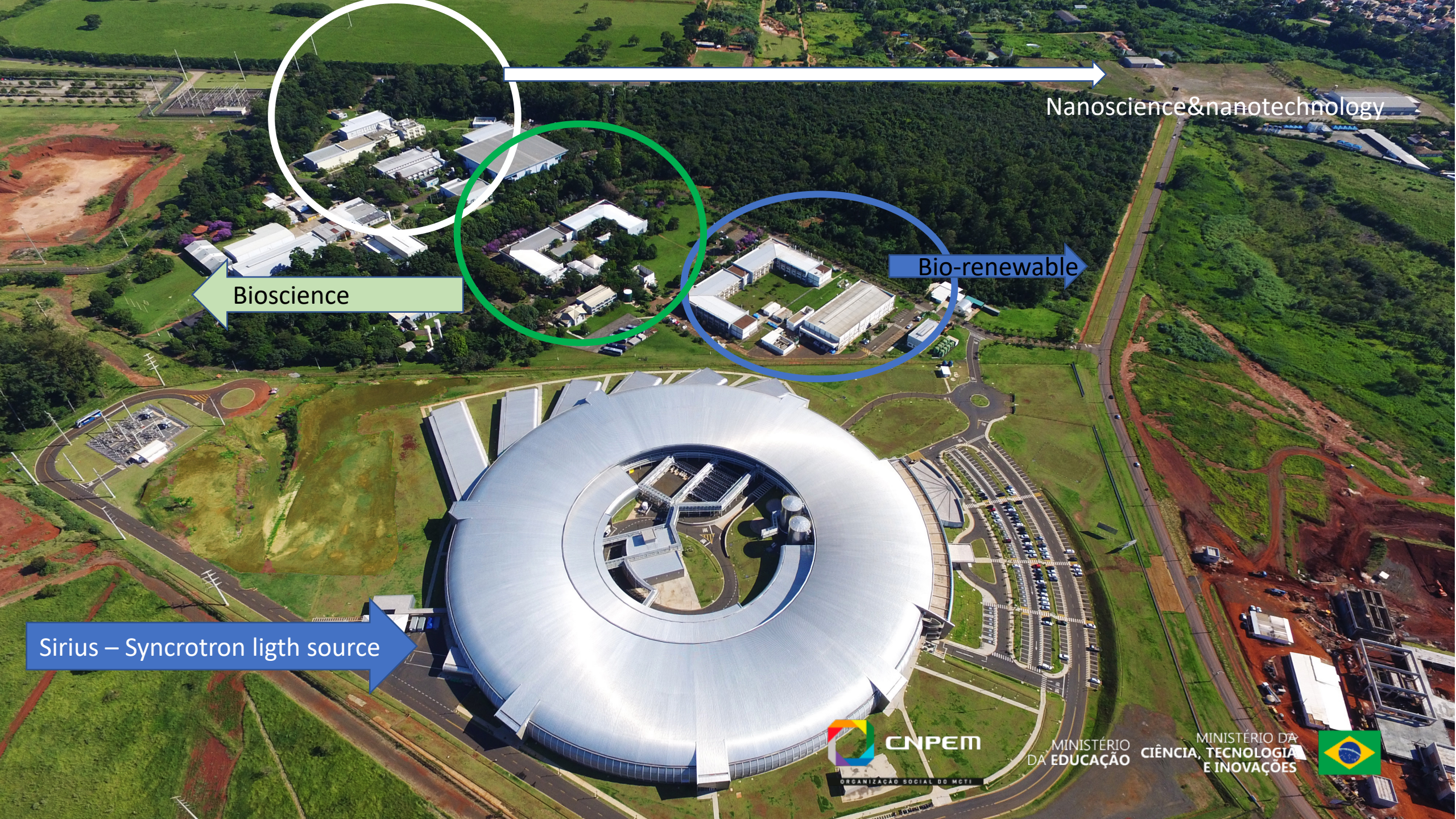




A.FAZZIO



Nanoscience & nanotechnology

Bio-renewable

Bioscience

Sirius - Synchrotron light source



CNPq

ORGANIZAÇÃO SOCIAL DO MCTI

MINISTÉRIO DA EDUCAÇÃO

MINISTÉRIO DA CIÊNCIA, TECNOLOGIA E INOVAÇÕES





ilum school of
science



“Unveiling quantum phase transition by disorder and defects in 2D-materials: Jacutingaite family”

@ Jacutingaite-family : A class of topological materials

@ Topological insulating phase arising in Jacutingaite- family ordered and random alloys.

@ Vacancies – driven Quantum Spin Hall on transition metal dichalcogenides.



Topological Insulators are called “topological” because the wave functions describing their electronic states span a Hilbert space that has a nontrivial topology... they opened a new window for understanding the elaborate workings of nature.

Consequence?... a gapless interface state necessarily shows up when the insulator is physically terminated and faces an ordinary insulator (including the vacuum).

Which invariant?

(Time Reversal invariant)

$$\mathbb{Z}_2 = \frac{1}{2\pi} \left[\oint_{\partial \text{HBZ}} d\mathbf{k} \cdot \mathbf{A}(\mathbf{k}) - \int_{\text{HBZ}} d^2k \Omega_z(\mathbf{k}) \right] \text{ mod}(2)$$

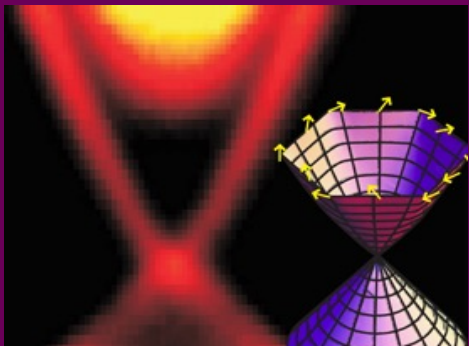
$$\vec{A}_n(\vec{k}) = -i \langle u_{n\vec{k}} | \vec{\nabla}_k | u_{n\vec{k}} \rangle$$

Berry connection:

$$\vec{\Omega}_n(\vec{k}) = \vec{\nabla}_k \times \mathbf{A}_n(\vec{k})$$

Berry curvature

Isolantes topológicos $\mathbb{Z}_2 = 1$
 Isolantes triviais $\mathbb{Z}_2 = 0$





Why Jacutingaite-family ?

New candidates for topological materials:

- (i) large topological gap.
- (ii) structural stability.
- (iii) accessible synthesis route.



@ Pt_2HgSe_3 is a naturally occurring mineral discovered in Brazil in 2008.

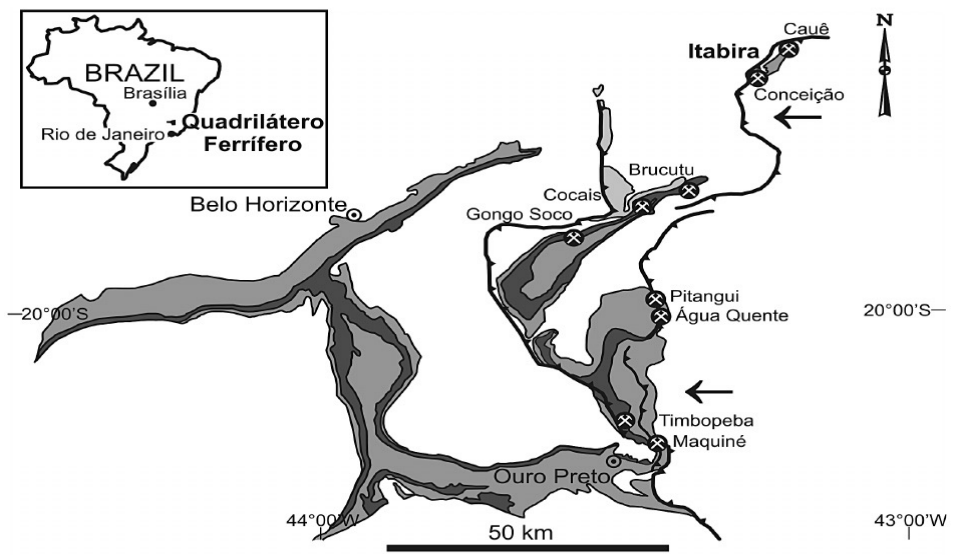
@ In 3D-form is predicted a dual topology, weak topological insulator and topological crystalline insulator.

@ Its monolayer form, a place for manifestation of the Kane-Mele topological phase

@ Also Pt_2HgSe_3 has been synthesized and also Pd-based in the same structure Pd_2HgSe_3 .



BRAZILIAN TOPOLOGICAL!!!



- Paleoproterozoic Minas SG Itabira Group (dark grey) itabirite, dolomite
- City, town
- Palladiferous gold, jacutinga-style veins
- Thrust fault (~0.6Ga Brasiliano orogeny)
- Mean tectonic transport (Brasiliano orogeny)



One of the largest mining companies in the world - Vale do Rio Doce

doi: 10.1111/j.1365-3121.2007.00783.x

Platinum enrichment at low temperatures and related microstructures, with examples of hongshiite (PtCu) and empirical ' Pt_2HgSe_3 ' from Itabira, Minas Gerais, Brazil 2008

A. R. Cabral,¹ H. F. Galbiatti,² R. Kwitko-Ribeiro³ and B. Lehmann⁴
¹Department of Geology: Exploration Geology, Rhodes University, PO Box 94, Grahamstown 6140, South Africa; ²Companhia Vale do Rio Doce, 35900-900 Itabira-MG, Brazil; ³Desenvolvimento de Projetos Minerários, Companhia Vale do Rio Doce, Rodovia BR 381/km 450, 33040-900 Santa Luzia-MG, Brazil; ⁴Institut für Mineralogie und Mineralische Rohstoffe, Technische Universität Clausthal, Adolph-Roemer-Str. 2A, Clausthal-Zellerfeld, D-38678, Germany



@ Pt_2HgSe_3 is a naturally occurring mineral discovered in Brazil in 2008.

@ In 3D-form is predicted a dual topology, weak topological insulator and topological crystalline insulator.

@ its monolayer form, a place for manifestation of the Kane-Mele topological phase

@ Also Pt_2HgSe_3 has been synthesized and also Pd-based in the same structure Pd_2HgSe_3 .

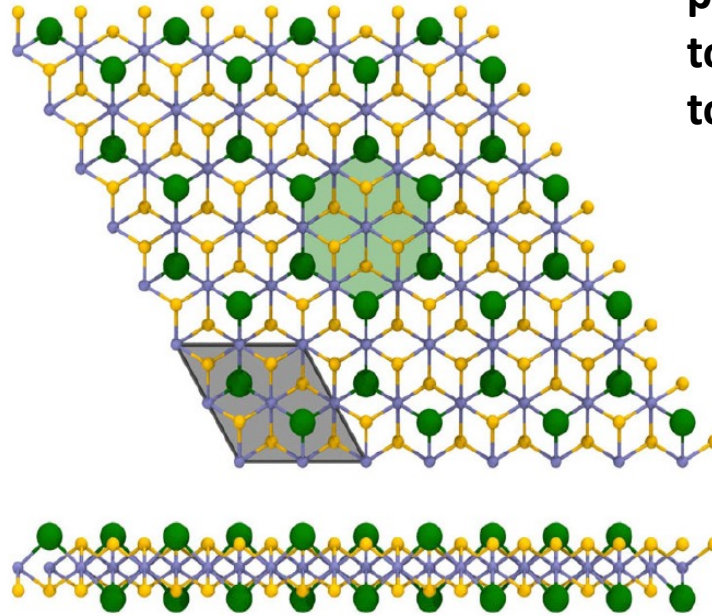
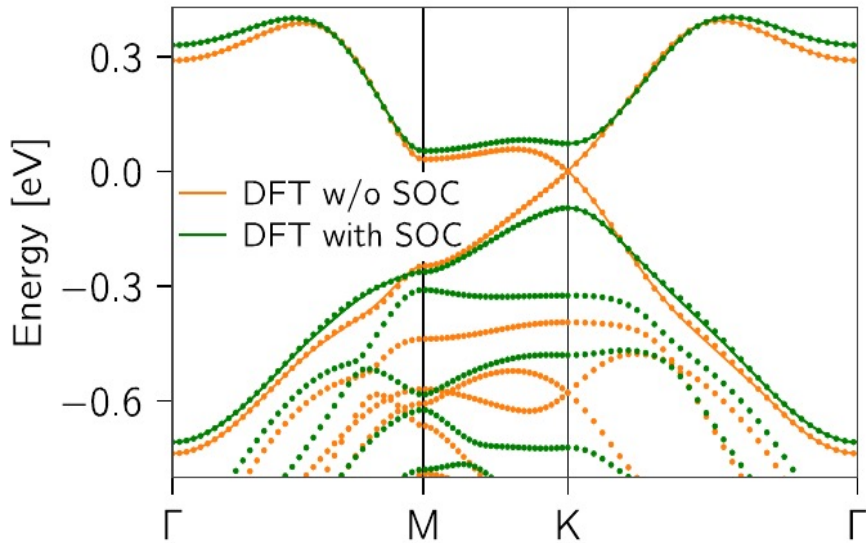
First theoretical paper



Prediction of a Large-Gap and Switchable Kane-Mele Quantum Spin Hall Insulator

Antimo Marrazzo,^{*} Marco Gibertini, Davide Campi, Nicolas Mounet, and Nicola Marzari[†]

Theory and Simulation of Materials (THEOS) and National Centre for Computational Design and Discovery of Novel Materials (MARVEL), École Polytechnique Fédérale de Lausanne, 1015 Lausanne, Switzerland



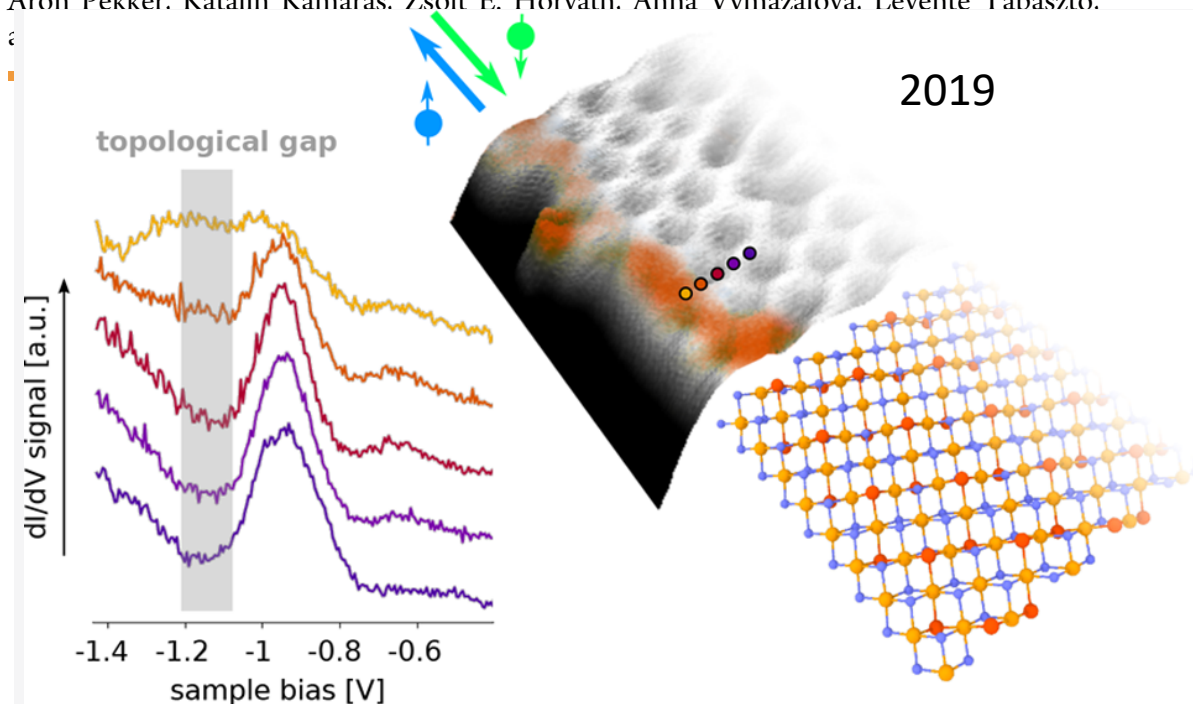
its monolayer(2D) form, a place for manifestation of the Kane-Mele topological phase. Whereas in 3D-form is predict a dual topology , weak topological insulator and topological crystalline insulator.

PRL 2018

Its atomic structure can be viewed as a the transition metal dichalcogenide (TMD) PtSe₂ with a structural phase where ¼ of the chalcogenides are replaced by Hg.

Signature of Large-Gap Quantum Spin Hall State in the Layered Mineral Jacutingaite

Konrad Kandrai, Péter Vancsó, Gergő Kukucska, János Koltai, György Baranka, Ákos Hoffmann, Áron Pekker, Katalin Kamarás, Zsolt E. Horváth, Anna Vymazalová, Levente Tapasztó.



ARTICLE OPEN

Check for updates

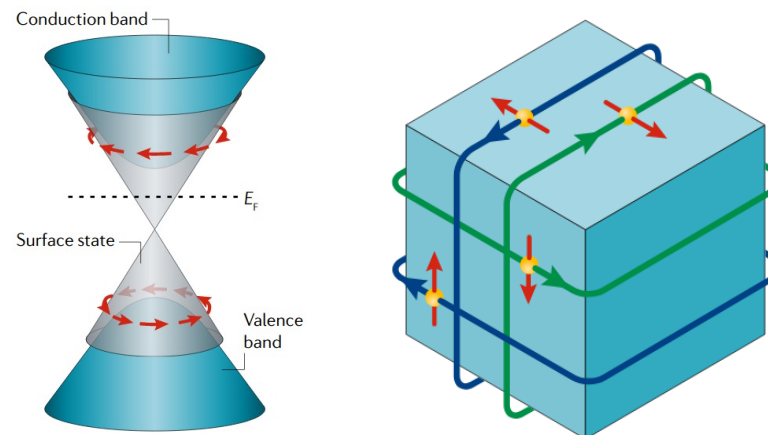
Pressure-induced superconductivity and structure phase transition in Pt₂HgSe₃

Cuiying Pei^{1,8}, Suhua Jin^{1,8}, Peihao Huang^{2,8}, Anna Vymazalova³, Lingling Gao¹, Yi Zhao¹, Weizheng Cao¹, Changhua Li¹, Peter Nemes-Incze⁴, Yulin Chen^{1,5,6}, Hanyu Liu^{2,7,8}, Gang Li^{1,5,8} and Yanpeng Qi^{1,8}

PHYSICAL REVIEW LETTERS 124, 106402 (2020)

Bulk and Surface Electronic Structure of the Dual-Topology Semimetal Pt₂HgSe₃

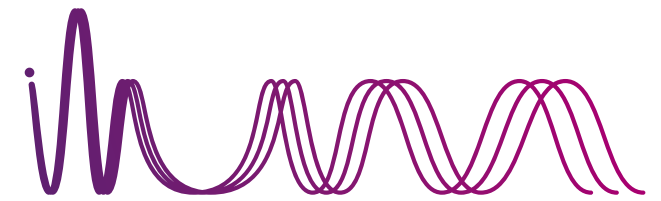
I. Cucchi¹, A. Marrazzo¹, E. Cappelli¹, S. Riccò¹, F. Y. Bruno^{1,3}, S. Lisi¹, M. Hoesch^{4,5}, T. K. Kim⁴, C. Cacho⁴, C. Besnard¹, E. Giannini¹, N. Marzari², M. Gibertini^{1,2}, F. Baumberger^{1,6} and A. Tamai^{1,*}



2020



Jacuntingaite-family >>>



Thermodynamic and mechanical stables

27 materials

M= Ni, Pd, Pt;
N= Zn, Cd, Hg;
X= S, Se, Te

Periodic Table of the Elements

State of matter (color of name)
 GAS LIQUID SOLID UNKNOWN

Subcategory in the metal-metalloid-nonmetal trend (color of background)
 Alkali metals, Alkaline earth metals, Transition metals, Lanthanides, Actinides, Post-transition metals, Metalloids, Reactive nonmetals, Noble gases, Unknown chemical properties

1 IA 1 H Hydrogen 1.008 1	2 IIA 4 Be Beryllium 9.012 4	3 IIIB 21 Sc Scandium 44.956 21	4 IVB 22 Ti Titanium 47.887 22	5 VB 23 V Vanadium 50.942 23	6 VIB 24 Cr Chromium 51.996 24	7 VIIB 25 Mn Manganese 54.938 25	8 VIIIB 26 Fe Iron 55.845 26	9 VIIIB 27 Co Cobalt 58.933 27	10 VIIIB 28 Ni Nickel 58.693 28	11 IB 29 Cu Copper 63.546 29	12 IIB 30 Zn Zinc 65.38 30	13 IIIA 5 B Boron 10.81 5	14 IVA 6 C Carbon 12.011 6	15 VA 7 N Nitrogen 14.007 7	16 VIA 8 O Oxygen 15.999 8	17 VIIA 9 F Fluorine 18.998 9	18 VIIIA 10 Ne Neon 20.180 10																		
3 IIIA 11 Na Sodium 22.990 11	4 IIA 12 Mg Magnesium 24.305 12	5 IIIB 13 Al Aluminum 26.982 13	6 IVB 14 Si Silicon 28.086 14	7 VB 15 P Phosphorus 30.974 15	8 VIB 16 S Sulfur 32.06 16	9 VIIB 17 Cl Chlorine 35.45 17	10 VIIIB 18 Ar Argon 39.948 18	11 IB 19 K Potassium 39.098 19	12 IIB 20 Ca Calcium 40.078 20	13 IIIA 31 Ga Gallium 69.723 31	14 IVA 32 Ge Germanium 72.64 32	15 VA 33 As Arsenic 74.922 33	16 VIA 34 Se Selenium 78.96 34	17 VIIA 35 Br Bromine 79.904 35	18 VIIIA 36 Kr Krypton 83.798 36	19 IB 37 Rb Rubidium 85.468 37	20 IIA 38 Sr Strontium 87.62 38	21 IIIB 39 Y Yttrium 88.906 39	22 IVB 40 Zr Zirconium 91.224 40	23 VB 41 Nb Niobium 92.906 41	24 VIB 42 Mo Molybdenum 95.94 42	25 VIIB 43 Tc Technetium 98 43	26 VIIIB 44 Ru Ruthenium 101.07 44	27 VIIIB 45 Rh Rhodium 102.91 45	28 VIIIB 46 Pd Palladium 106.42 46	29 IB 47 Ag Silver 107.87 47	30 IIB 48 Cd Cadmium 112.41 48	31 IIIA 49 In Indium 114.82 49	32 IVA 50 Sn Tin 118.71 50	33 VA 51 Sb Antimony 121.76 51	34 VIA 52 Te Tellurium 127.6 52	35 VIIA 53 I Iodine 126.91 53	36 VIIIA 54 Xe Xenon 131.29 54		
55 IIA 55 Cs Cesium 132.905 55	56 IIA 56 Ba Barium 137.33 56	57-71 Lanthanides	72 IVB 72 Hf Hafnium 178.49 72	73 VB 73 Ta Tantalum 180.948 73	74 VIB 74 W Tungsten 183.84 74	75 VIIB 75 Re Rhenium 186.21 75	76 VIIIB 76 Os Osmium 190.23 76	77 VIIIB 77 Ir Iridium 192.22 77	78 VIIIB 78 Pt Platinum 195.08 78	79 IB 79 Au Gold 196.97 79	80 IIB 80 Hg Mercury 200.59 80	81 IIIA 81 Tl Thallium 204.38 81	82 IVA 82 Pb Lead 207.2 82	83 VA 83 Bi Bismuth 208.98 83	84 VIA 84 Po Polonium 209 84	85 VIIA 85 At Astatine 210 85	86 VIIIA 86 Rn Radon 222 86	87 IIA 87 Fr Francium 223 87	88 IIA 88 Ra Radium 226 88	89-103 Actinides	104 IVB 104 Rf Rutherfordium 261 104	105 VB 105 Db Dubnium 262 105	106 VIB 106 Sg Seaborgium 263 106	107 VIIB 107 Bh Bohrium 264 107	108 VIIIB 108 Hs Hassium 265 108	109 VIIIB 109 Mt Meitnerium 266 109	110 VIIIB 110 Ds Darmstadtium 268 110	111 IB 111 Rg Roentgenium 269 111	112 IIB 112 Cn Copernicium 277 112	113 IIIA 113 Nh Nihonium 278 113	114 IVA 114 Fl Flerovium 285 114	115 VA 115 Mc Moscovium 286 115	116 VIA 116 Lv Livermorium 287 116	117 VIIA 117 Ts Tennessine 289 117	118 VIIIA 118 Og Oganesson 294 118
57 Lanthanum 138.91 57	58 Cerium 140.12 58	59 Praseodymium 140.91 59	60 Neodymium 144.24 60	61 Promethium 145 61	62 Samarium 150.36 62	63 Europium 151.96 63	64 Gadolinium 157.25 64	65 Terbium 158.93 65	66 Dysprosium 162.50 66	67 Holmium 164.93 67	68 Erbium 167.26 68	69 Thulium 168.93 69	70 Ytterbium 173.05 70	71 Lutetium 174.97 71	89 Actinium 227 89	90 Thorium 232.04 90	91 Protactinium 231.04 91	92 Uranium 238.03 92	93 Neptunium 237 93	94 Plutonium 244 94	95 Americium 243 95	96 Curium 247 96	97 Berkelium 247 97	98 Californium 251 98	99 Einsteinium 252 99	100 Fermium 257 100	101 Mendelevium 258 101	102 Nobelium 259 102	103 Lawrencium 260 103						

We employ density functional theory simulations (DFT)



- >Spin-orbit coupling
- >PBE functional

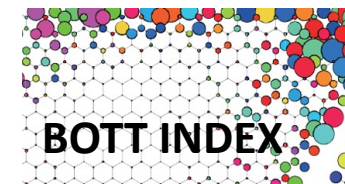
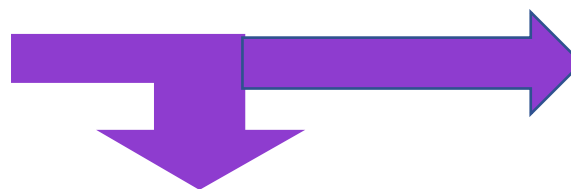
TRANS-*sampa*



Ballistic Electronic transport

WANNIER90

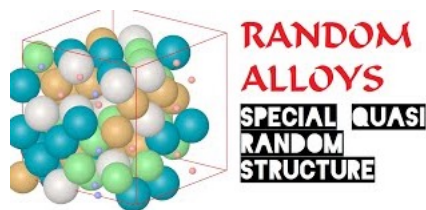
- >Localized basis Hamiltonian
- >Bloch to Wannier function transformation



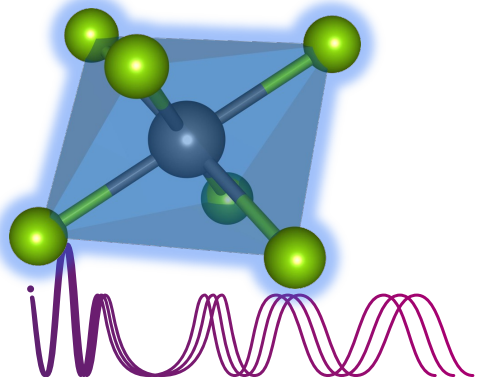
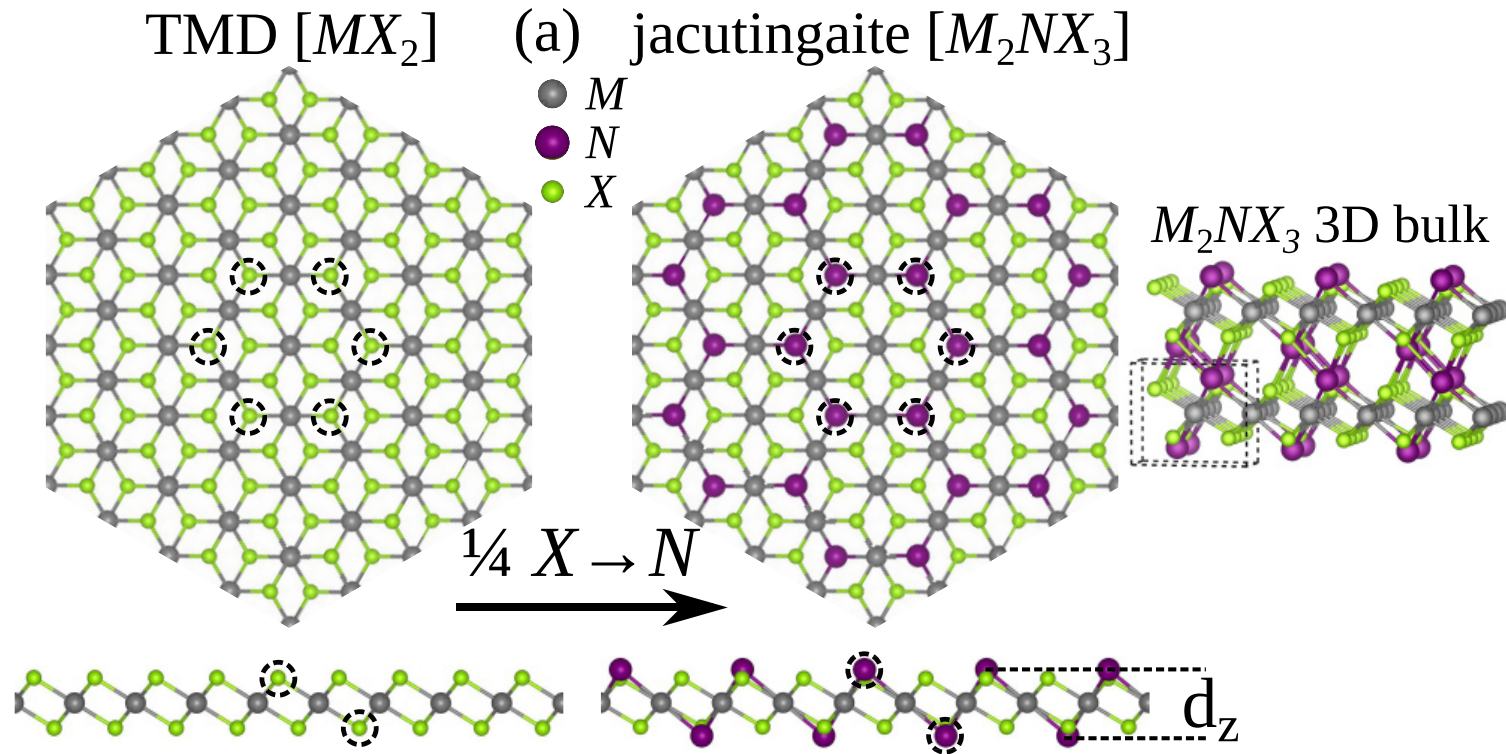
Z2



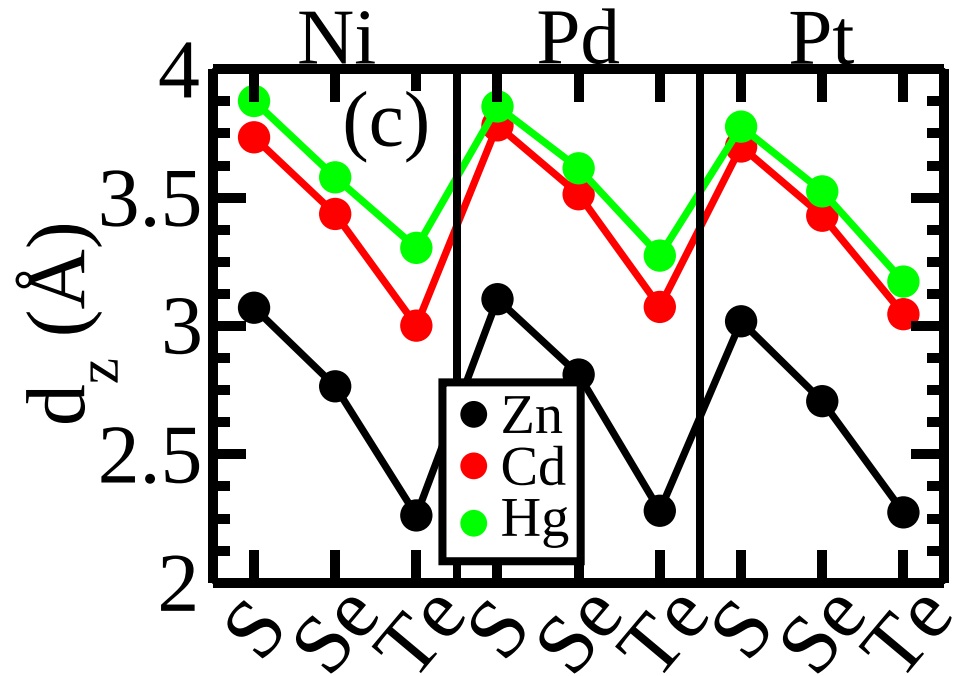
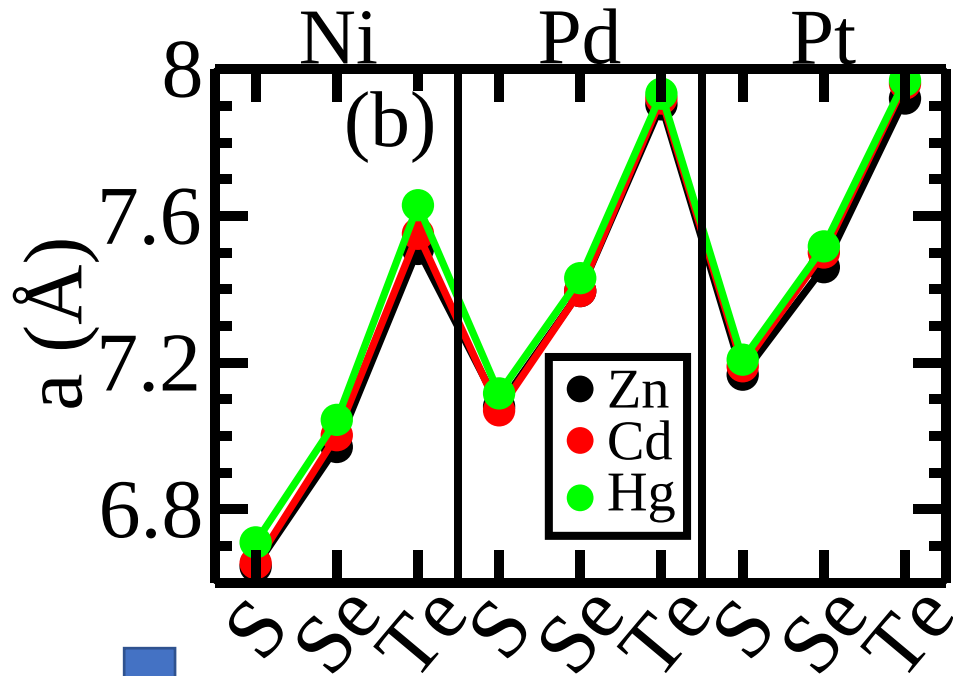
- >Topological invariant (Soluyanov-Vanderbilt (PRB2011))
- >surface states' Green's function



Jacutingaite-like share the same backbone geometry of TMD(MX_2)-1T $\rightarrow M_2NX_3$



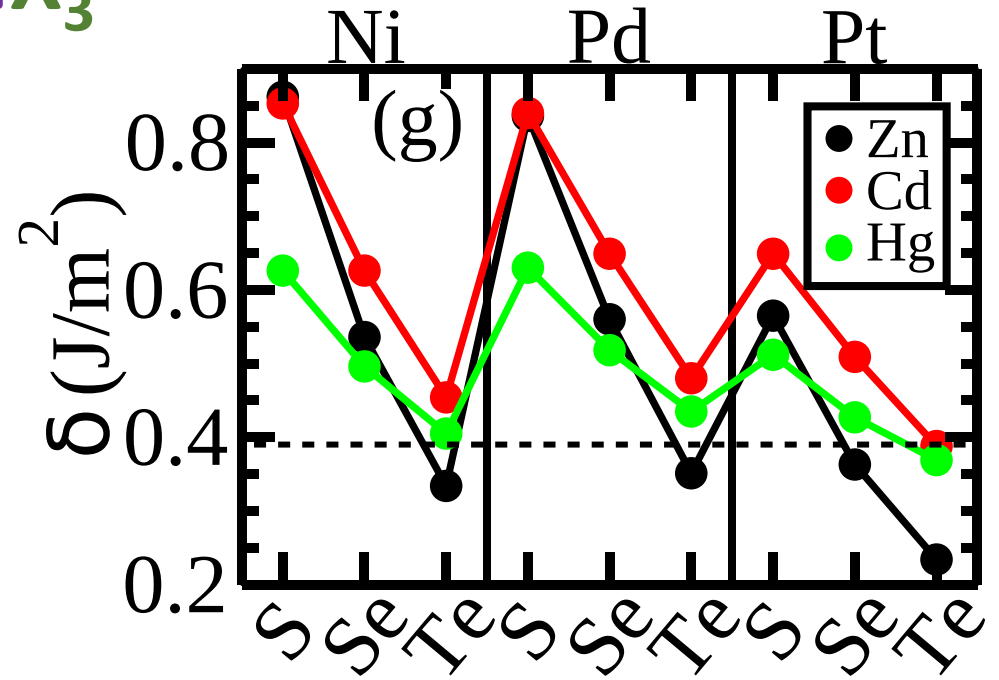
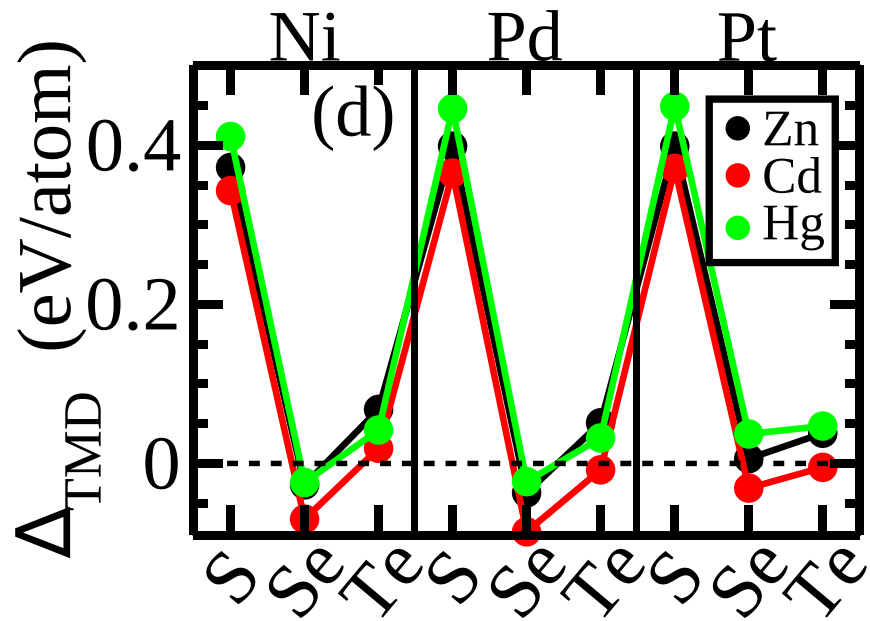
The chalcogenide atoms (X) are partially replaced by transition metals (N), $M X_2 \rightarrow M_2 N X_3$, resulting in buckled $N-M-N$ bonds.



The lattice parameter of M_2NX_3 , are practically independent of transition metal

The N atoms form triangular lattices on the opposite sides of the MX_2 host, which in turn are rotated by 60° with respect to each other, giving rise to a buckled hexagonal lattice.

* And the equilibrium lattice constant of Pt_2NSe_3 for $N=Zn, Cd, Hg$ differ by less than 9% compared with 1T $PtSe_2$



$$\Delta_{\text{TMD}} = \Omega[M_2NX_3] - \Omega[MX_2]$$

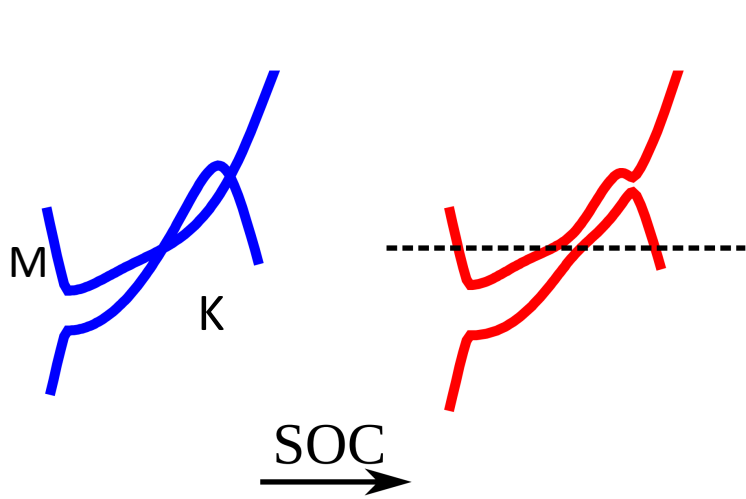
$$\Omega[x] = E[x] - \sum_i n_i \mu_i^{\text{bulk}}$$

Jacutingaite-like

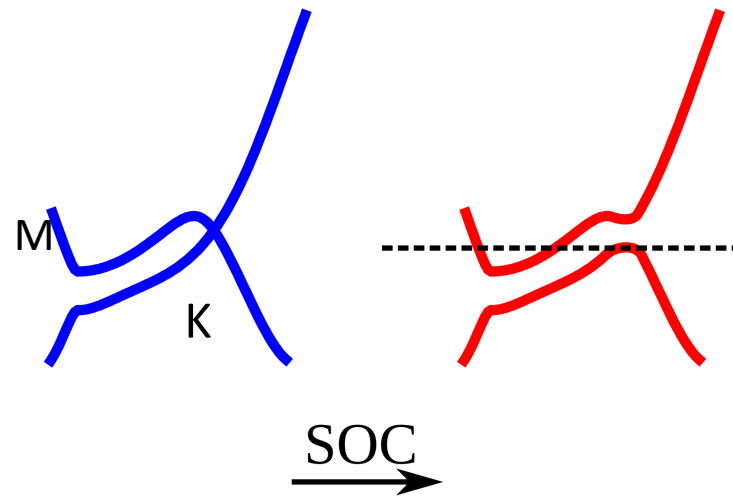
TMD

Cleavage energy((M_2NX_3 bulk) - the dashed line indicating the graphite cleavage barrier.

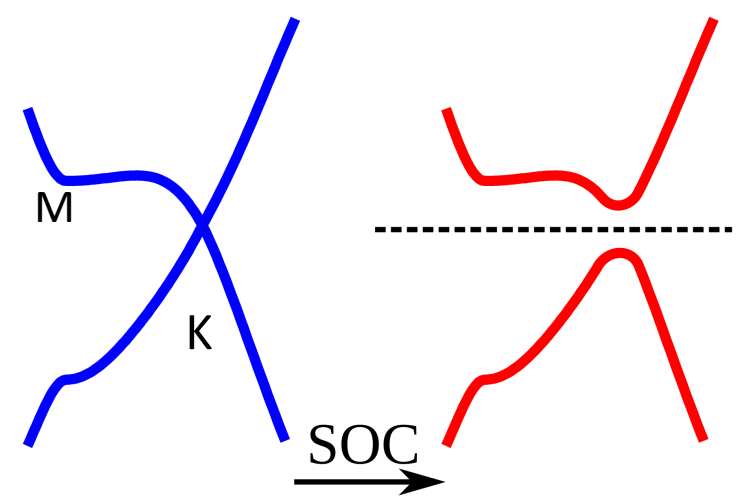
Schematic band structure around
Fermi-energy
M < > K Direction



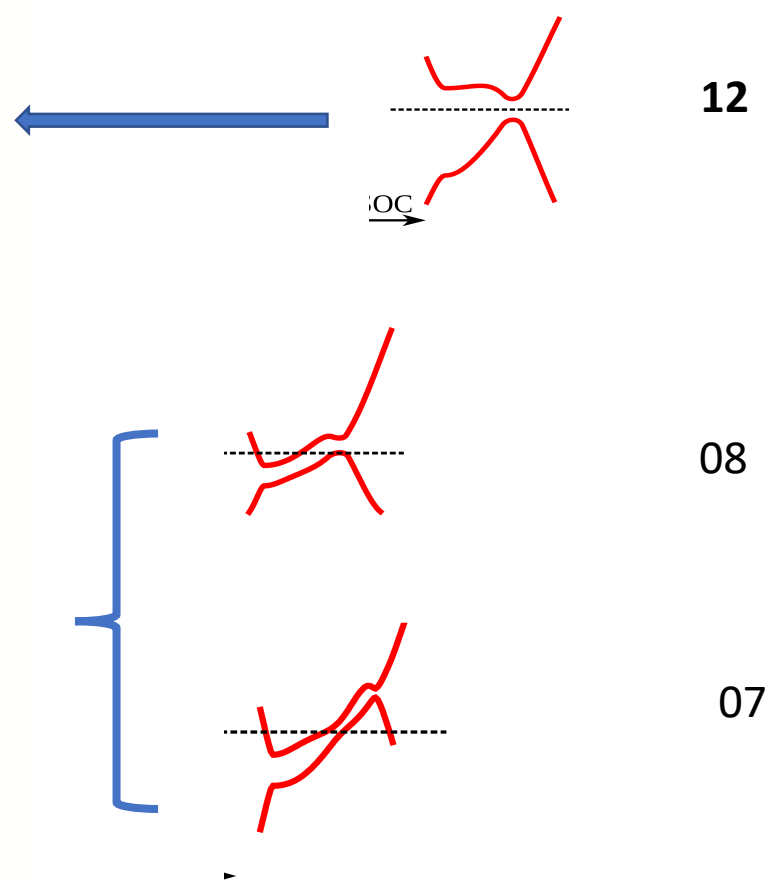
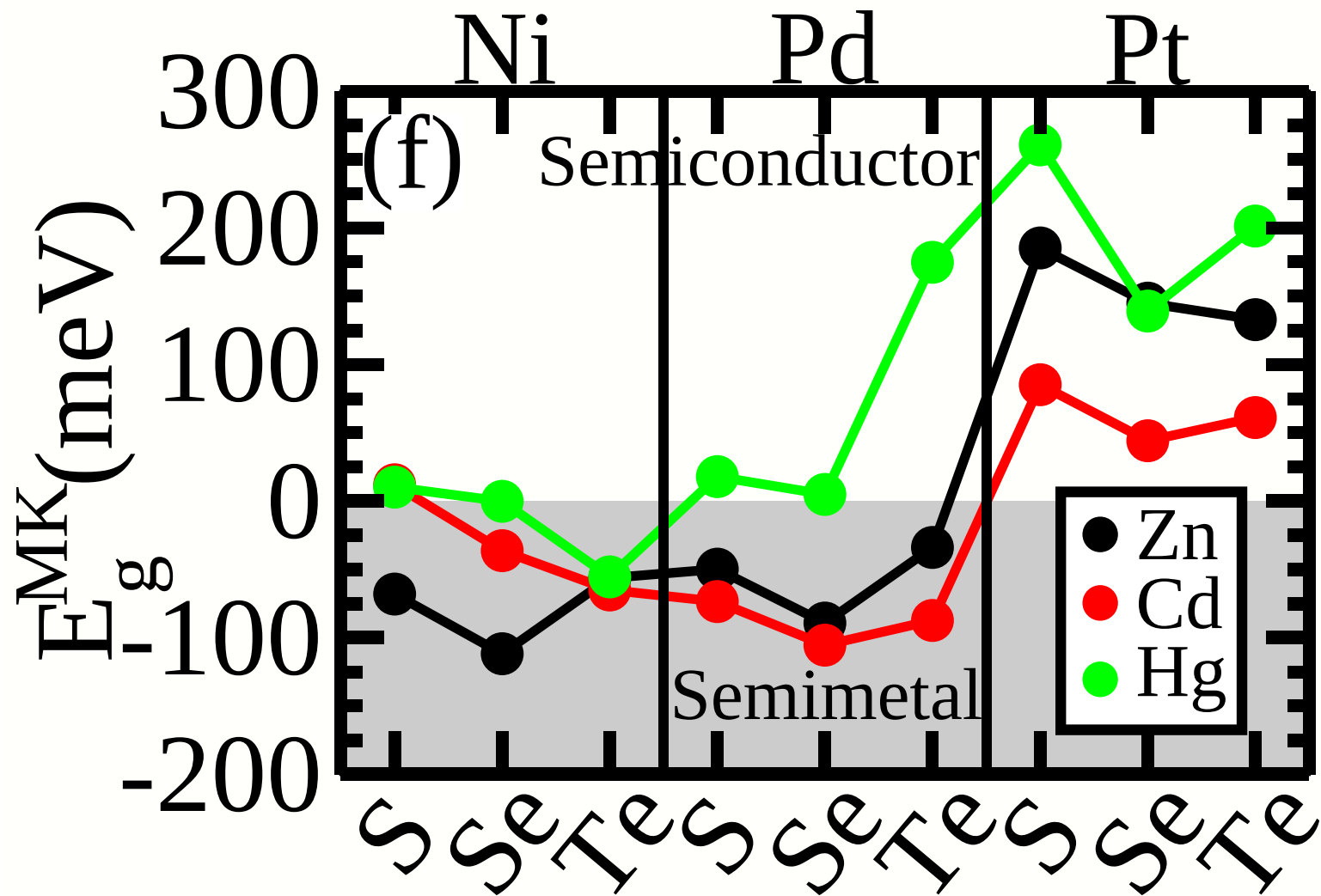
Trivial-
semimetal



Topological-
semimetal



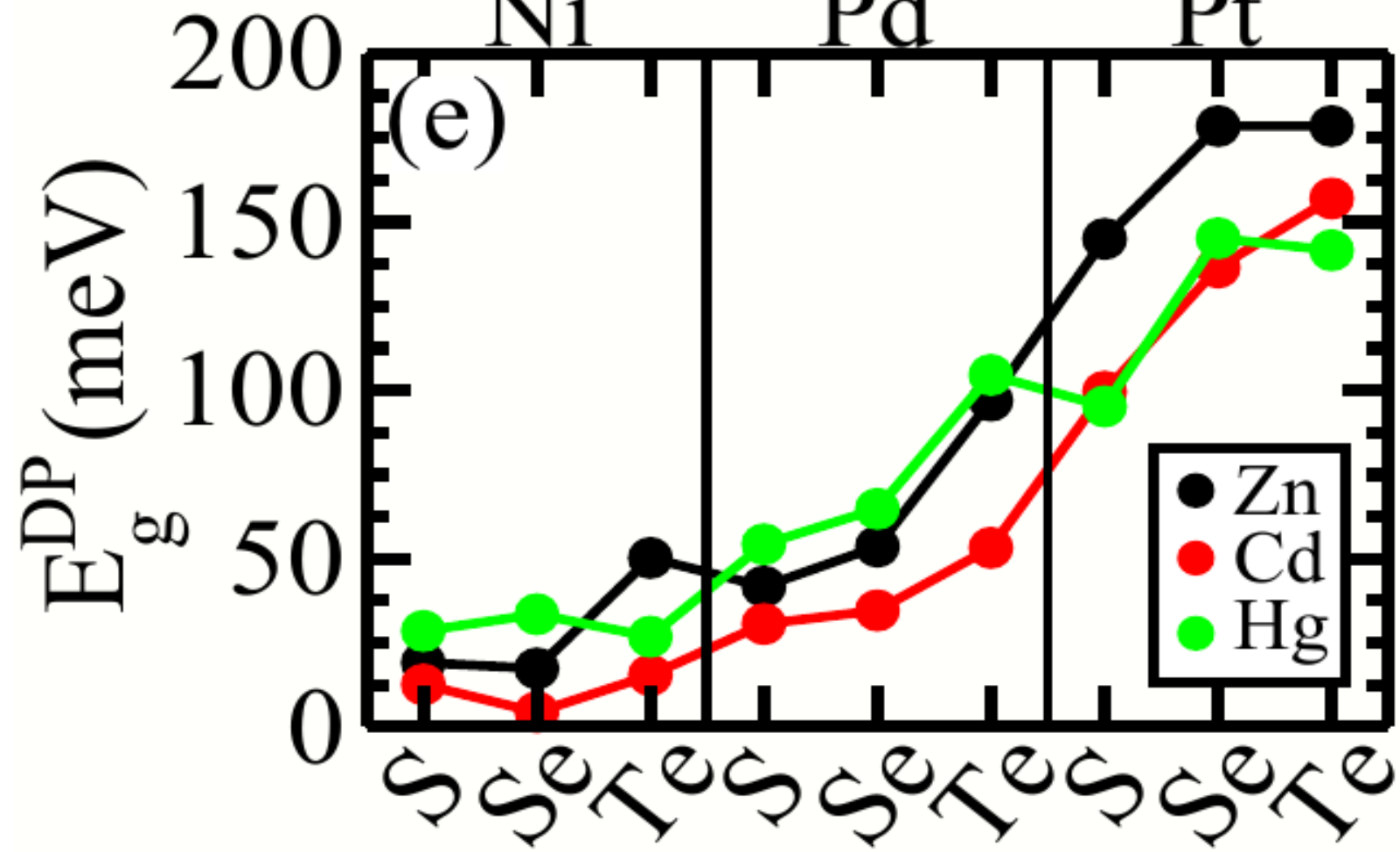
Topological-
insulator



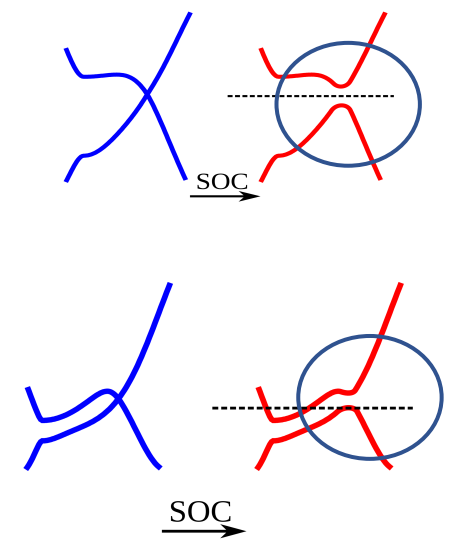


Ni_2NX_3 Pd_2NX_3 Pt_2NX_3

Ni Pd Pt



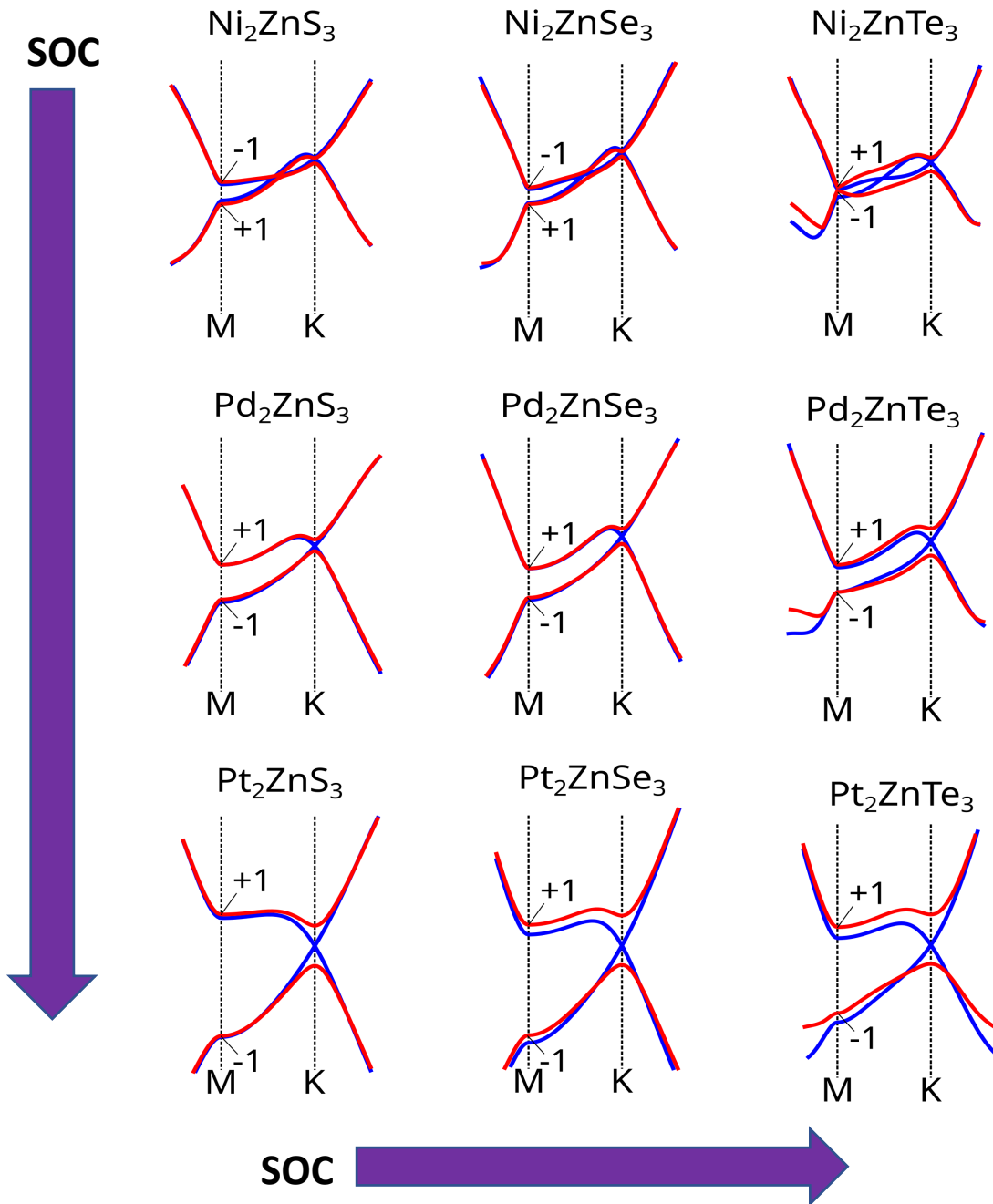
● Zn
● Cd
● Hg



Gap in Dirac-point (K)

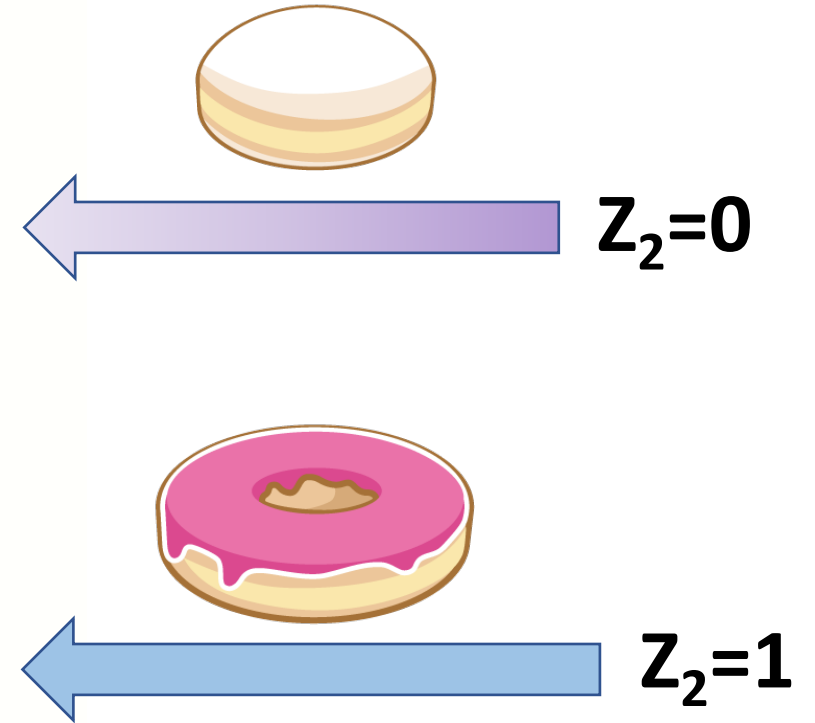
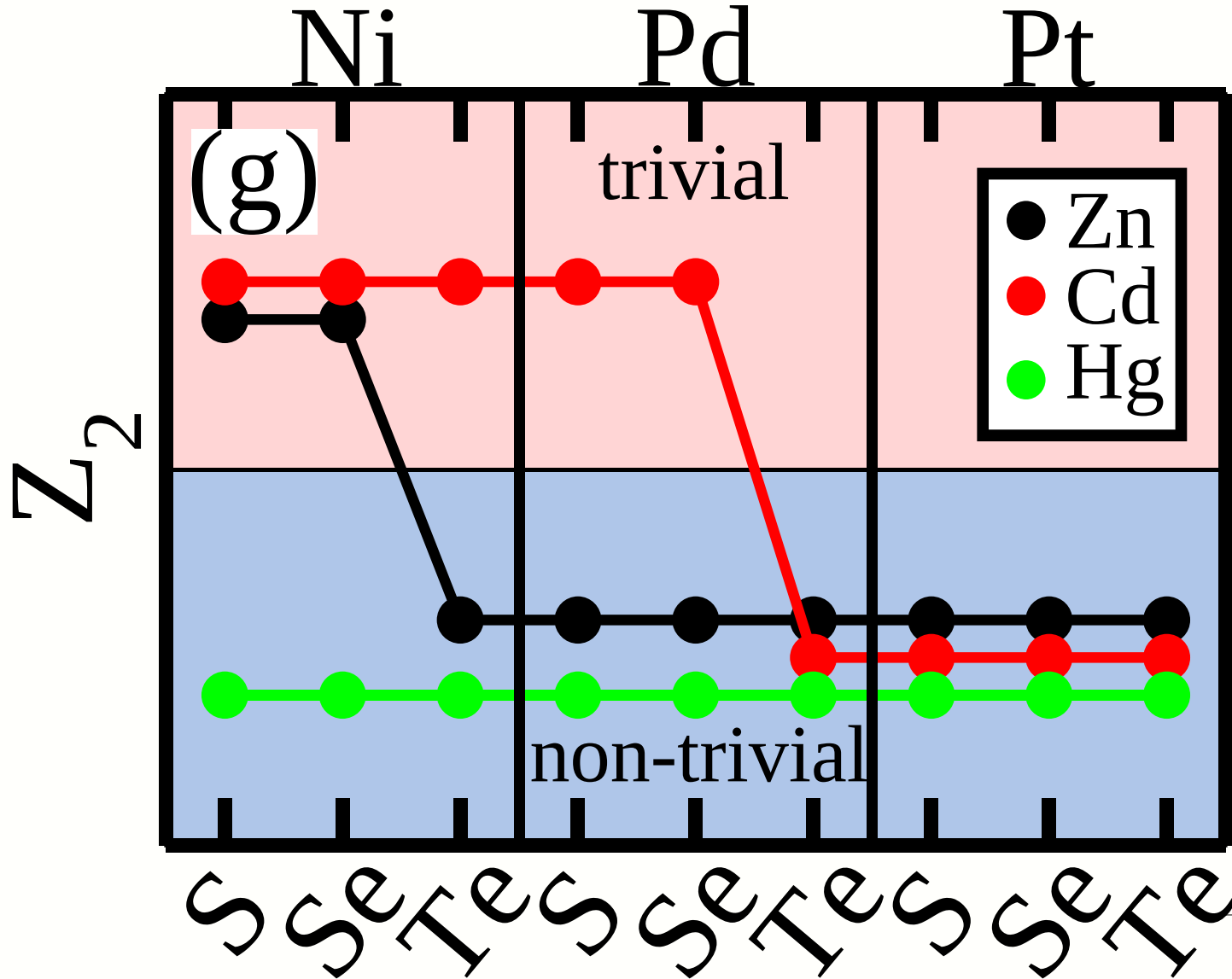
(27 materials)

No-SOC X SOC



Replacing transition metals and chalcogen

Pt₂HgSe₃-family



PHYSICAL REVIEW B 102, 235153 (2020)

Jacutingaite-family: A class of topological materials

F. Crasto de Lima^{1,*}, R. H. Miwa^{2,†} and A. Fazzio^{1,‡}

¹Brazilian Nanotechnology National Laboratory CNPEM, Caixa Postal 6192, 13083-970 Campinas, São Paulo, Brazil

²Instituto de Física, Universidade Federal de Uberlândia, Caixa Postal 593, 38400-902 Uberlândia, Minas Gerais, Brazil

Article

Tilkerodeite, Pd_2HgSe_3 , a New Platinum-Group Mineral from Tilkerode, Harz Mountains, Germany

Chi Ma ^{1,*}, Hans-Jürgen Förster ² and Günter Grundmann ³

¹ Division of Geological and Planetary Sciences, California Institute of Technology, Pasadena, CA 91125, USA

² Helmholtz Centre Potsdam German Research Centre for Geosciences GFZ, D-14473 Potsdam, Germany; forhj@gfz-potsdam.de

³ Eschenweg 6, D-32760 Detmold, Germany; grundmann.g@gmx.de

* Correspondence: chima@caltech.edu

• 2020



Then ...Pt₂HgSe₃-family

a) 12 Topological Insulators(Kane-Mele), 8 Topological Semi-Metal and 07 Trivial

b) The cleavage energies showed that these systems can be isolated in monolayers by exfoliation methods.

c) Pt₂ZnSe₃ and Pt₂ZnTe₃, present larger values of topological band gap compared with that of jacutingaite (Pt₂HgSe₃) .

....

“Unveiling quantum phase transition by disorder and defects in 2D-materials: Jacutingaite family”

@ Jacutingaite-family : A class of topological materials

@ Topological insulating phase arising in Jacutingaite- like ordered and random alloys.

@ Vacancies –driven Quantum Spin Hall on transition metal dichalcogenides.

ALLOYS

Topological insulating phase arising in transition metal dichalcogenide alloy

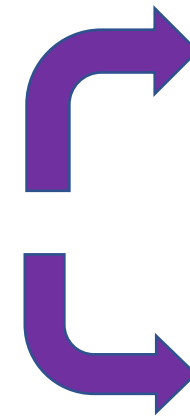


PtSe₂ is a semiconductor with trivial bandgap

>-> 25% of Se substituted by Hg >>->>>

Pt₂HgSe₃ is a topological insulator with a large bandgap

PtSe₂ monolayer -> Hg_{Se} -> Pt(Hg_xSe_{1-x})₂ alloy



Ordered

Random

Ordered alloys



$\text{Pt}(\text{Hg}_x\text{Se}_{1-x})_2$ with $x=0.25, 0.50, 0.75$ and 1.0

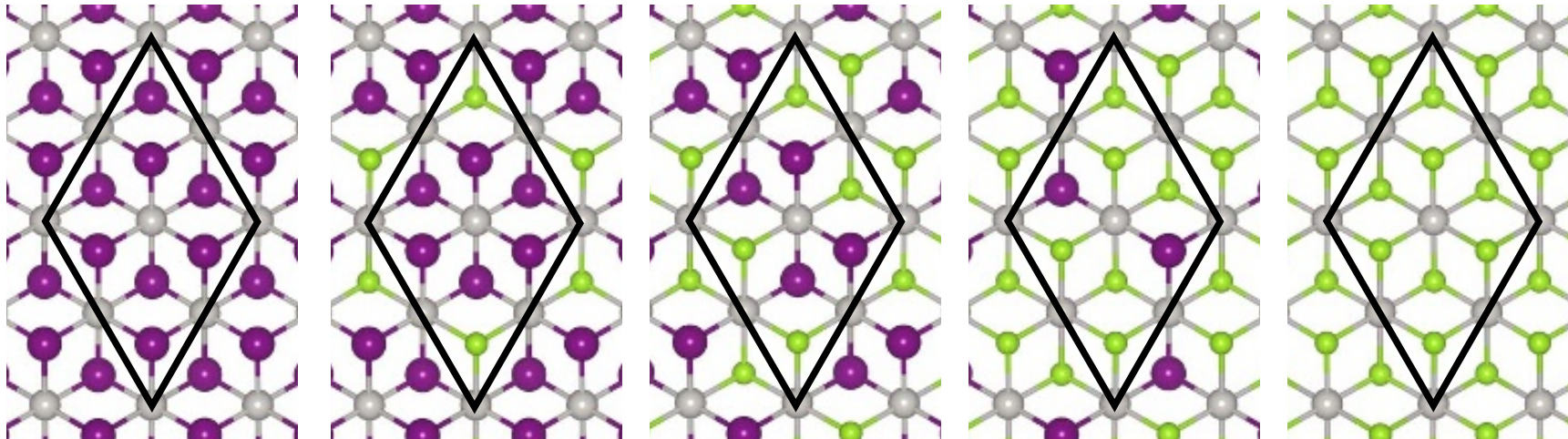
X=1.0

X=0.75

X=0.50

X=0.25

X=0.0



PtHg_2

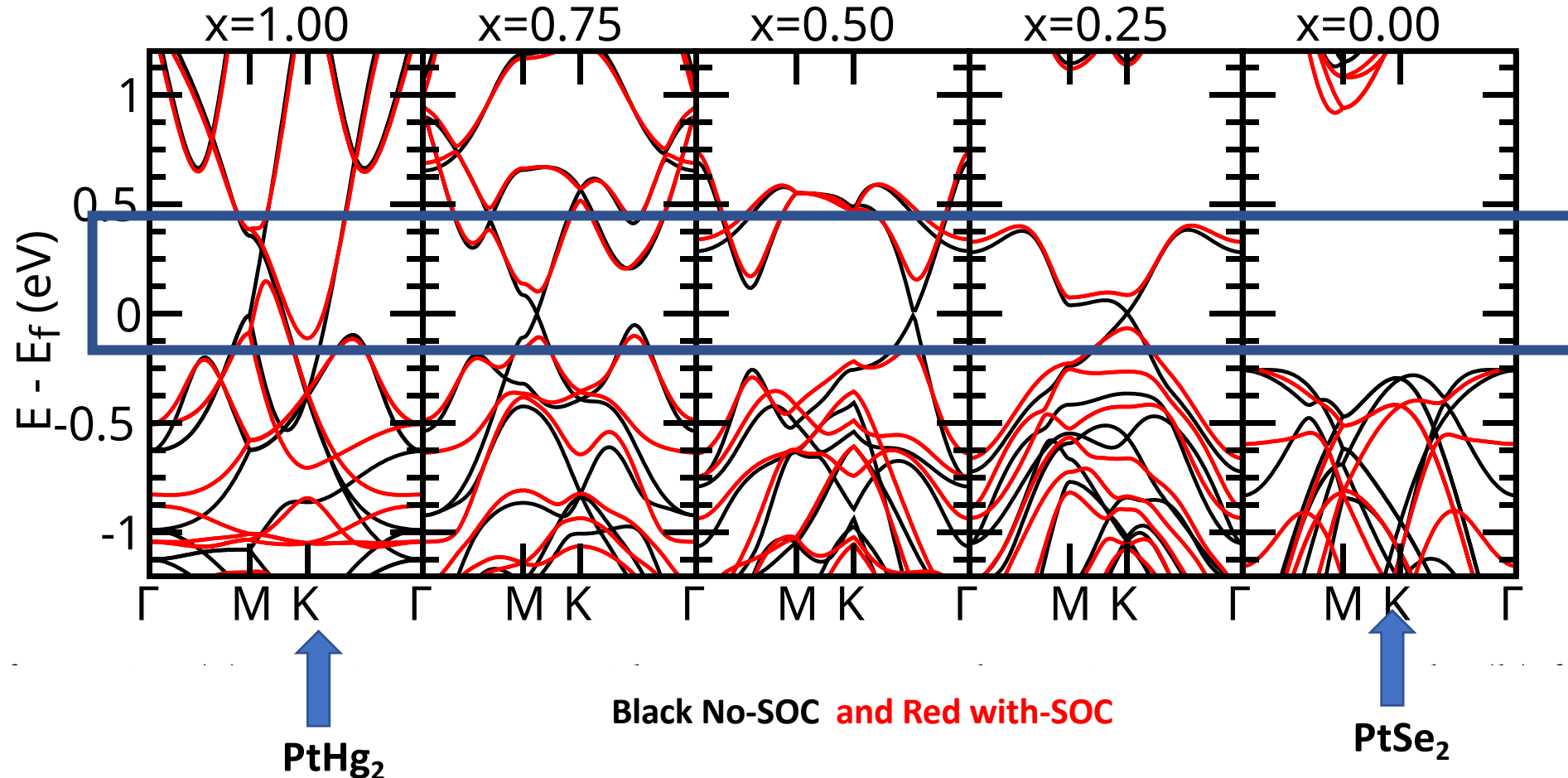
PtSe_2



Pt_2HgSe_3

Pt GRAY
Hg PURPLE
Se GREEN

Pt(Hg_xSe_{1-x})₂ with x=0.25, 0.50, 0.75 and 1.0



Black No-SOC and Red with-SOC

Metallic



Topological phase arise due to hybridization of the Hg s-orbitals with the Pt-dorbitals

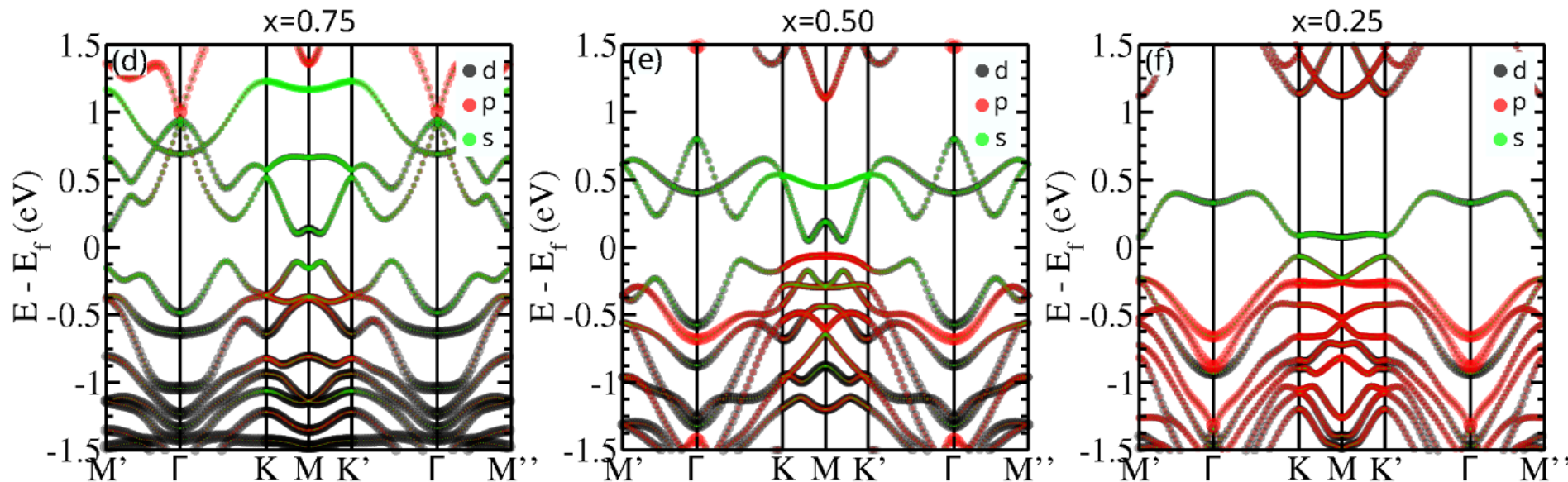
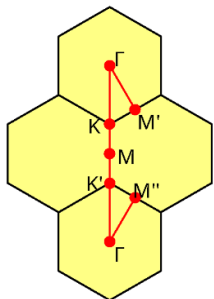


Insulator

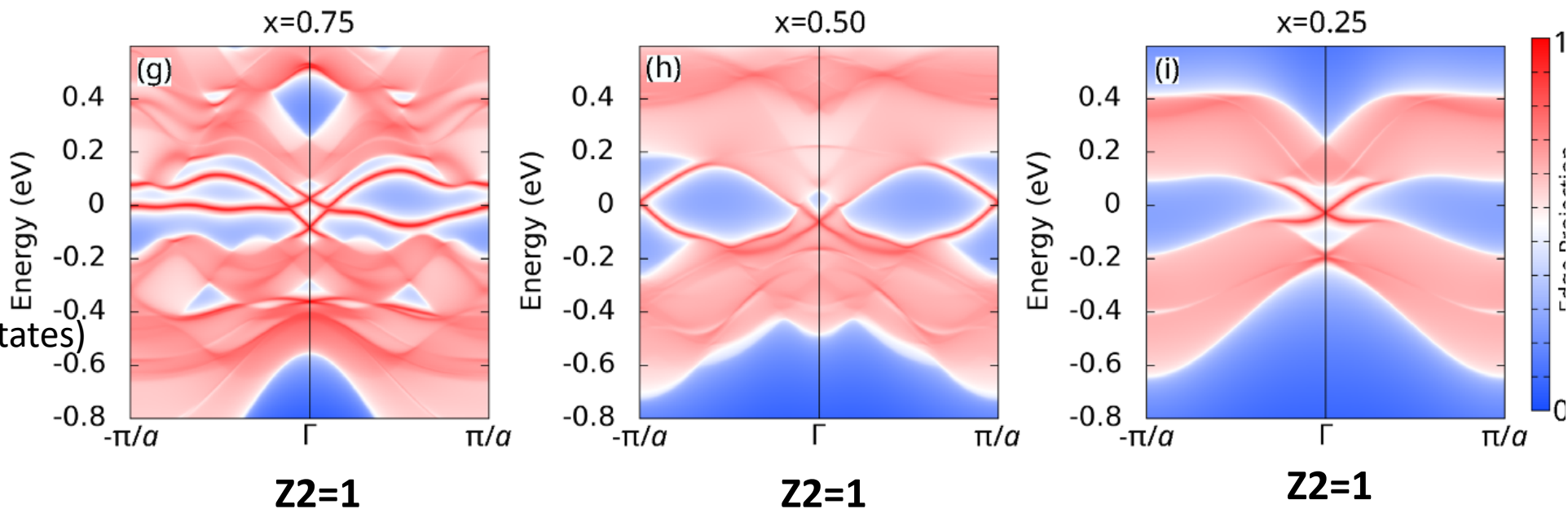
Pt(Hg_xSe_{1-x})₂ with x=0.25, 0.50, 0.75

All topological materials

(a)



Z₂=1



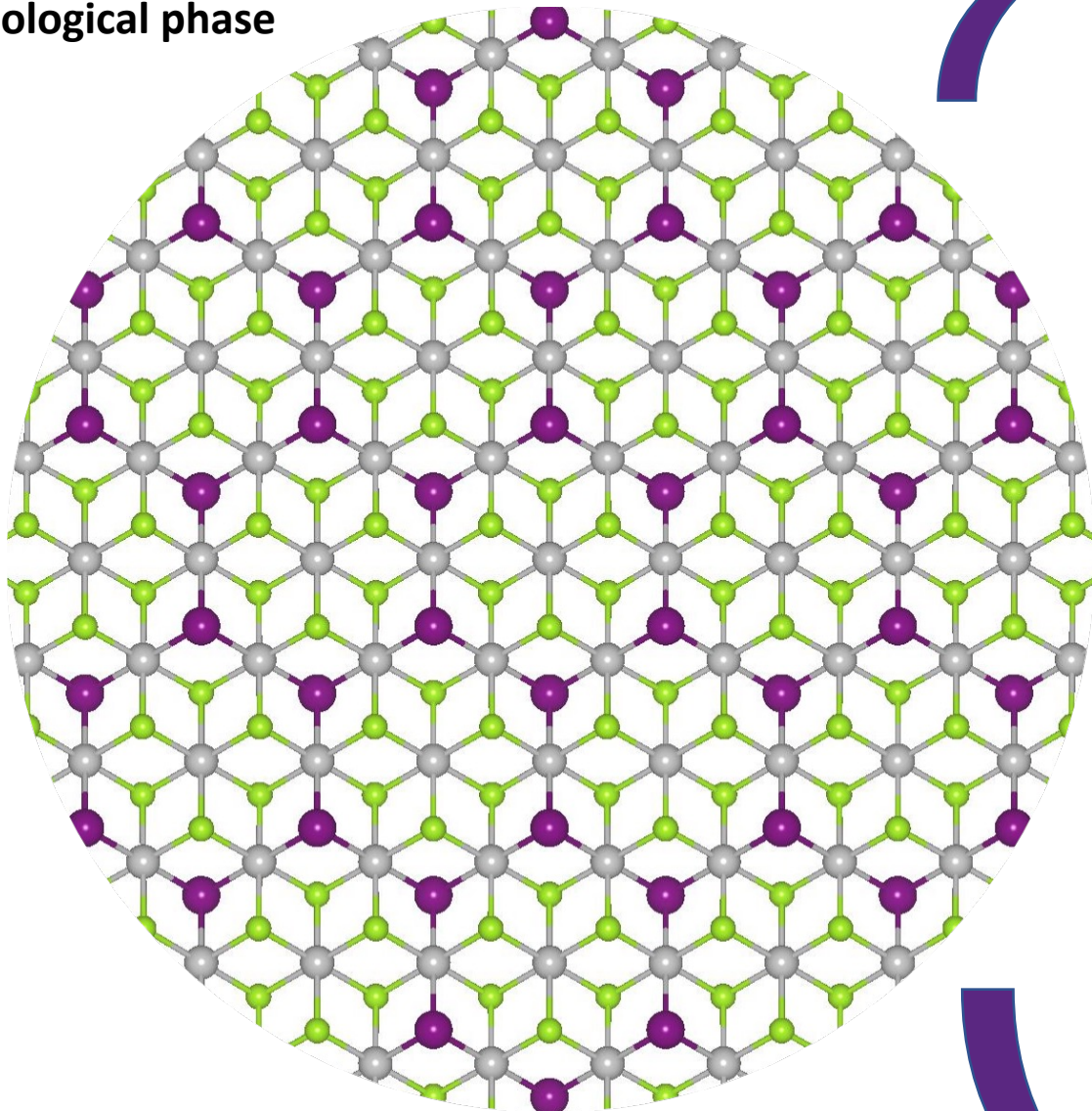
SEMI-INFINITE

 (projected edges states)

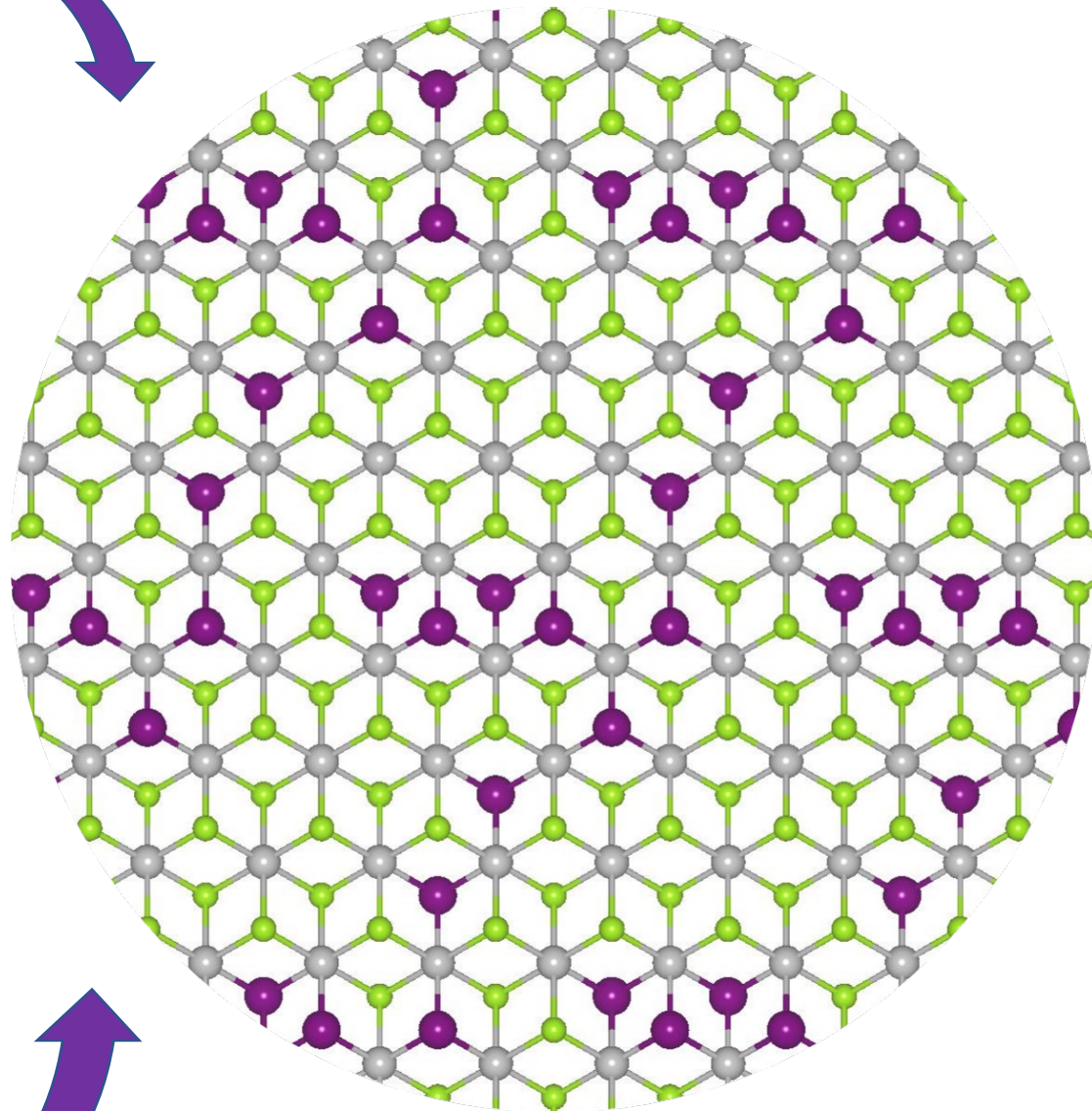
Our results reveal that the $\text{Pt}(\text{Hg}_x\text{Se}_{1-x})_2$ ordered alloys present a non-trivial topological phase

? ? ?

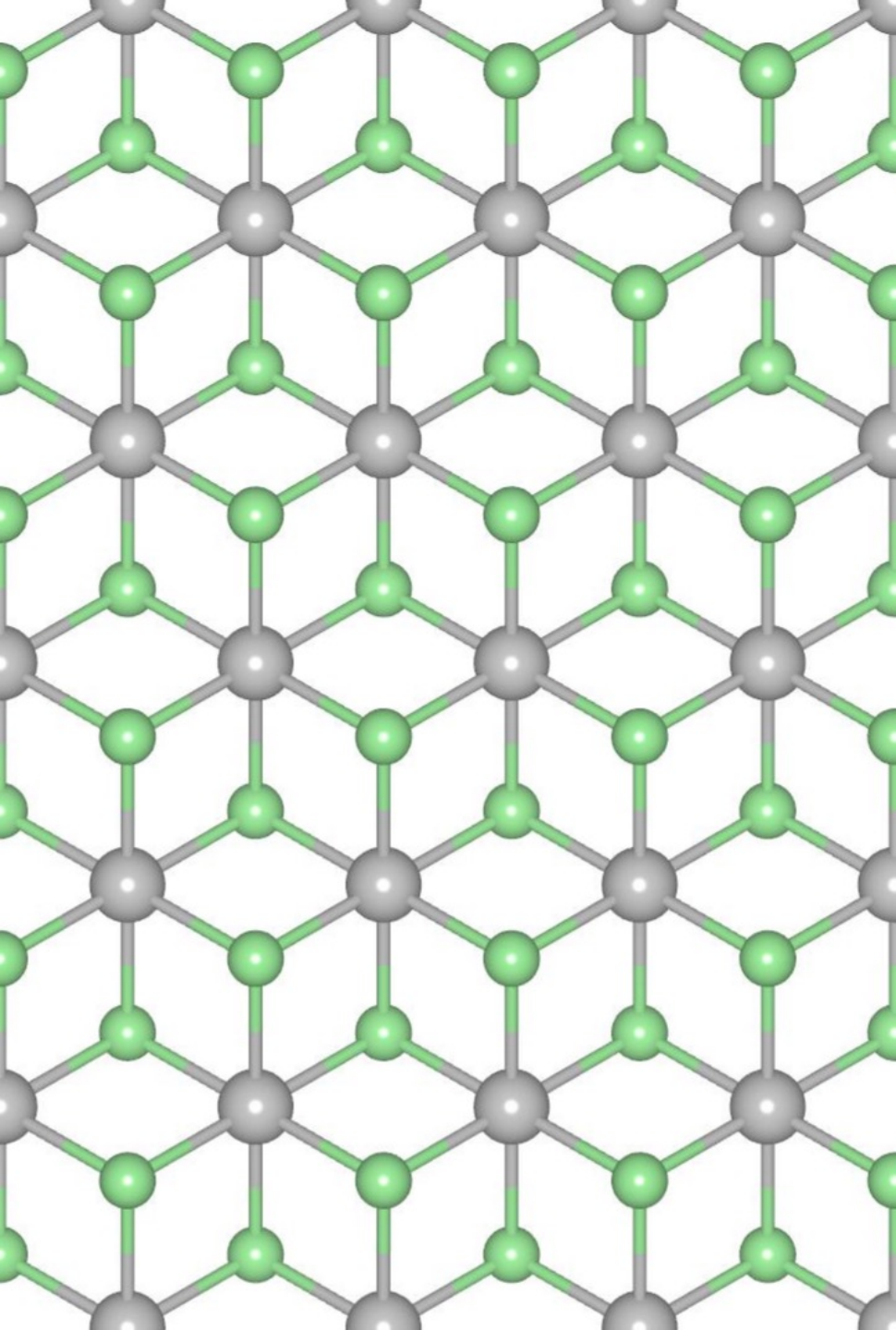
Random alloys ?



Ordered configuration



Random configuration

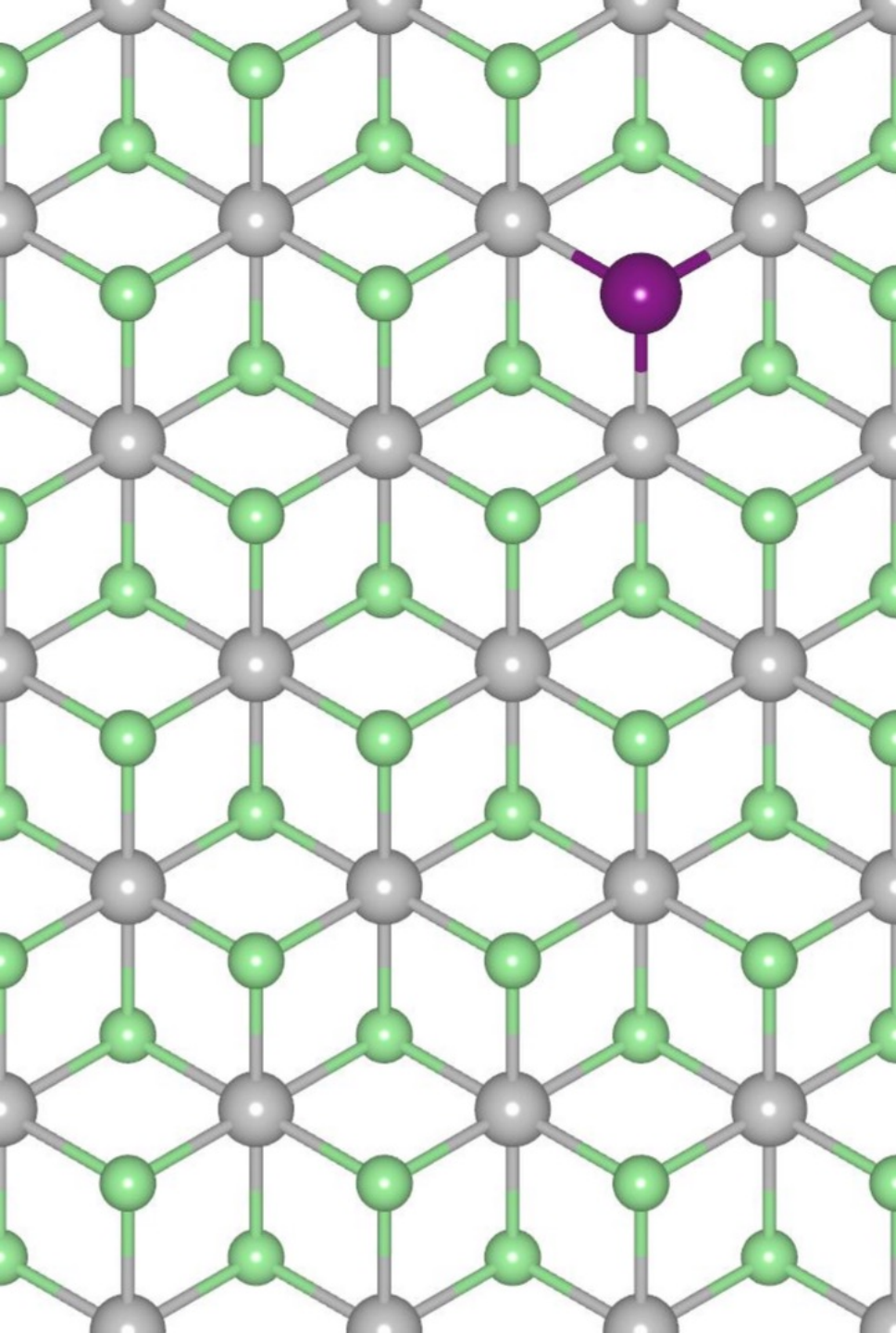


Hg–Hg-interaction embedded in PtSe₂ matrix

$$E_s = (E_{\text{system}} + n \mu_{\text{Se}} - E_{\text{PtSe}_2} - n \mu_{\text{Hg}}) / n$$

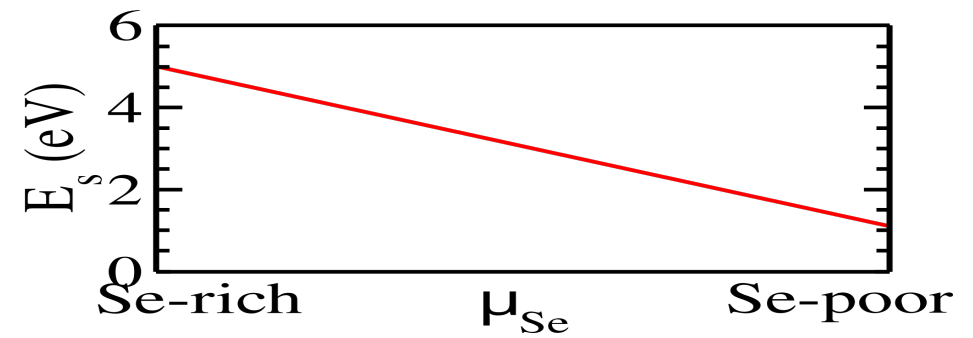
Tetragonal supercell 18.7Å x 32.4Å

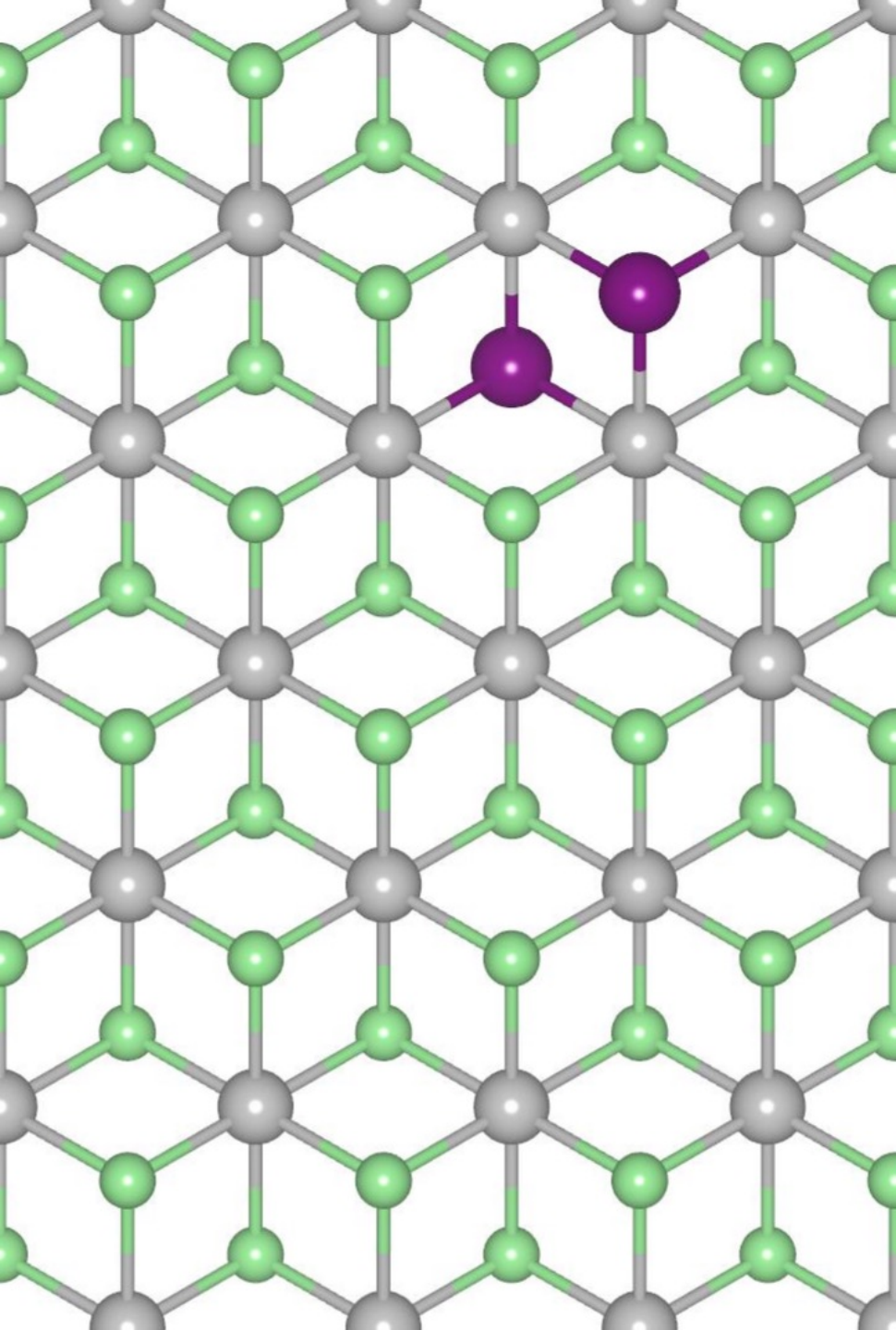
8x8 with 192 atoms.



>Substitutional energy for a single Hg ($n=1$)

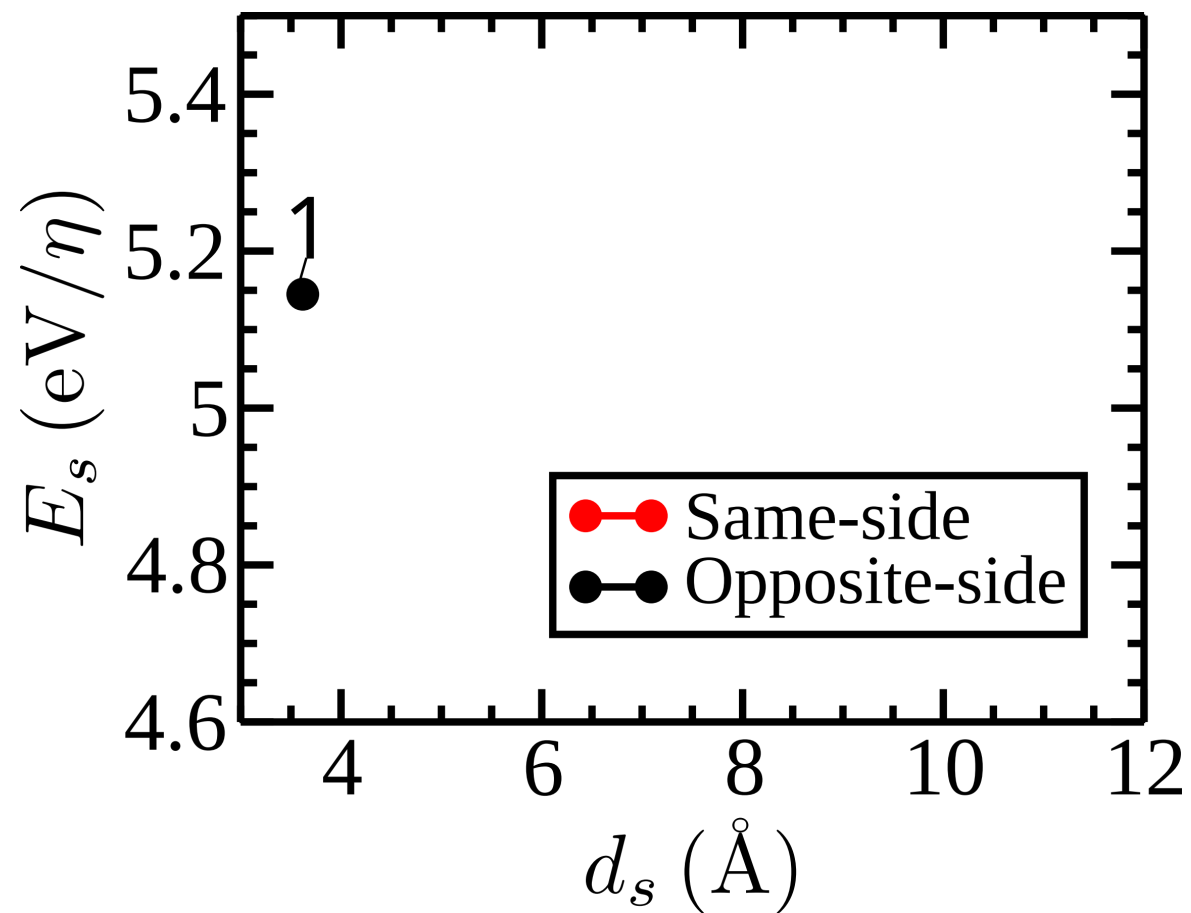
$$E_s = (E_{\text{system}} + n \mu_{\text{Se}} - E_{\text{PtSe}_2} - n \mu_{\text{Hg}}) / n$$

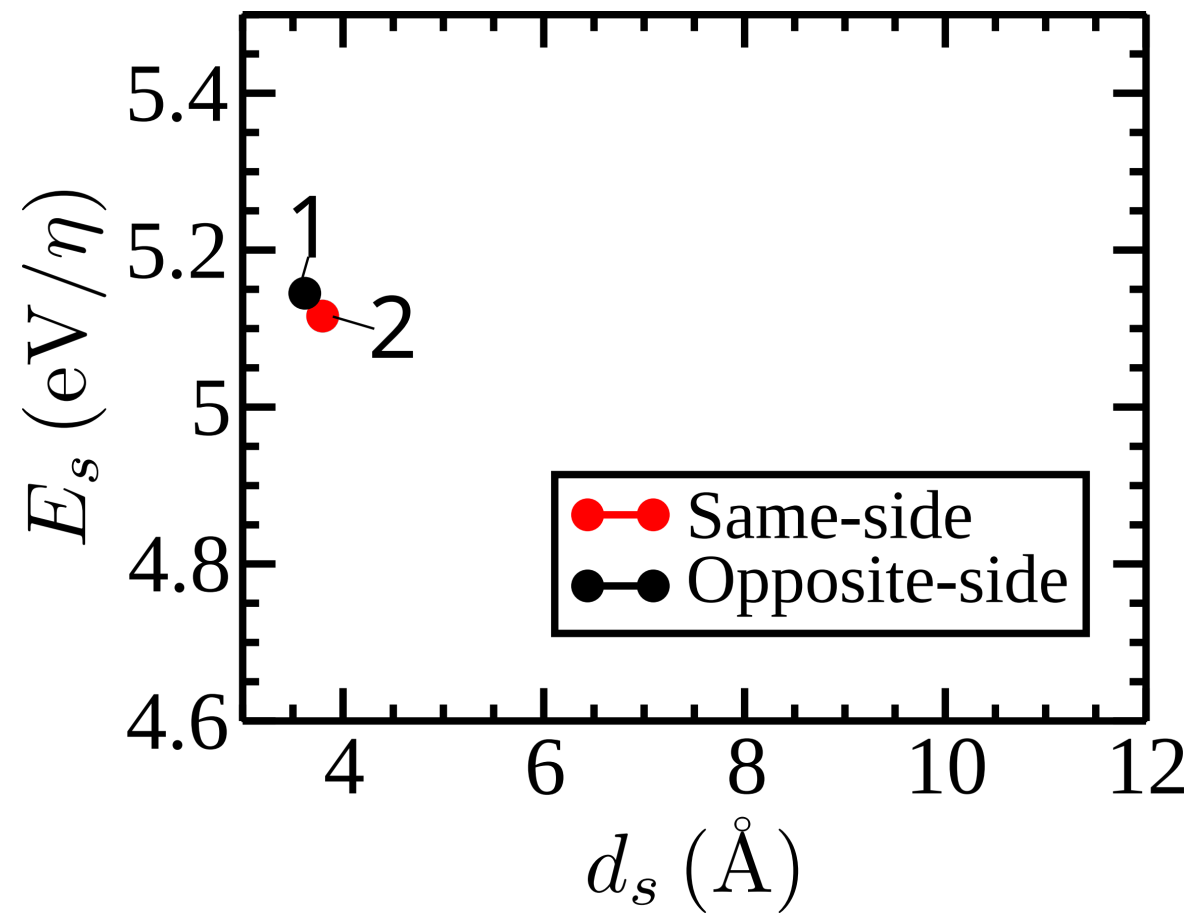
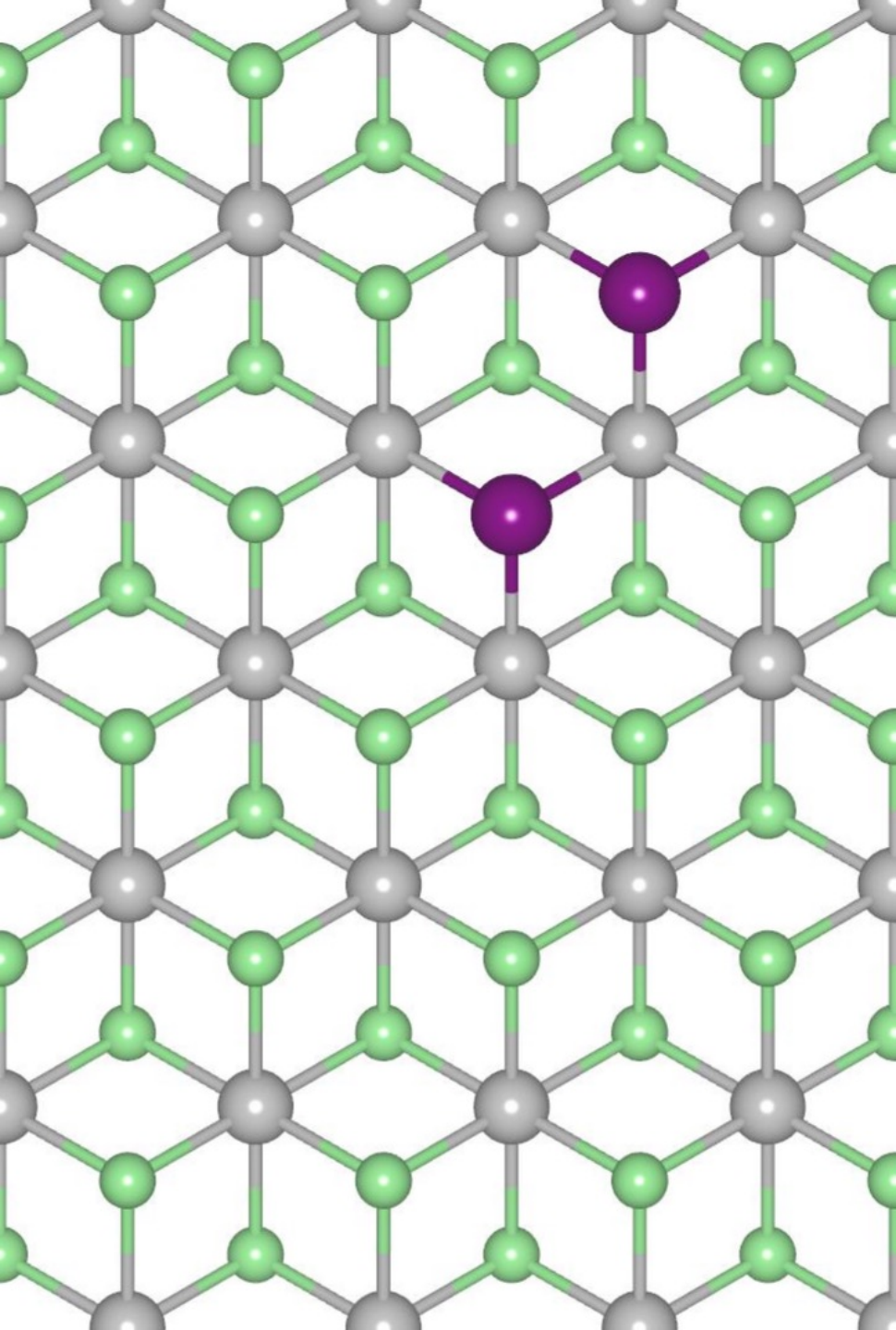


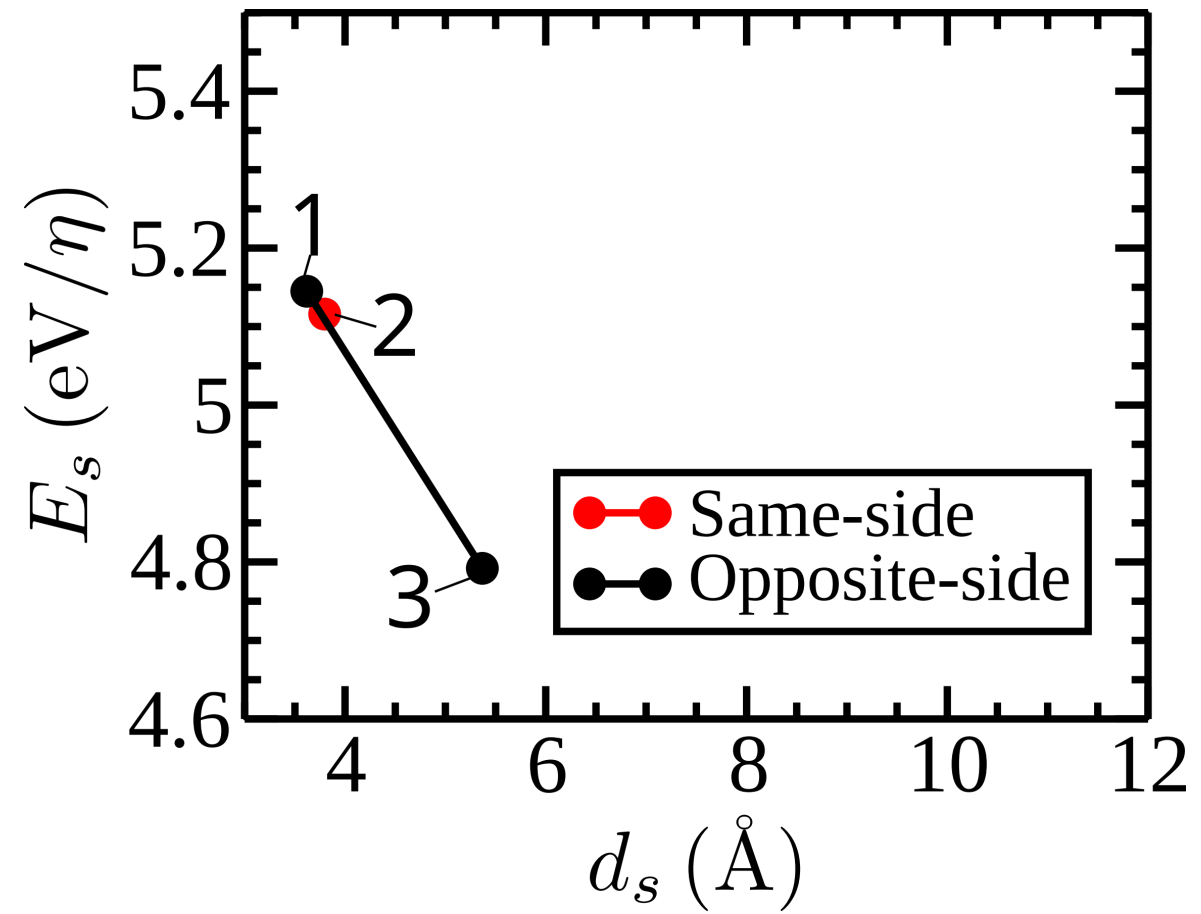
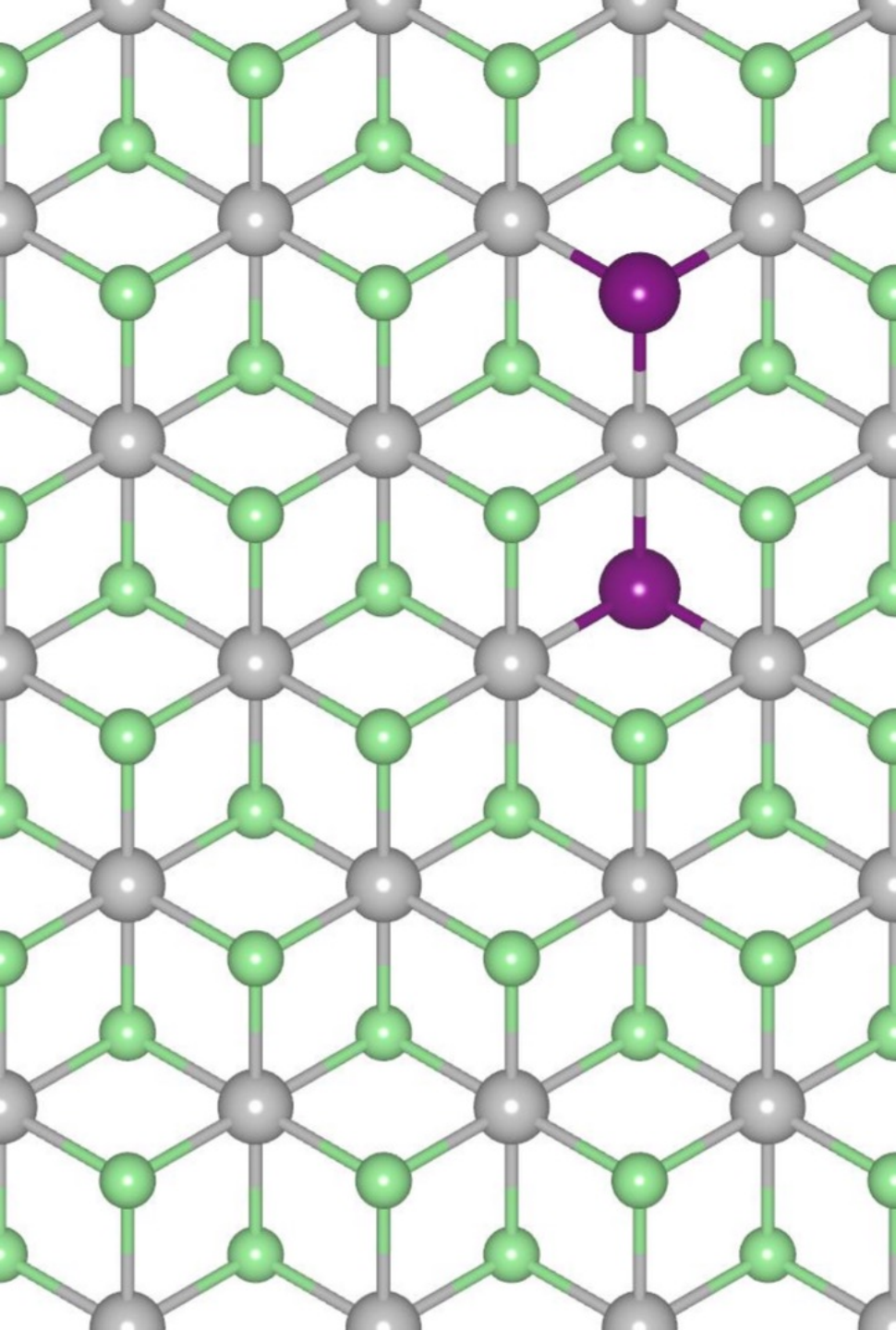


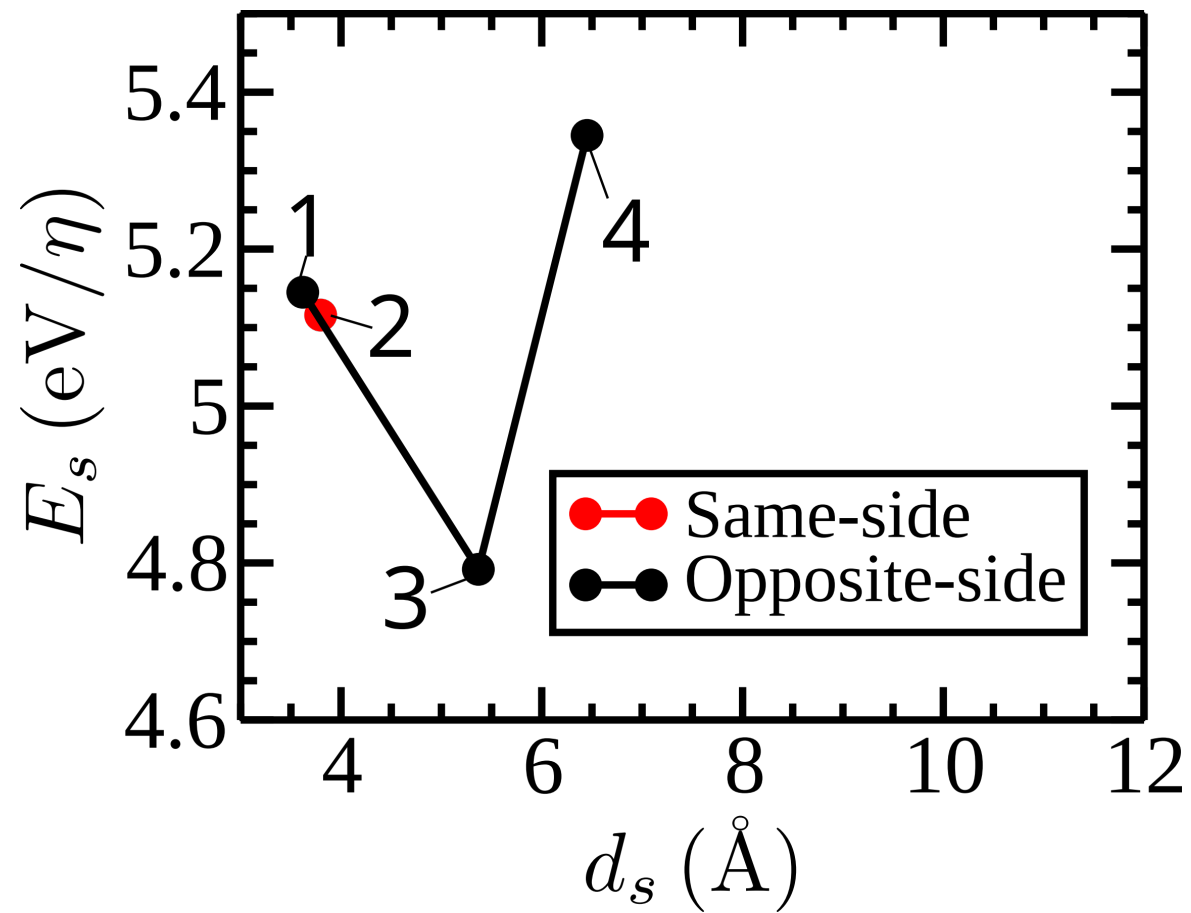
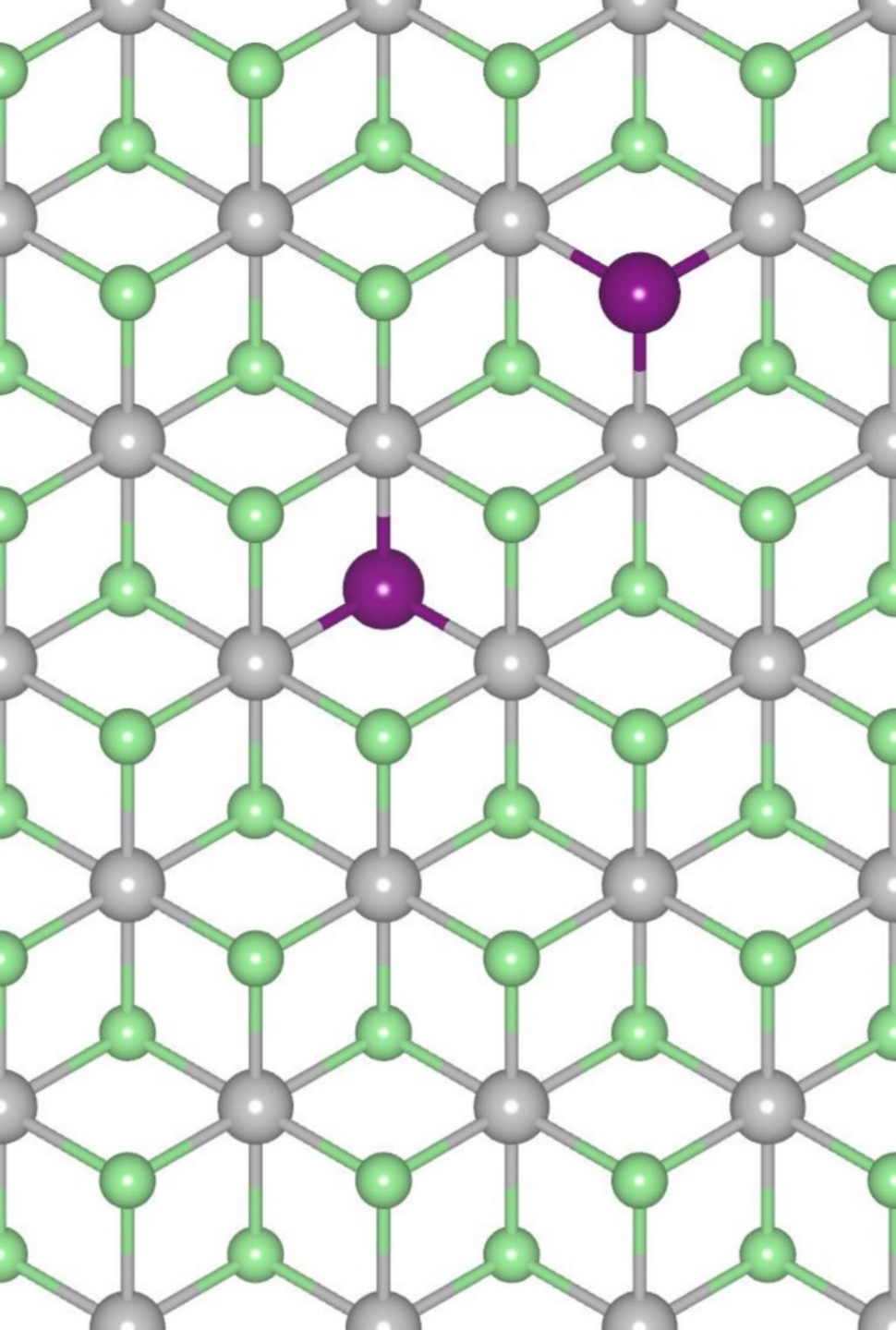
>Substitutional energy for interacting Hg pairs ($n=2$)

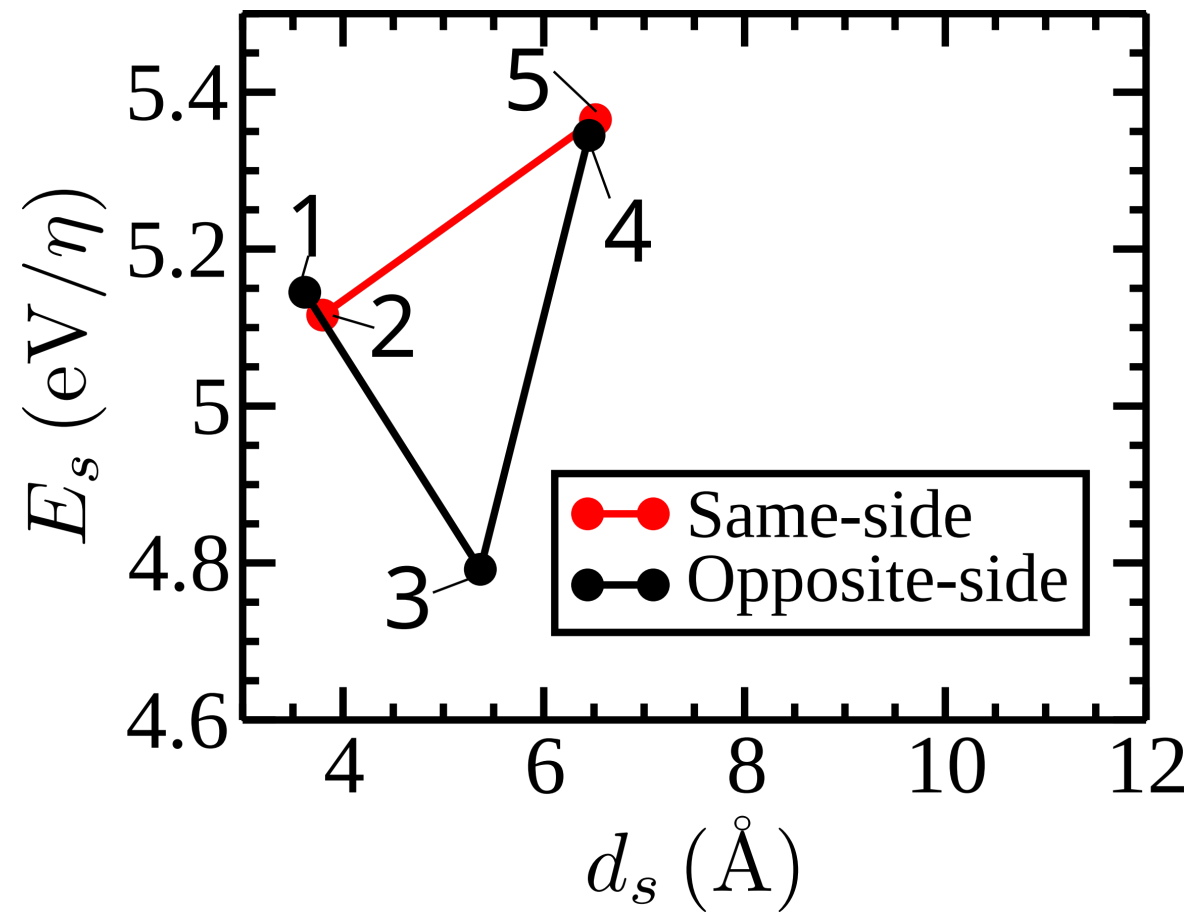
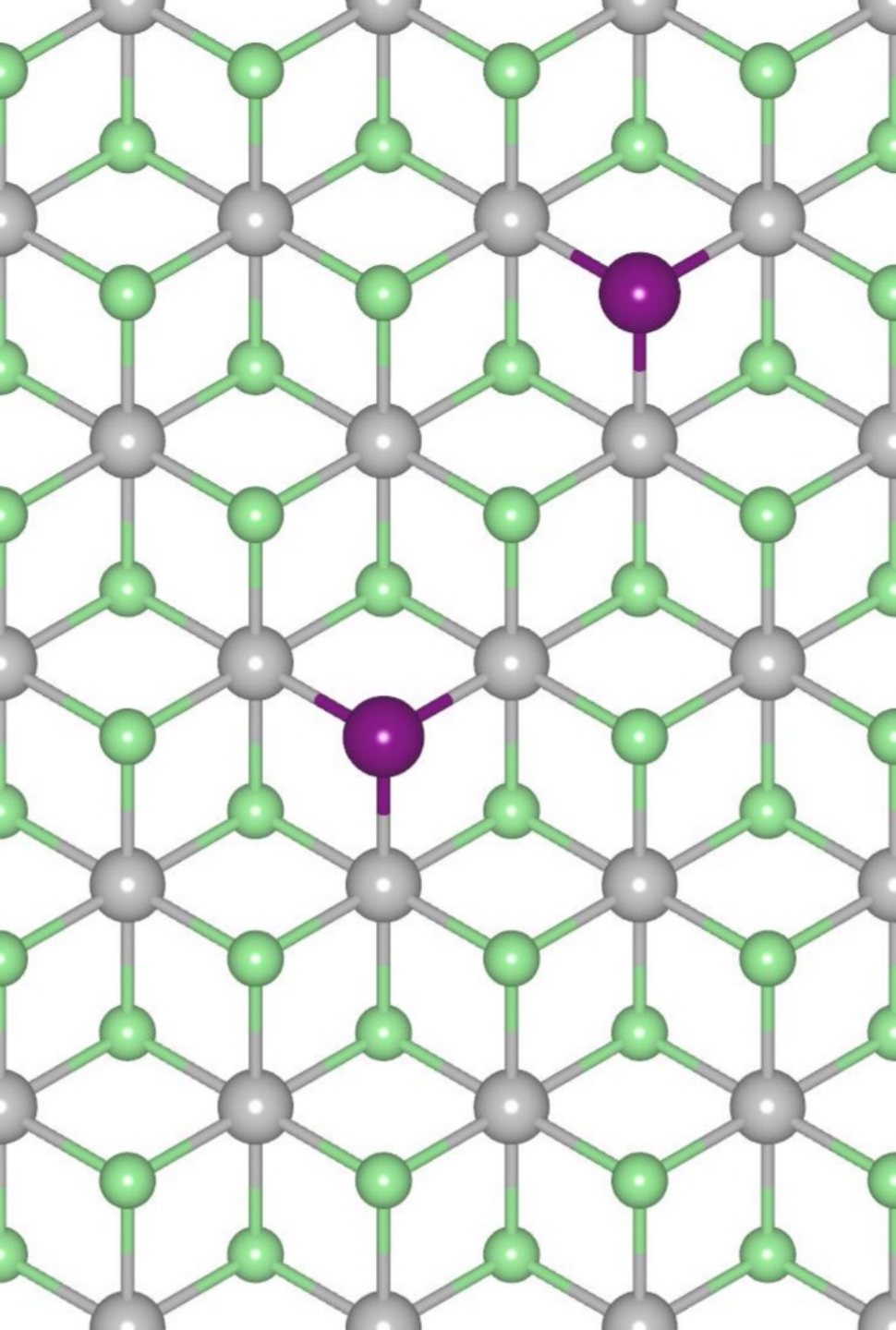
$$E_s = (E_{\text{system}} + n \mu_{\text{Se}} - E_{\text{PtSe}_2} - n \mu_{\text{Hg}}) / n$$

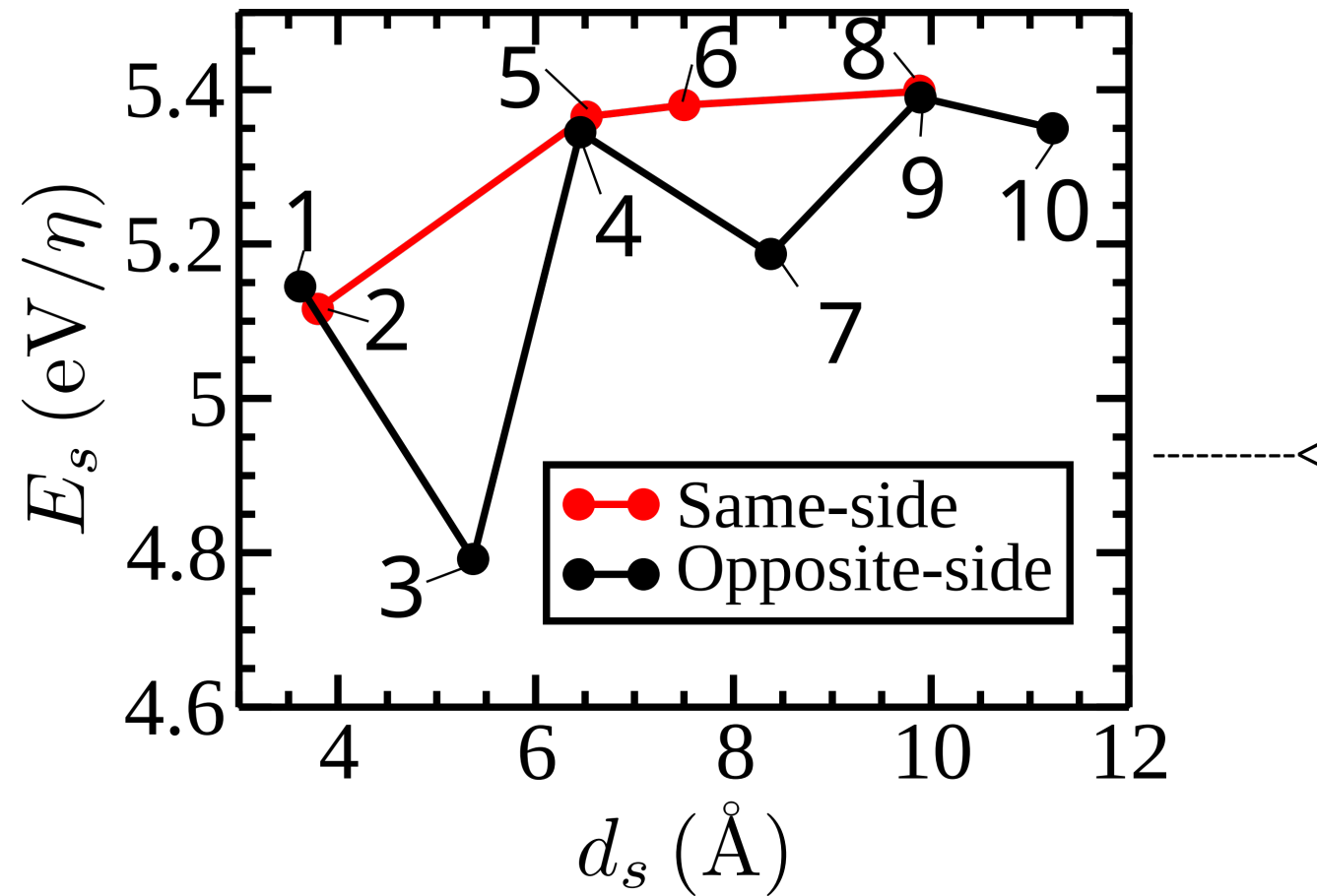
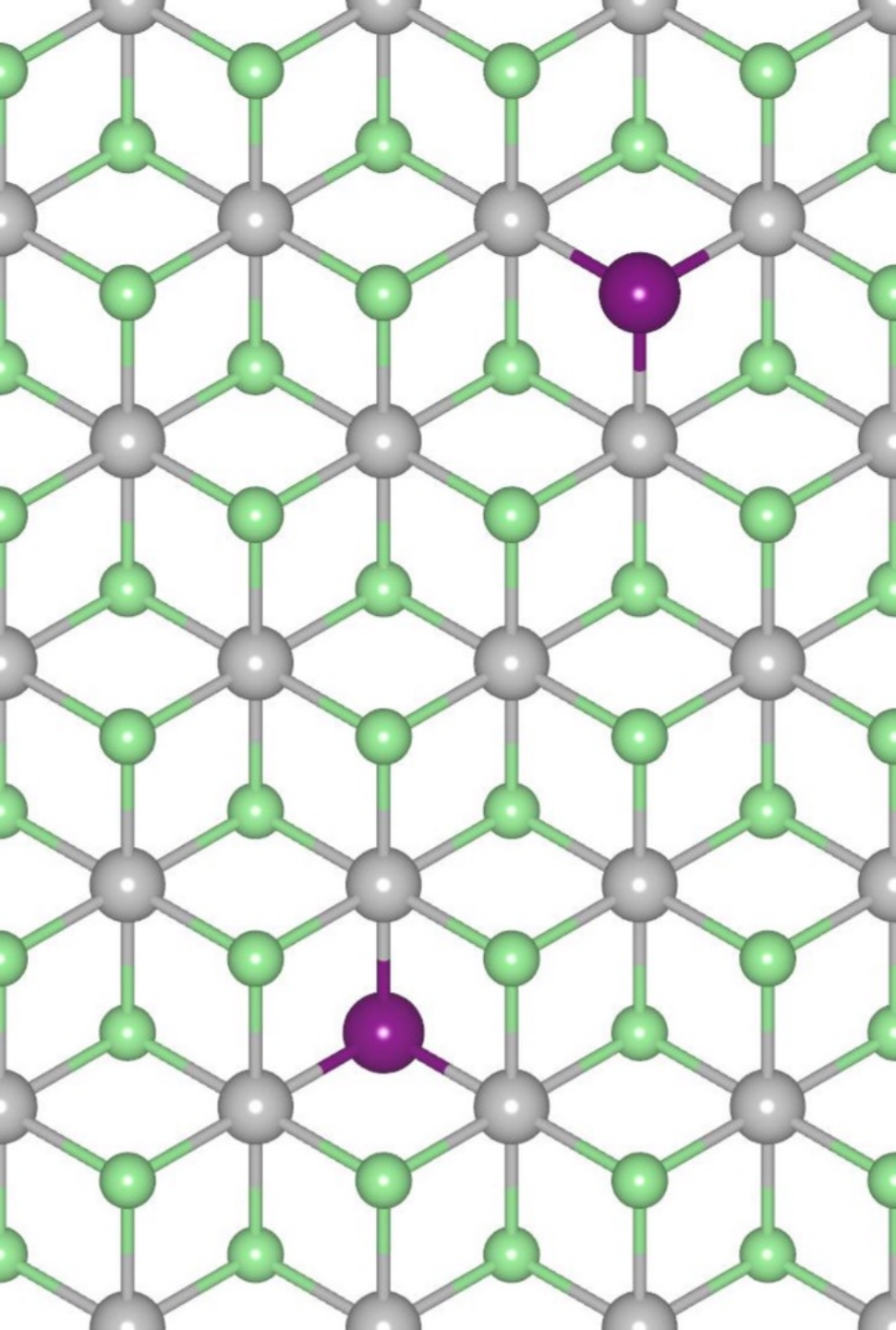






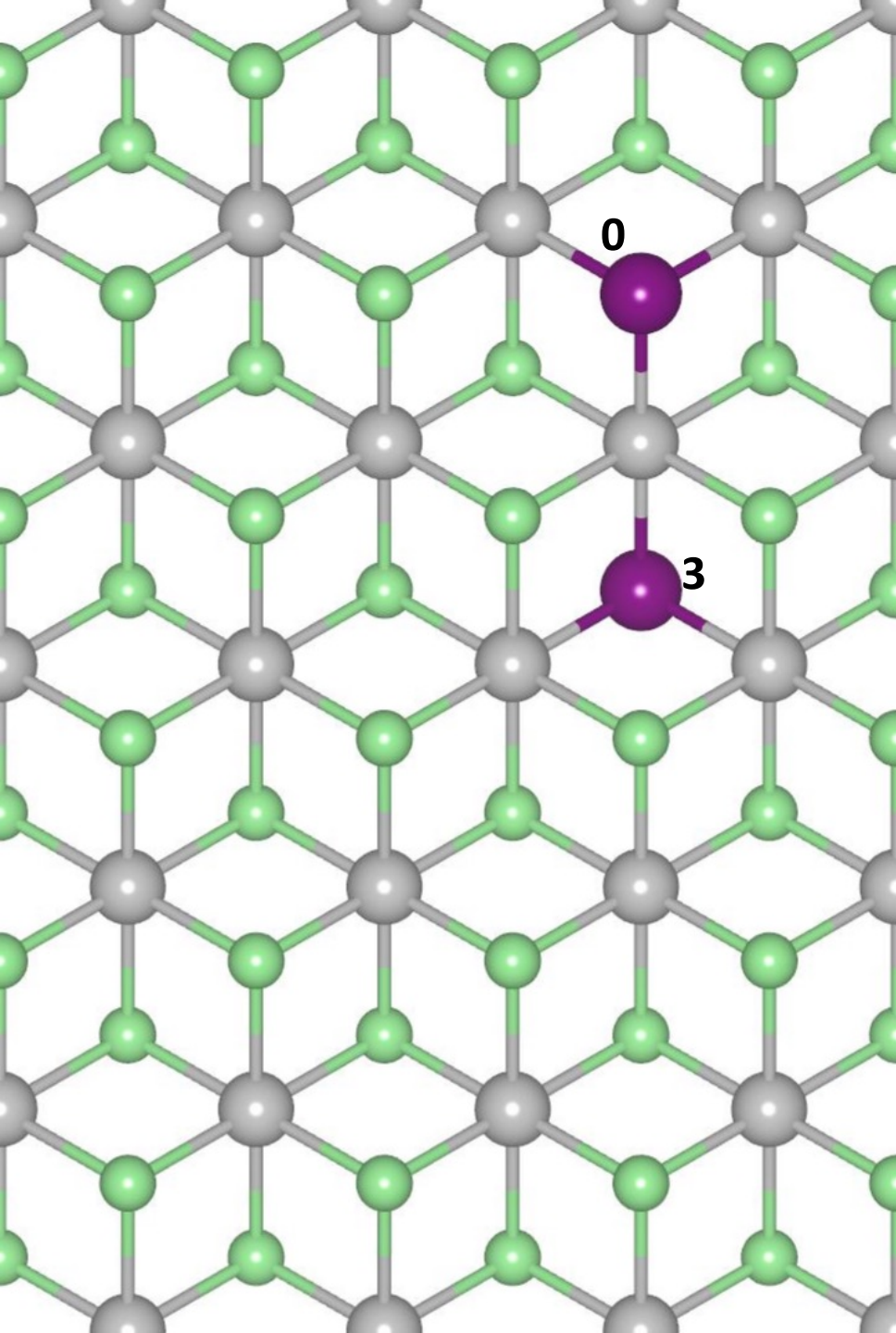






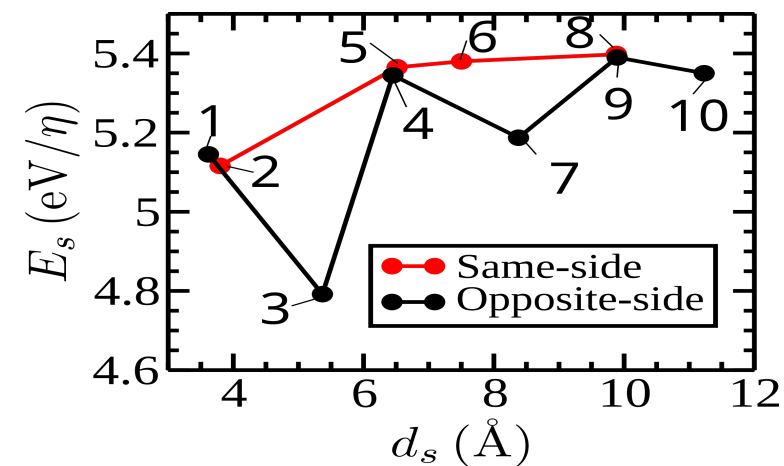
For distances greater than 11 \AA **NO** change in energy

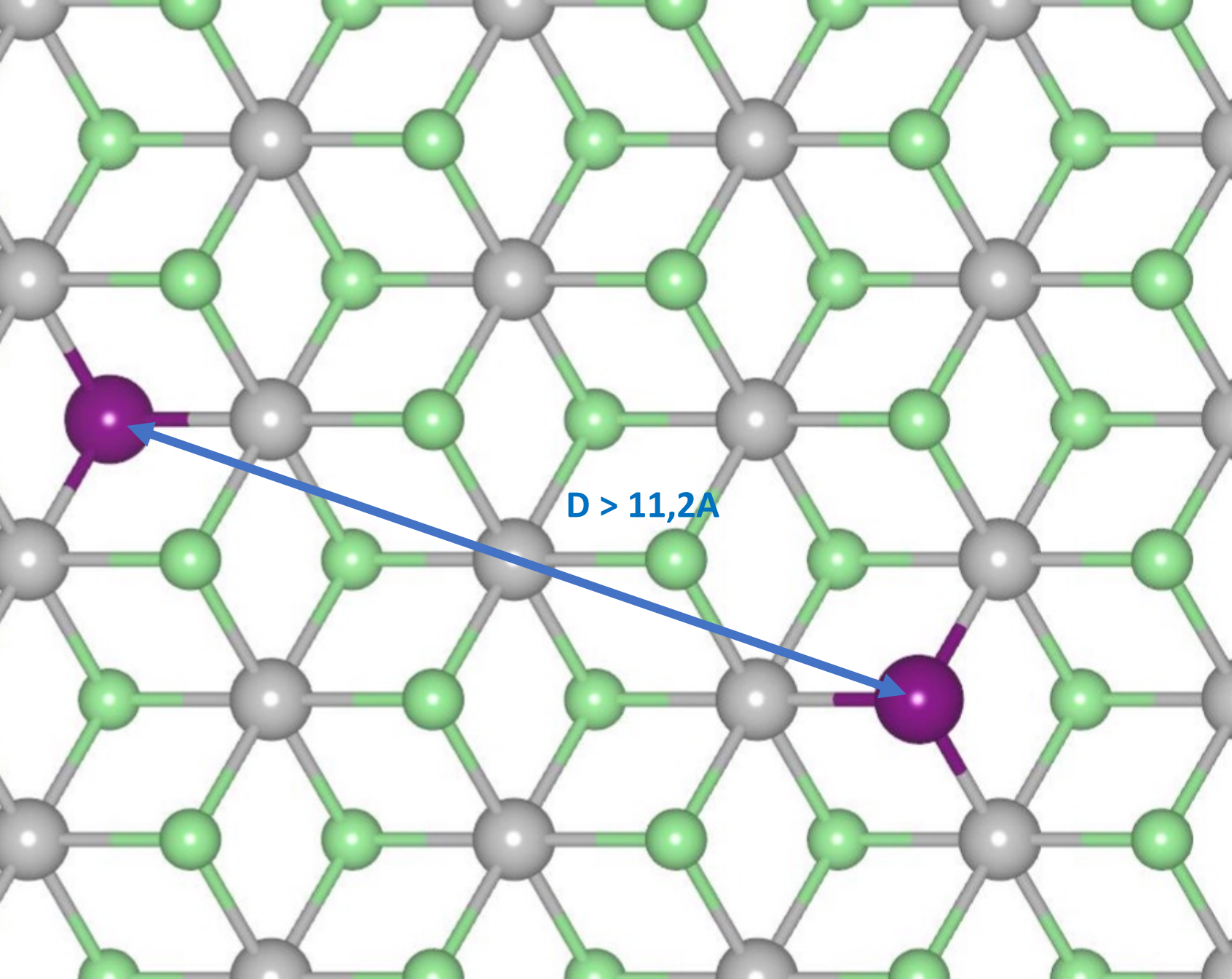
Tetragonal supercell 18.7 \AA x 32.4 \AA



Pair most stable $\text{Hg}^0\text{—Hg}^3$ bonds sharing the same Pt atoms

Hg-Pt-Hg exactly that found (that we expected) in the Pt_2HgSe_3 crystal

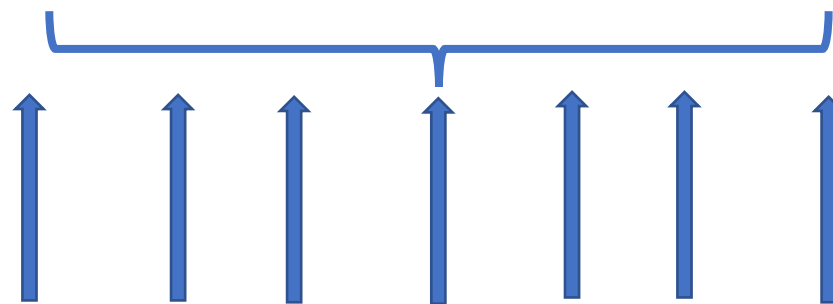
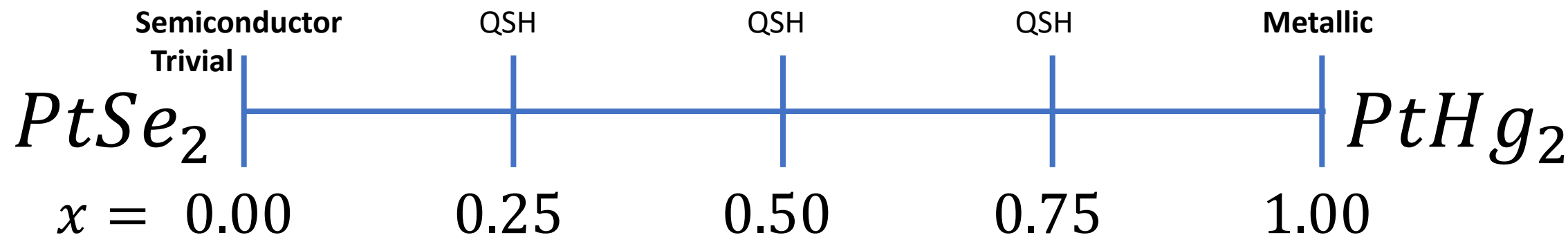




- The Hg “wavefunctions” are overlapping with each other up to $\sim 1,1\text{nm}$, defining a localization length



Order



SQS 1st-neighbor, 2st., 3st pair correlation exactly random.

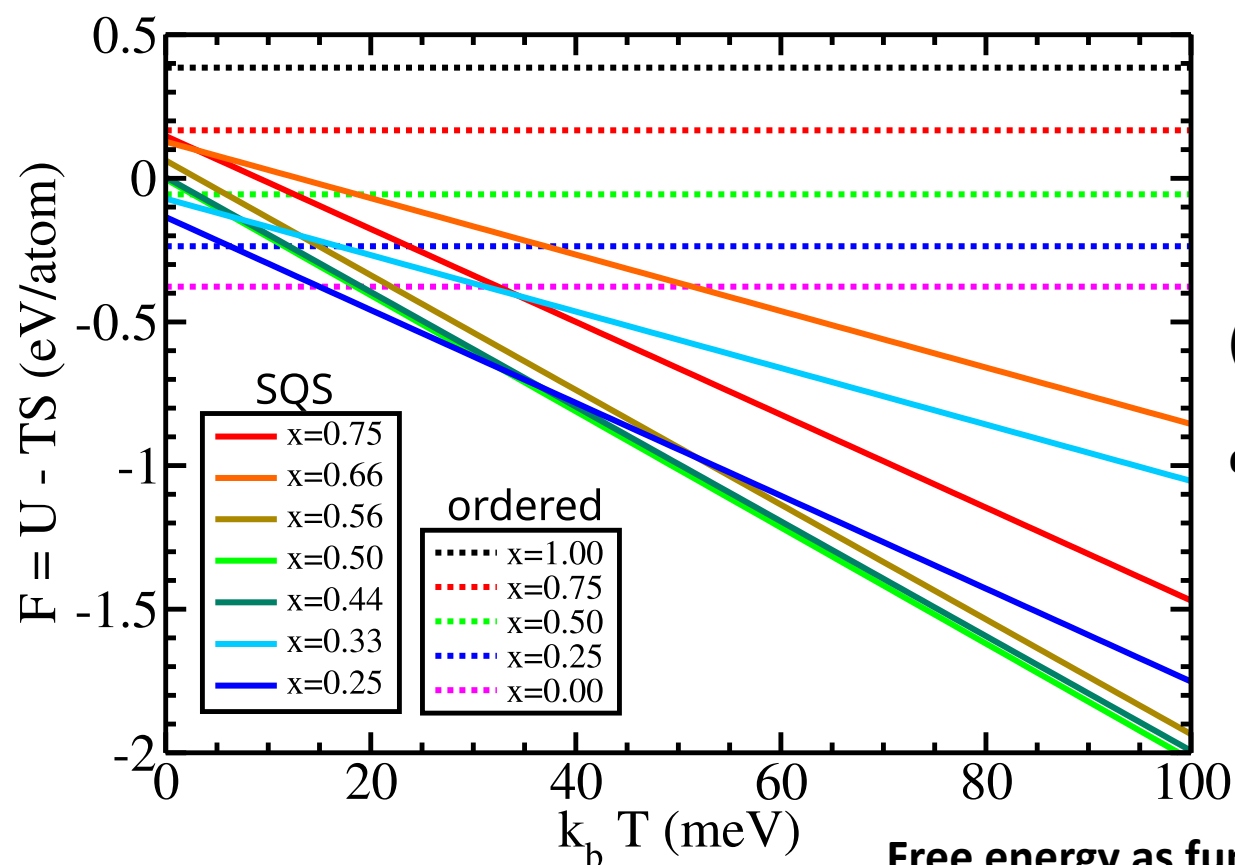
Disorder

$(x = 0.25, 0.33, 0.44, 0.50, 0.56, 0.66, 0.75)$

Random distribution



*To provide a more realistic description of random alloys > SQS (special quasi random) approach from $x=0.25$ to $x=0.75$ (Zunger et al PRL 1990)



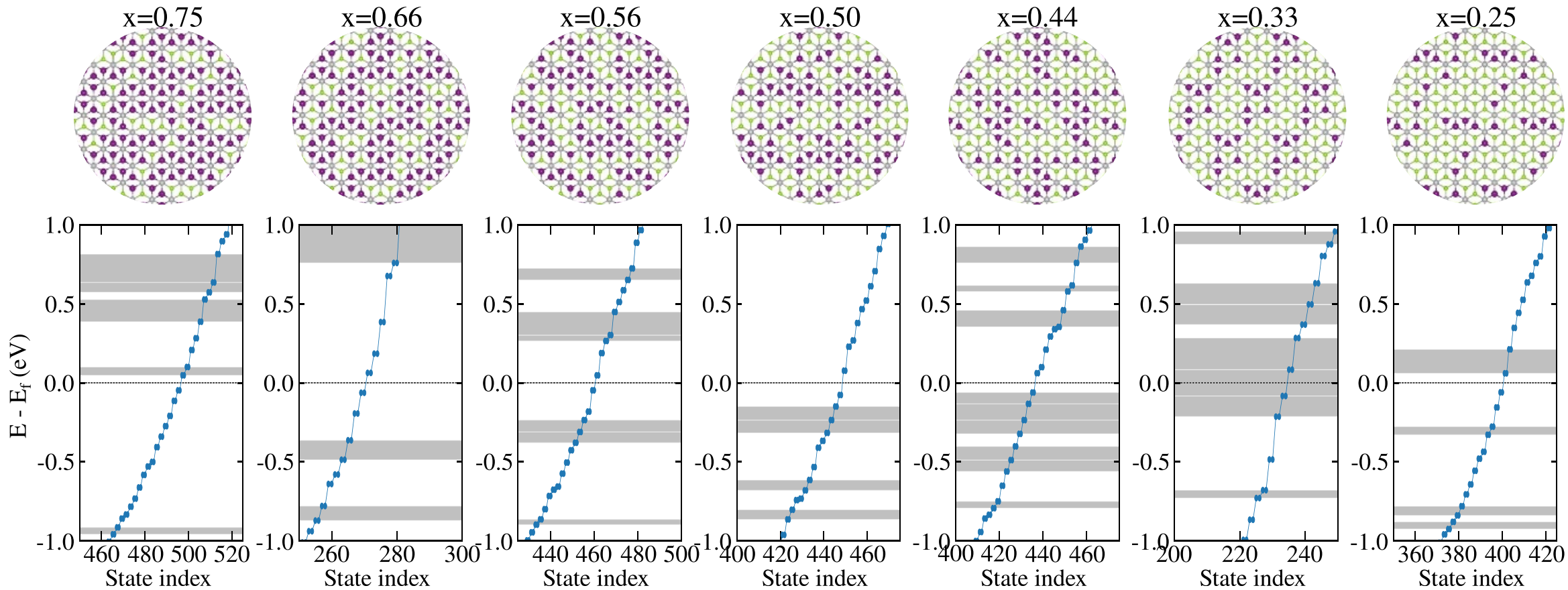
a function of temperature)

- (i) PtSe₂ energetic preference for $K_B T < 15 \text{ meV}$
- (ii) Above $\sim K_B T > 40 \text{ meV}$ PtHgSe random present lowest free energy

$$\Gamma_{1N} = \frac{1}{N_{1N}} \sum_{\langle ij \rangle} c_i c_j$$

$$(2x-1)^2$$

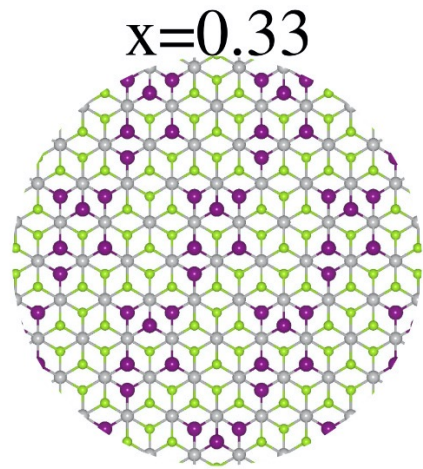
Free energy as function of temperature.



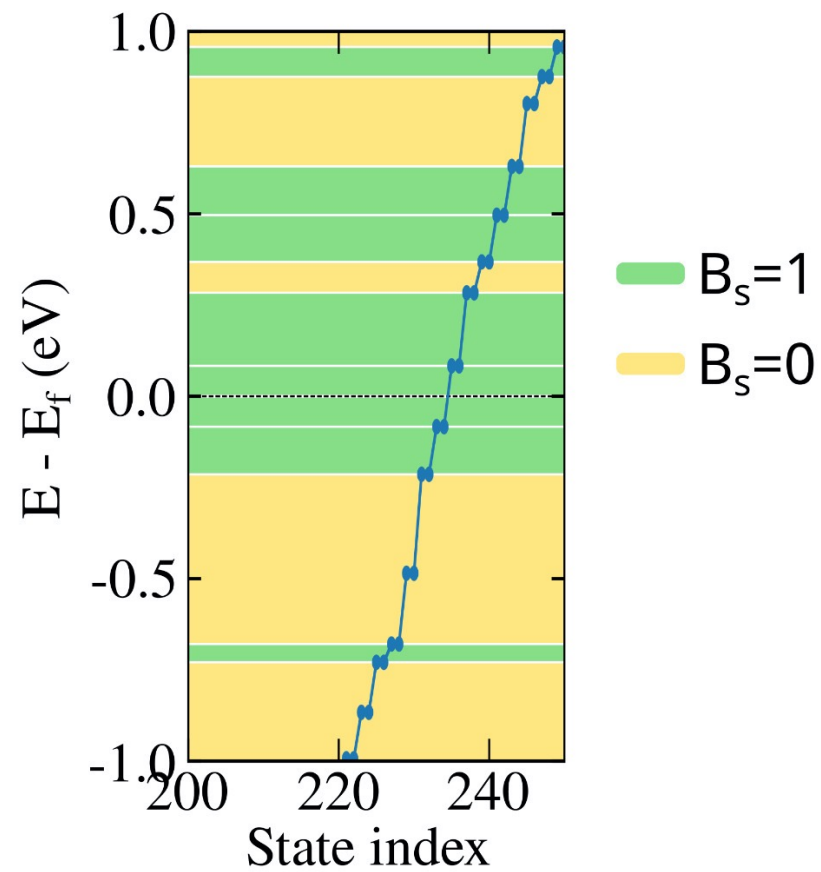
The blue point represents the eigenvalue of the Hamiltonian. The blue line is just a guide to the eye

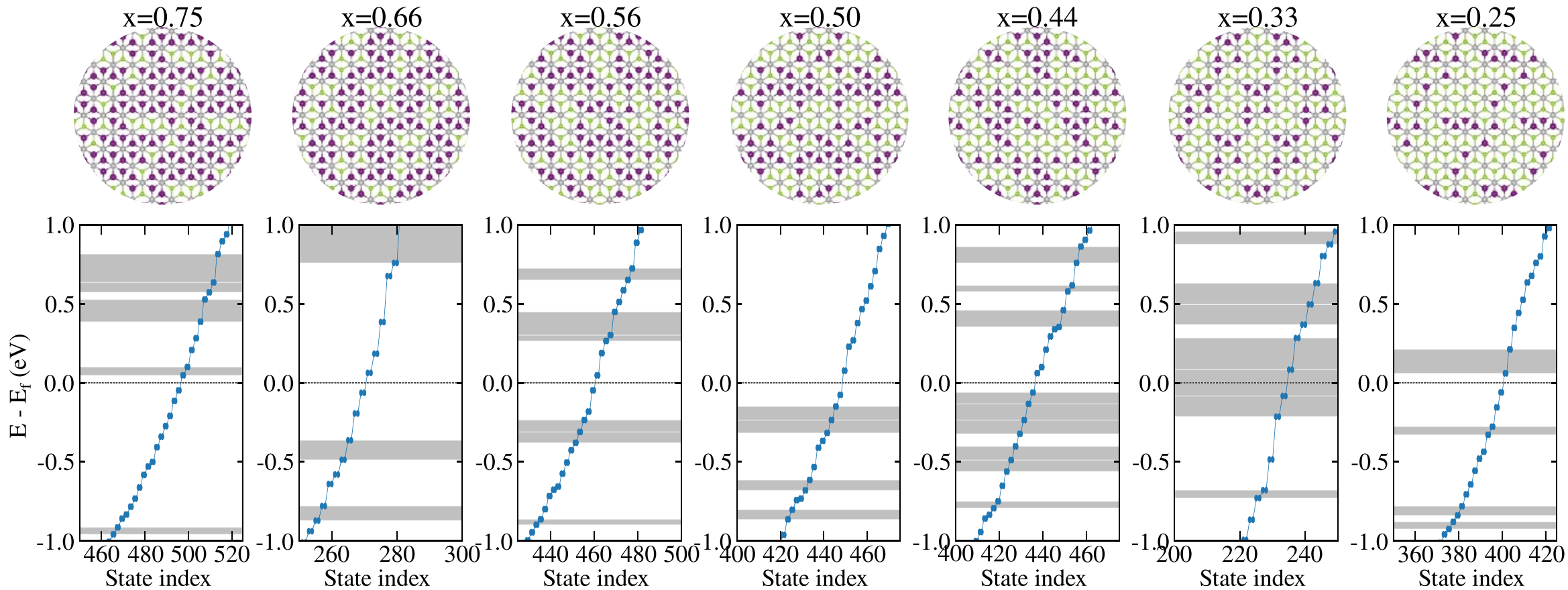
For a non-periodicity of the random alloy, we have computed a real space invariant : Spin Bott-index, which is equivalent to the spin-Chern number.





For a non-periodicity of the random alloy, we have computed a real space invariant :Spin Bott-index, which is equivalent to the spin-Chern number.

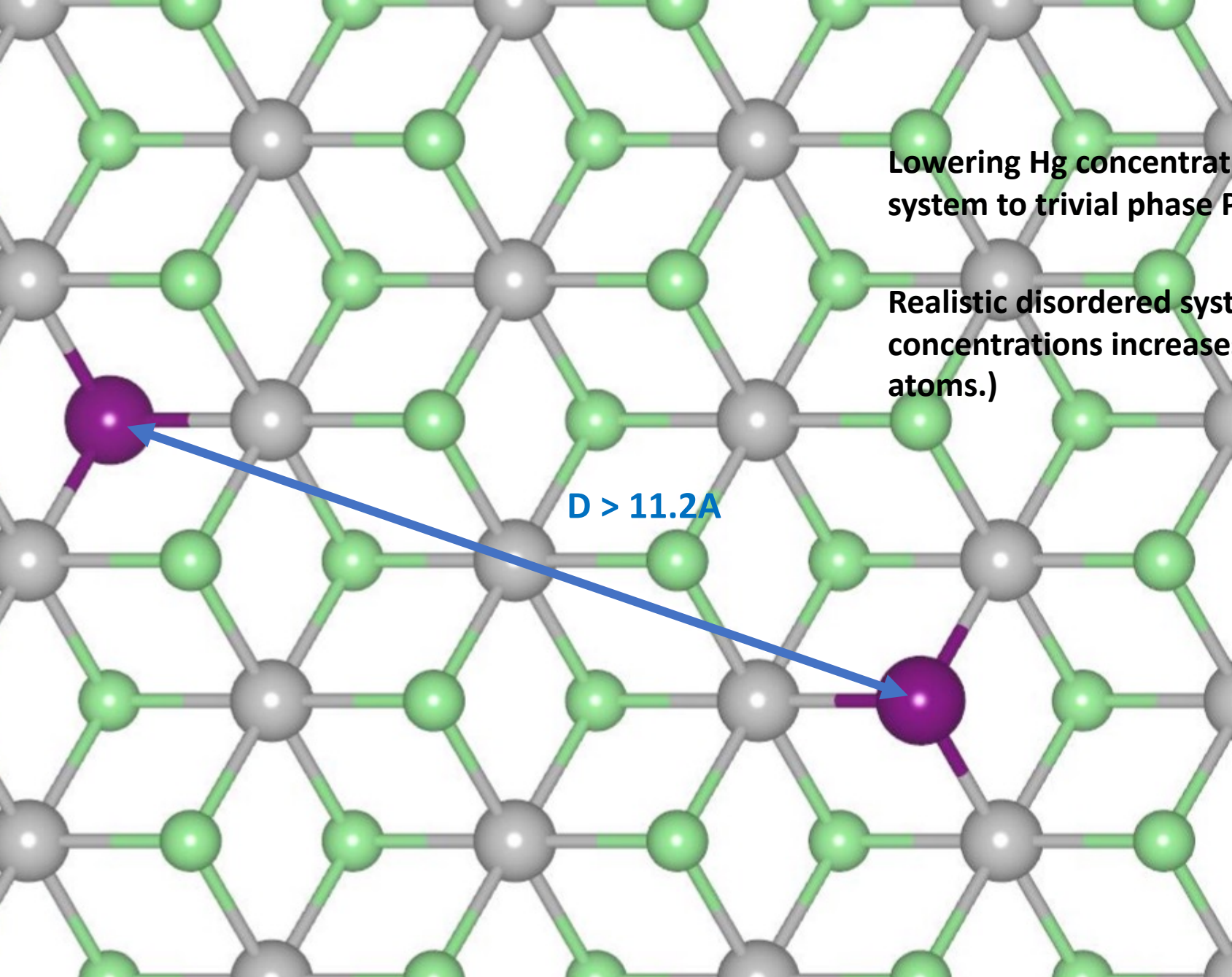




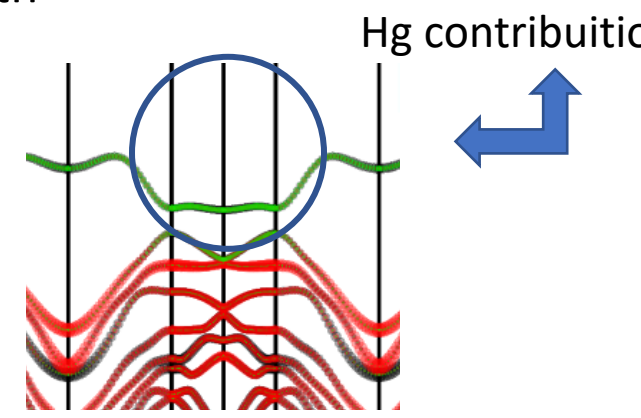
The blue point represents the eigenvalue of the Hamiltonian. The blue line is just a guide to the eye

For a non-periodicity of the random alloy, we have computed a real space invariant : Spin Bott-index, which is equivalent to the spin-Chern number.





- The Hg wavefunctions are overlapping with each other up to $\sim 1,0\text{nm}$, defining a localization length



Topological limit



* $x \rightarrow 0$ will lead the $\text{Pt}(\text{Hg}_x\text{Se}_{1-x})_2 \rightarrow \text{PtSe}_2$ trivial phase

** We will look at a NON-Trivial \leftrightarrow Trivial based on electron percolation limit

$c^{(s)} = c_+ - c_-$, (Chern number, integration over a closed surface of Berry connection)

$$c_j = \sum_n^{\text{occup}} \oint_C \vec{A}_n^{(j)} \cdot d\vec{k}, \quad \vec{A}_n^{(\sigma)} = i \langle n, \vec{k}, \sigma | \nabla_k | n, \vec{k}, \sigma \rangle$$

>fully localized wave functions are eigenfunction of the position operator:

$$\hat{x} = i \nabla_k$$

$$\therefore c_\sigma = \sum_n^{\text{occup}} x_n \oint_C dk = 0$$

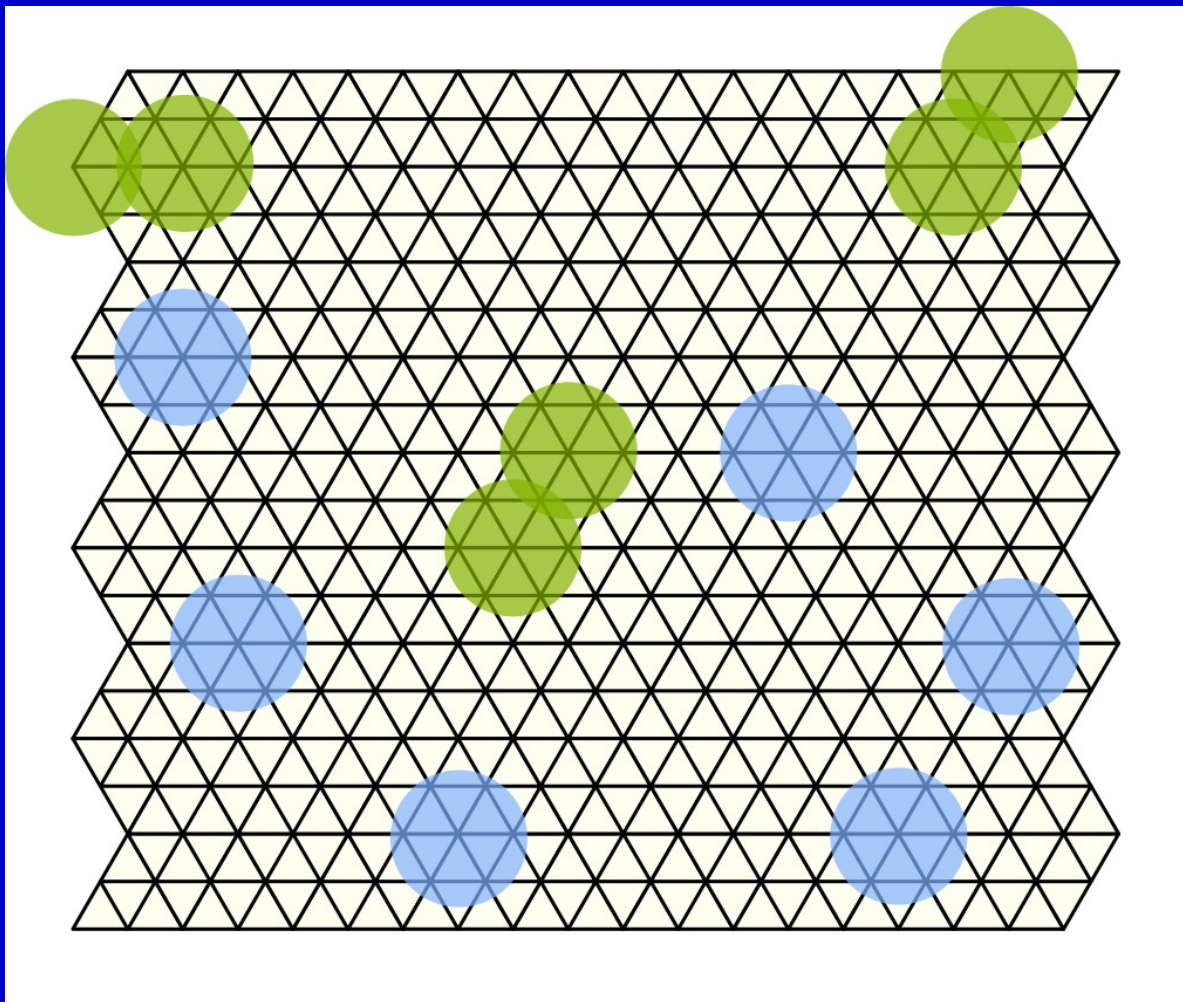
Non-zero Chern number requires the electronic states to **NOT** be completely localized (necessary but not sufficient).... For QSH phase.

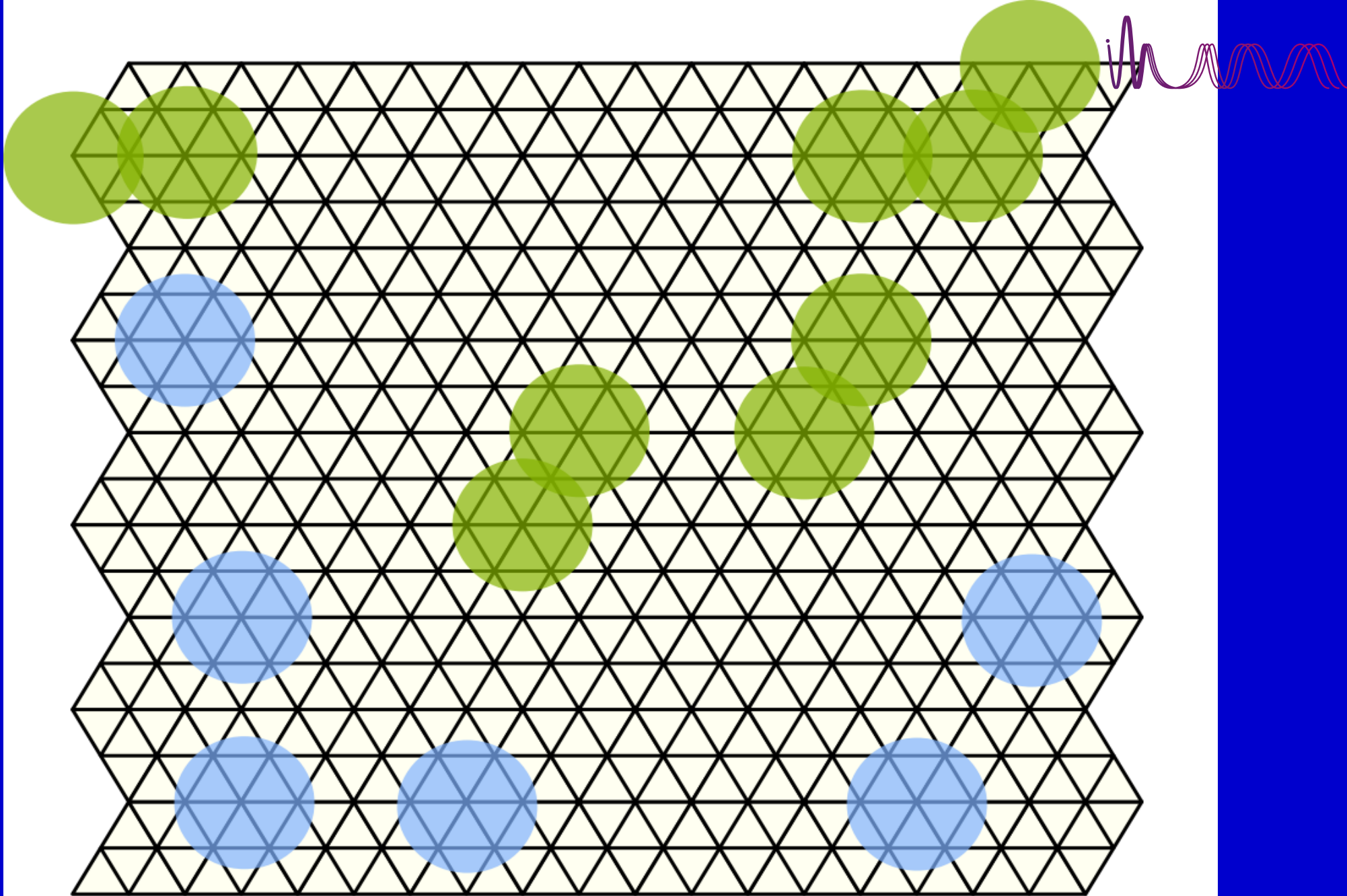


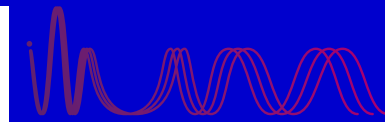
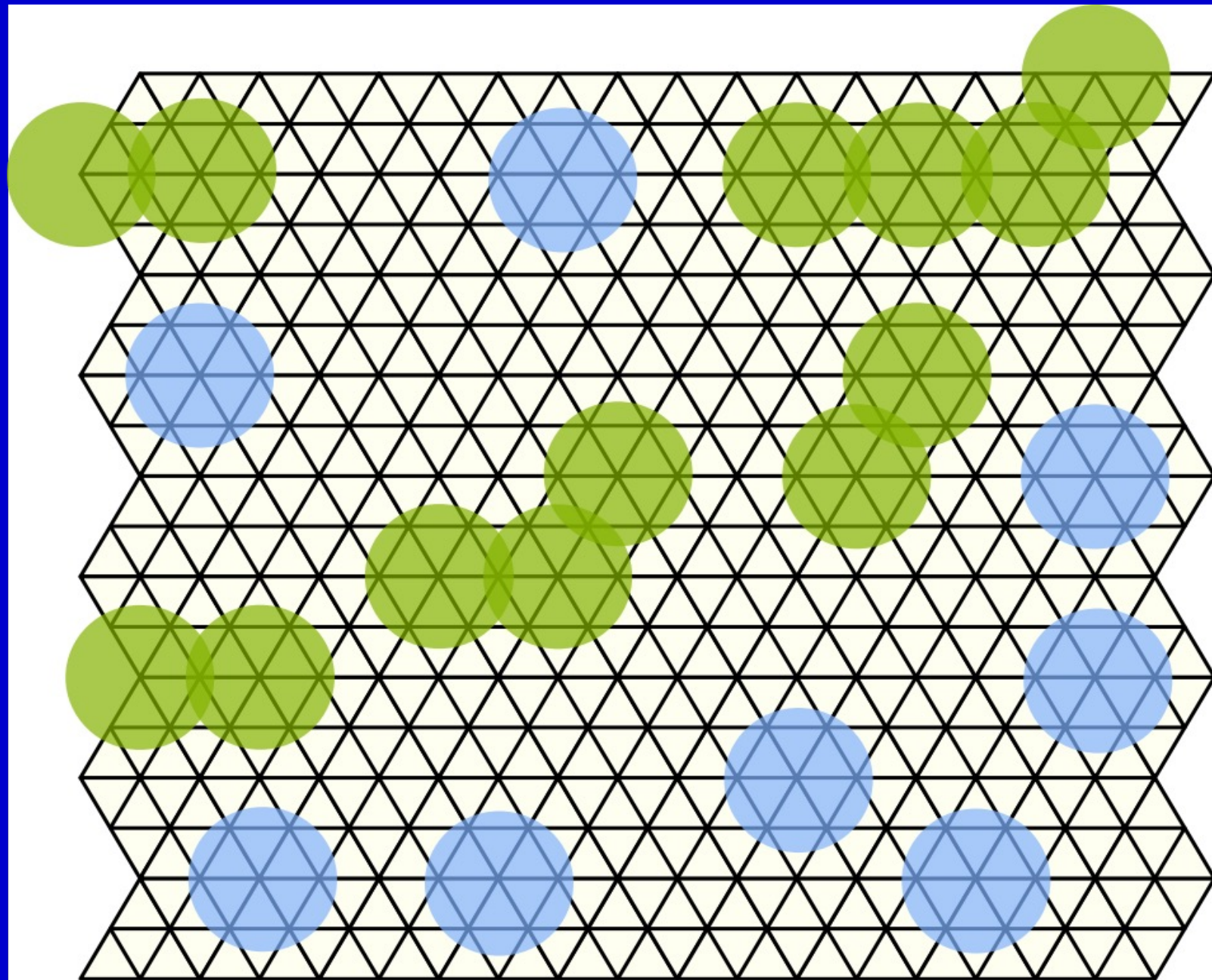
>Mathematically it can be found a **threshold of rigid disk concentration** where a random distribution guarantee a percolation in hexagonal lattices.

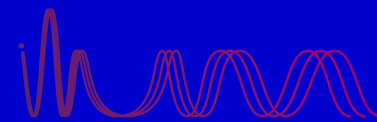
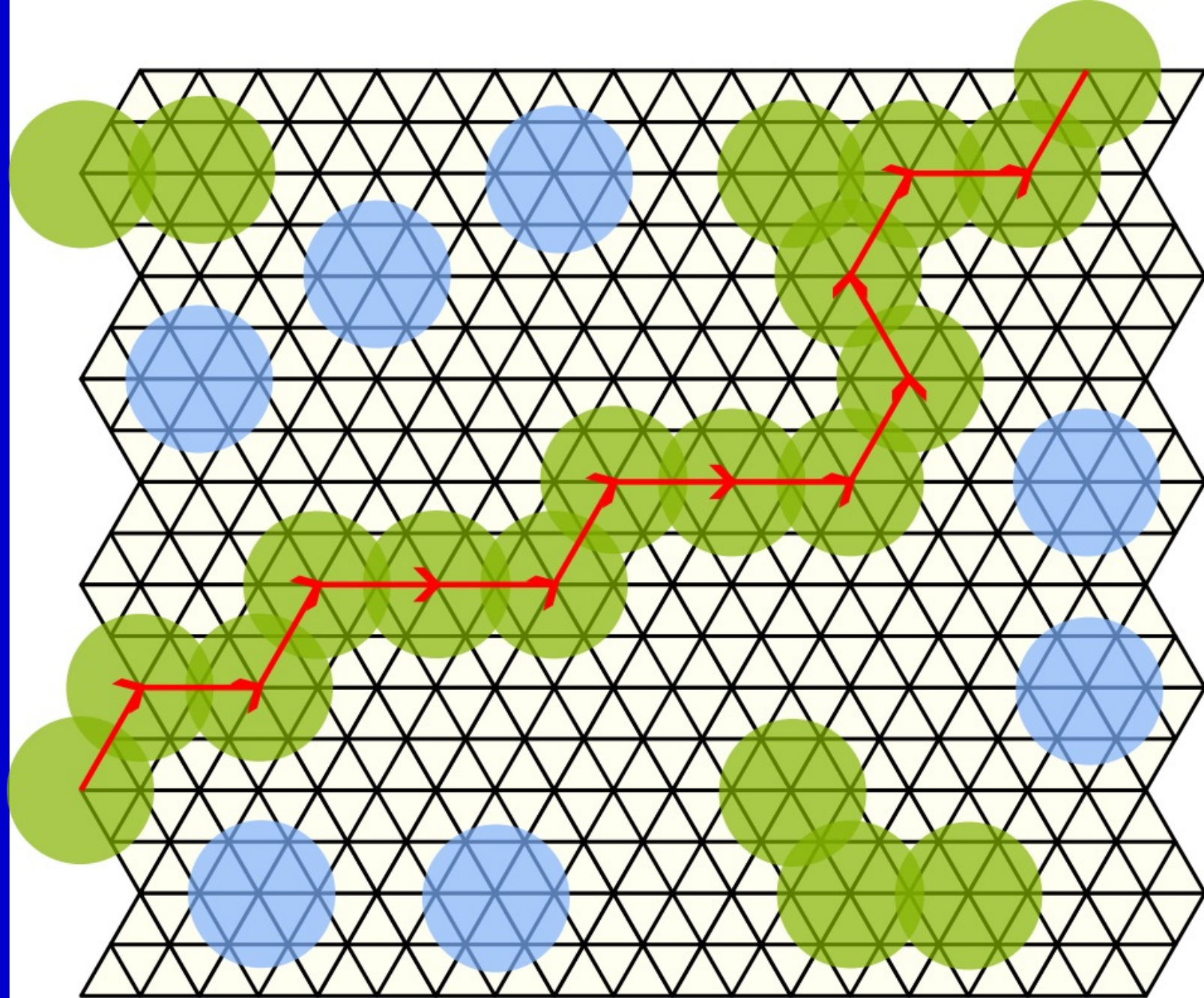
$$\phi_c = 1 - e^{-n_c} = 0.69$$

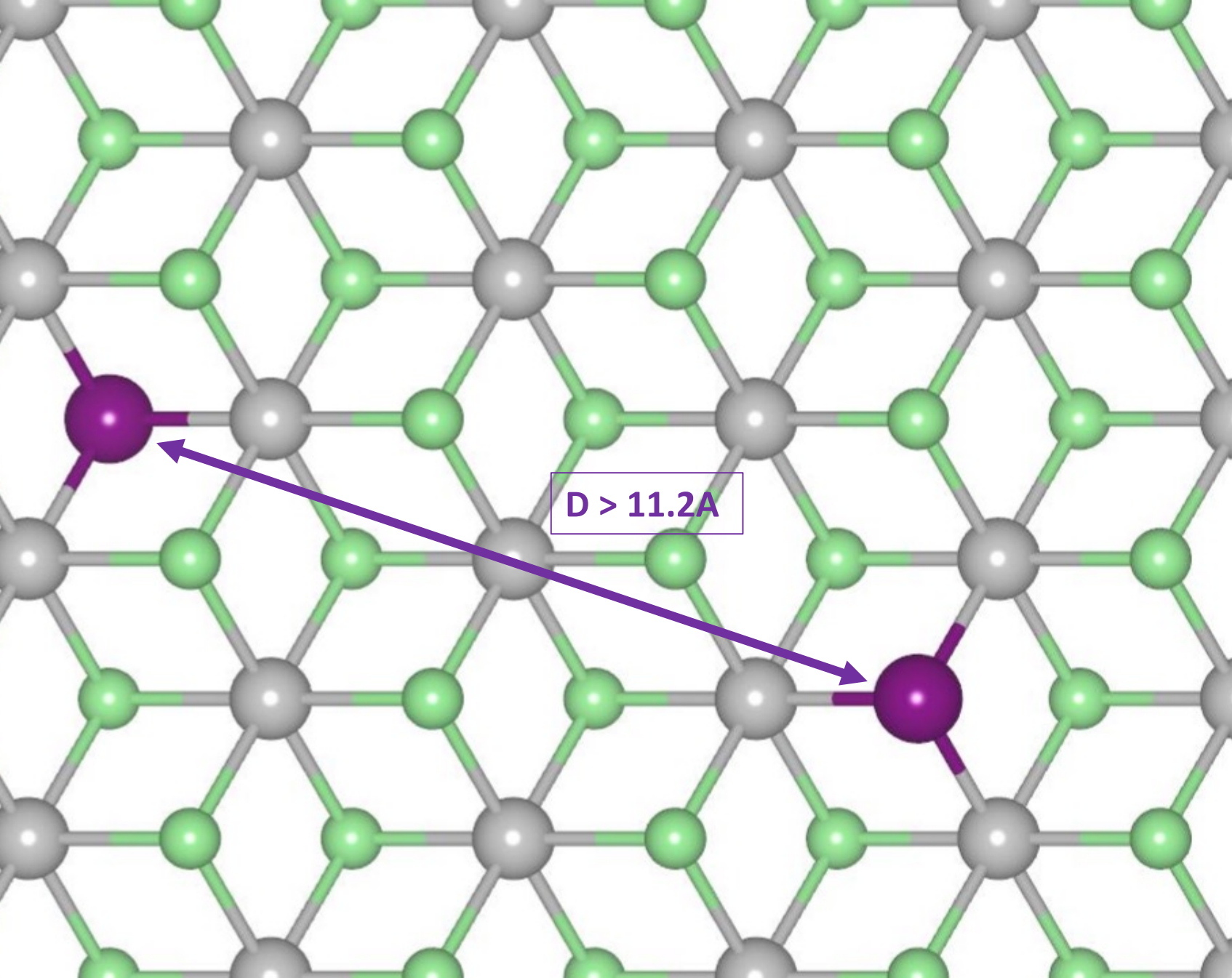
Using the disks-diameters 11A aWe stimated limit concentration..











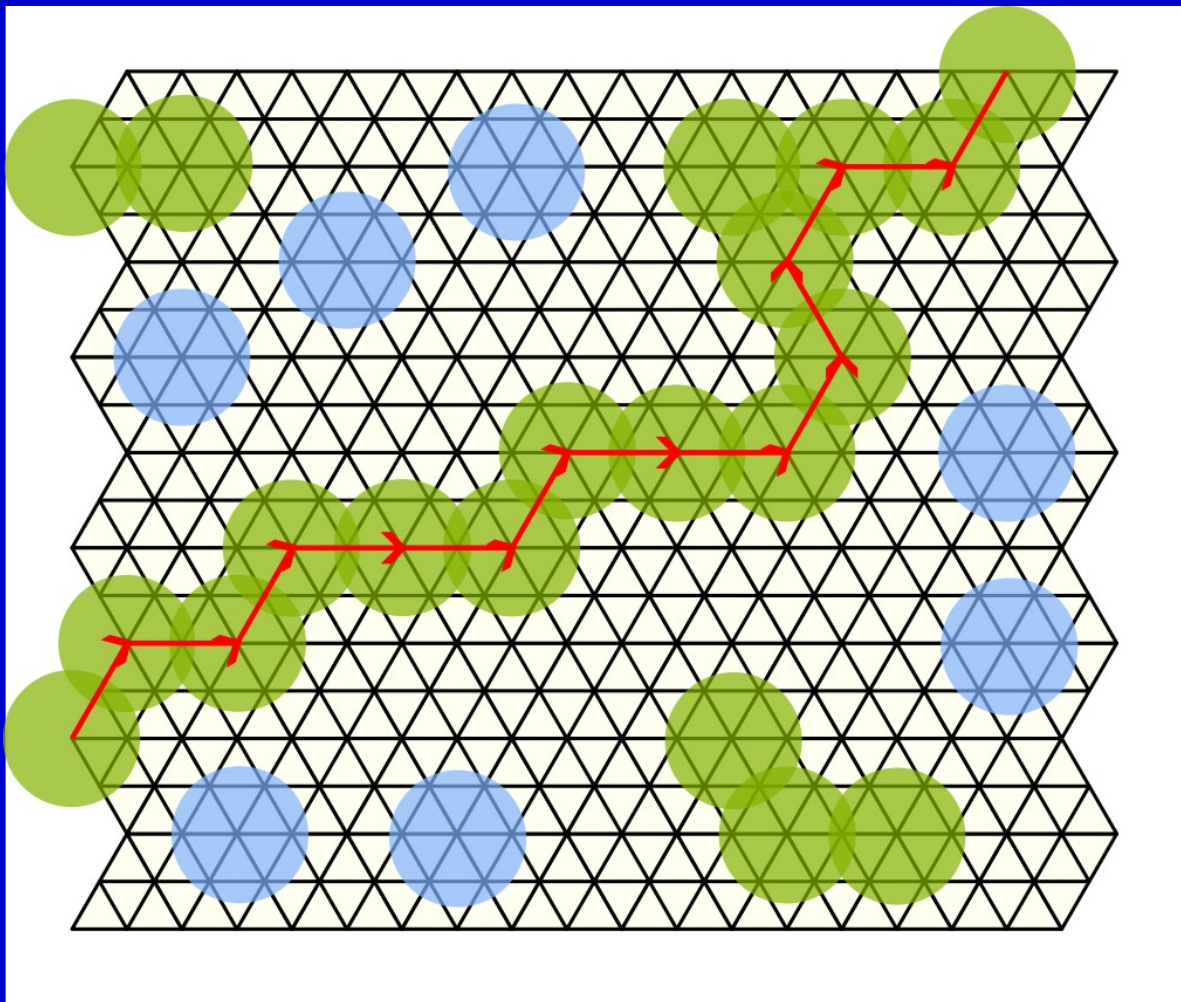


>Mathematically it can be found a threshold of Hg concentration where a random distribution guarantee a percolation of the **electrons hopping the Hg wave functions** (i.e. a non localization limit)

$$\phi_c = 1 - e^{-n_c} = 0.69$$

$$n_c = A_I/A_{UC}$$

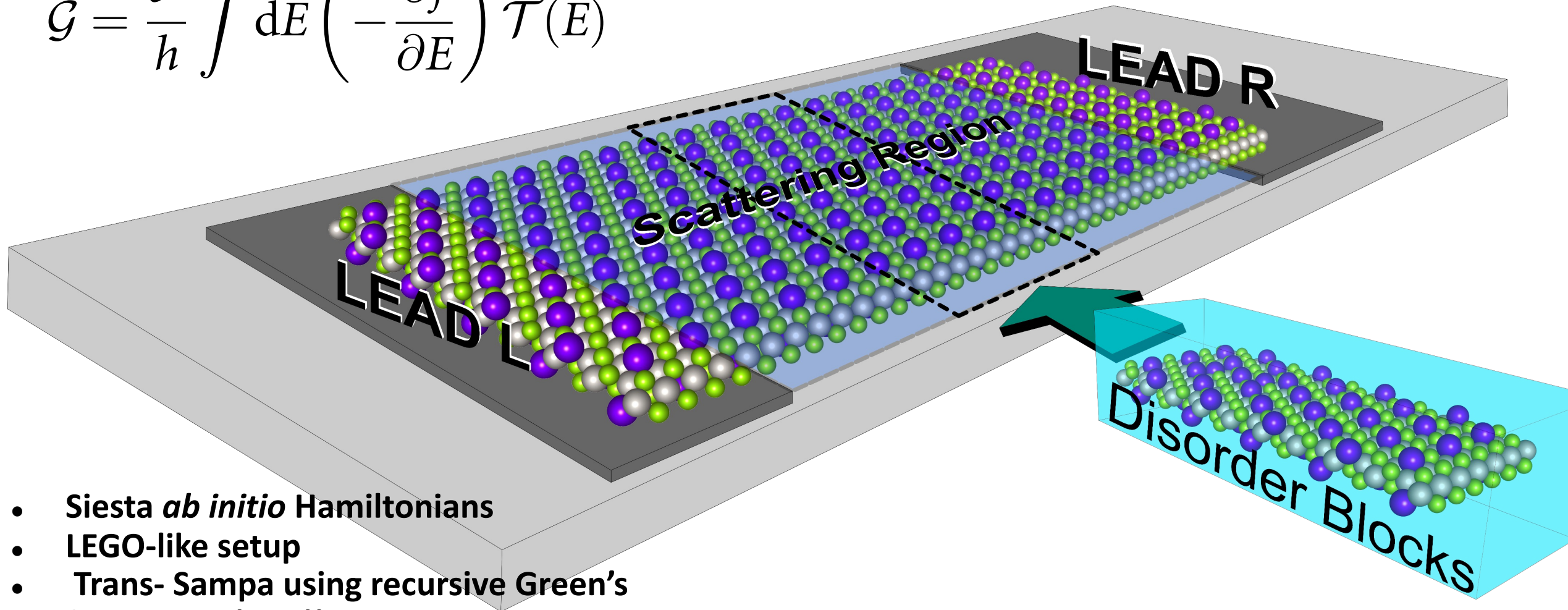
>This sets the necessary topological limit for random alloy at $x \sim 10\%$



Linear conductance
Landauer-Buttiker formula

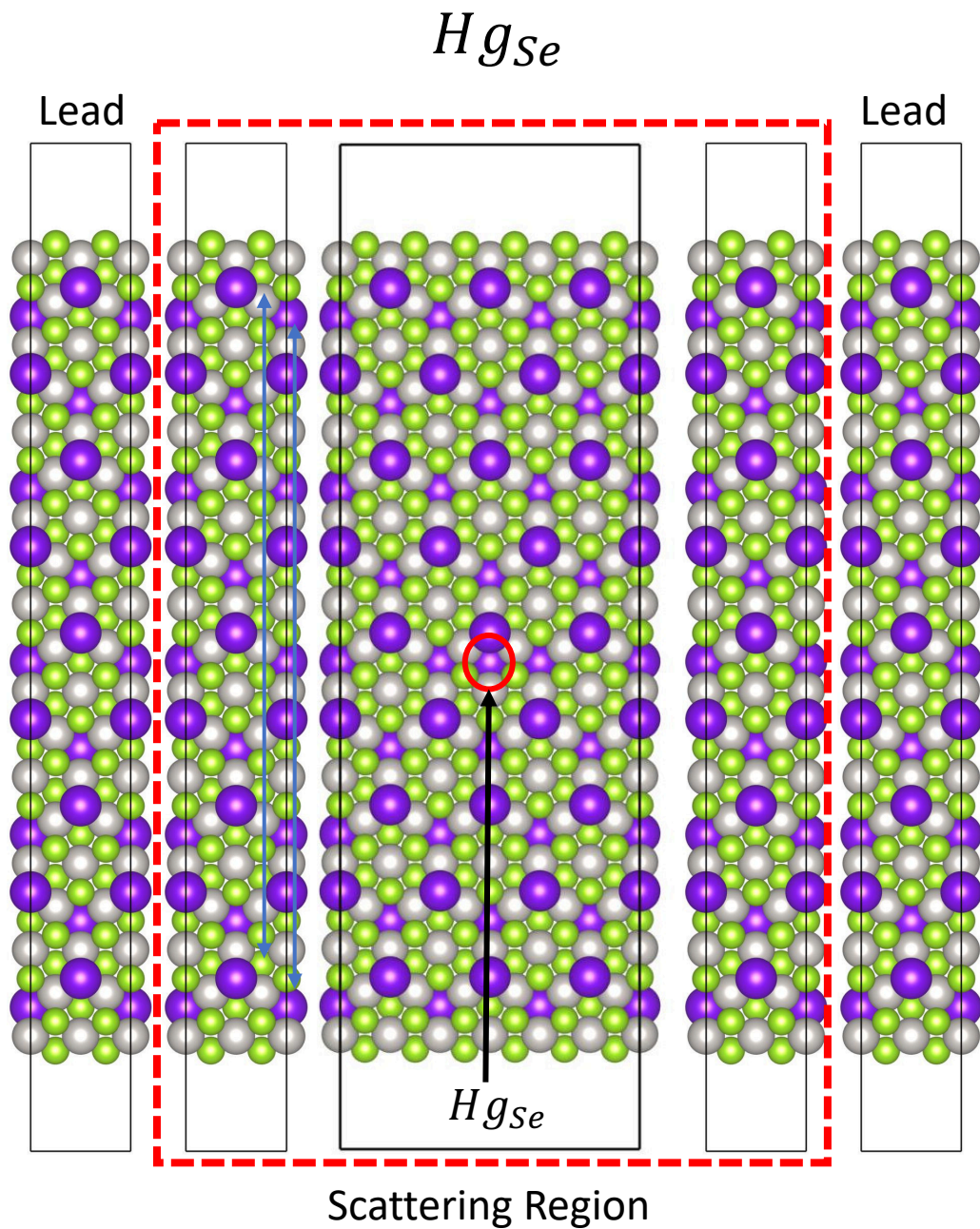


$$\mathcal{G} = \frac{e^2}{h} \int dE \left(-\frac{\partial f}{\partial E} \right) \mathcal{T}(E)$$

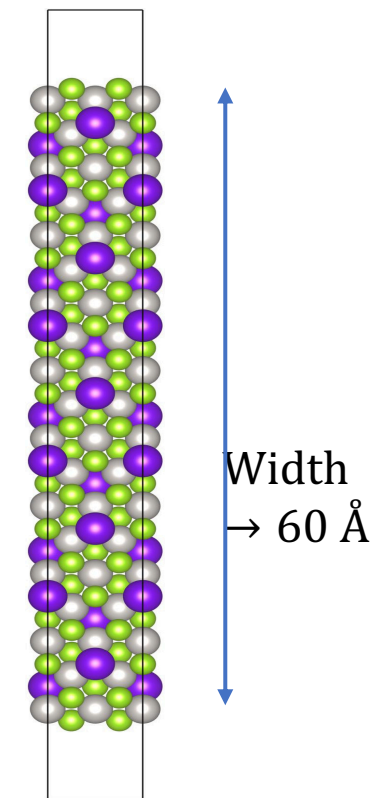
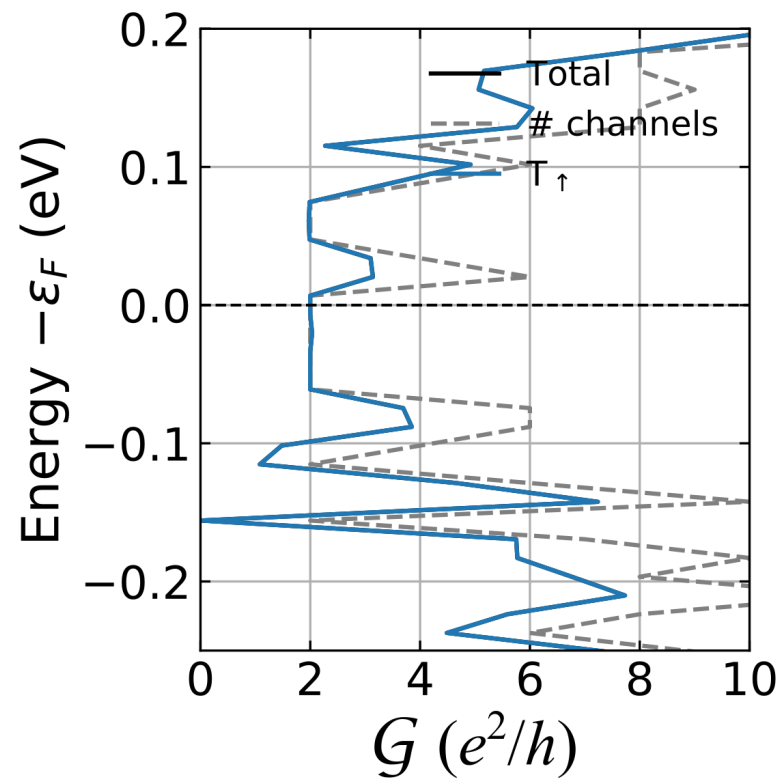


- Siesta *ab initio* Hamiltonians
- LEGO-like setup
- Trans- Sampa using recursive Green's functions +(SOC))

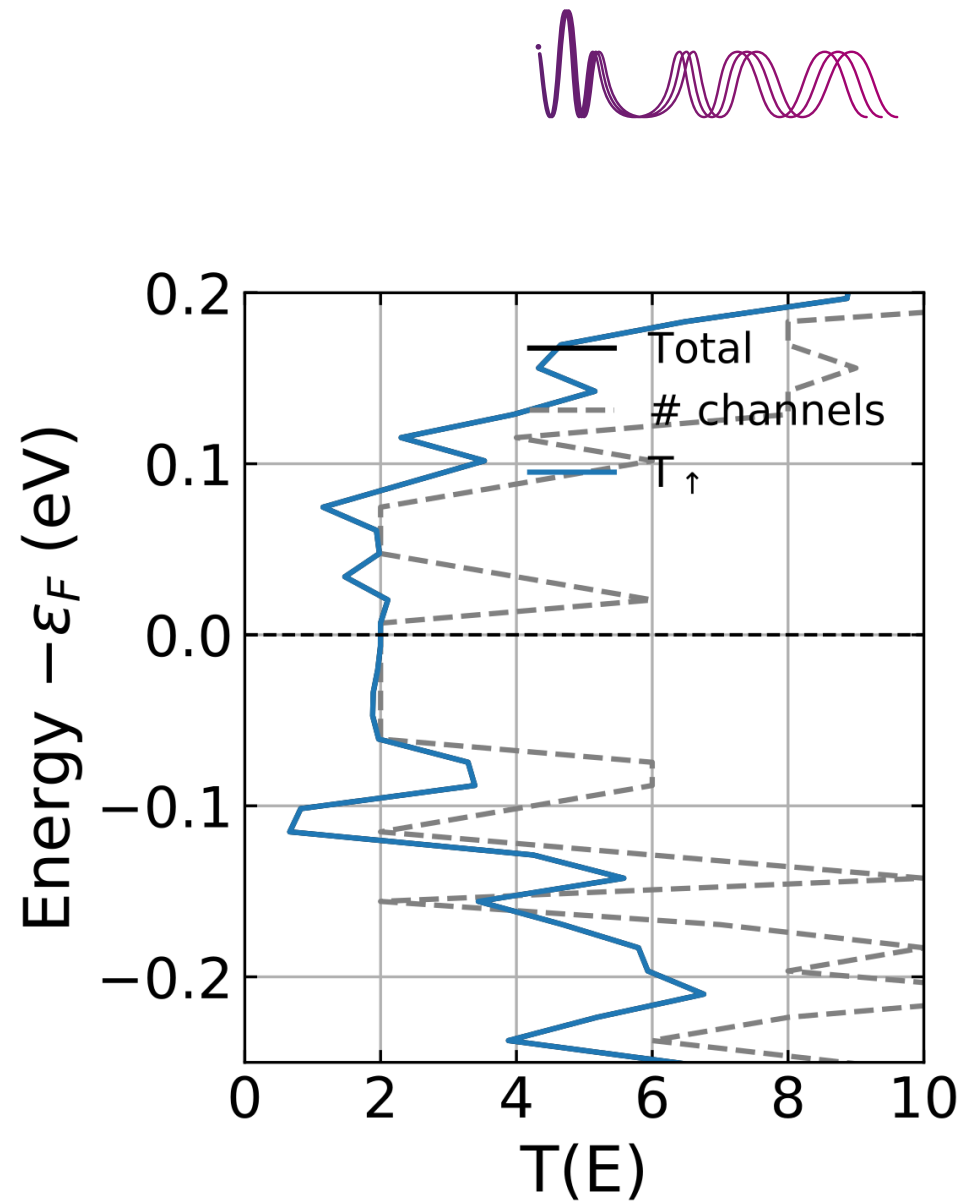
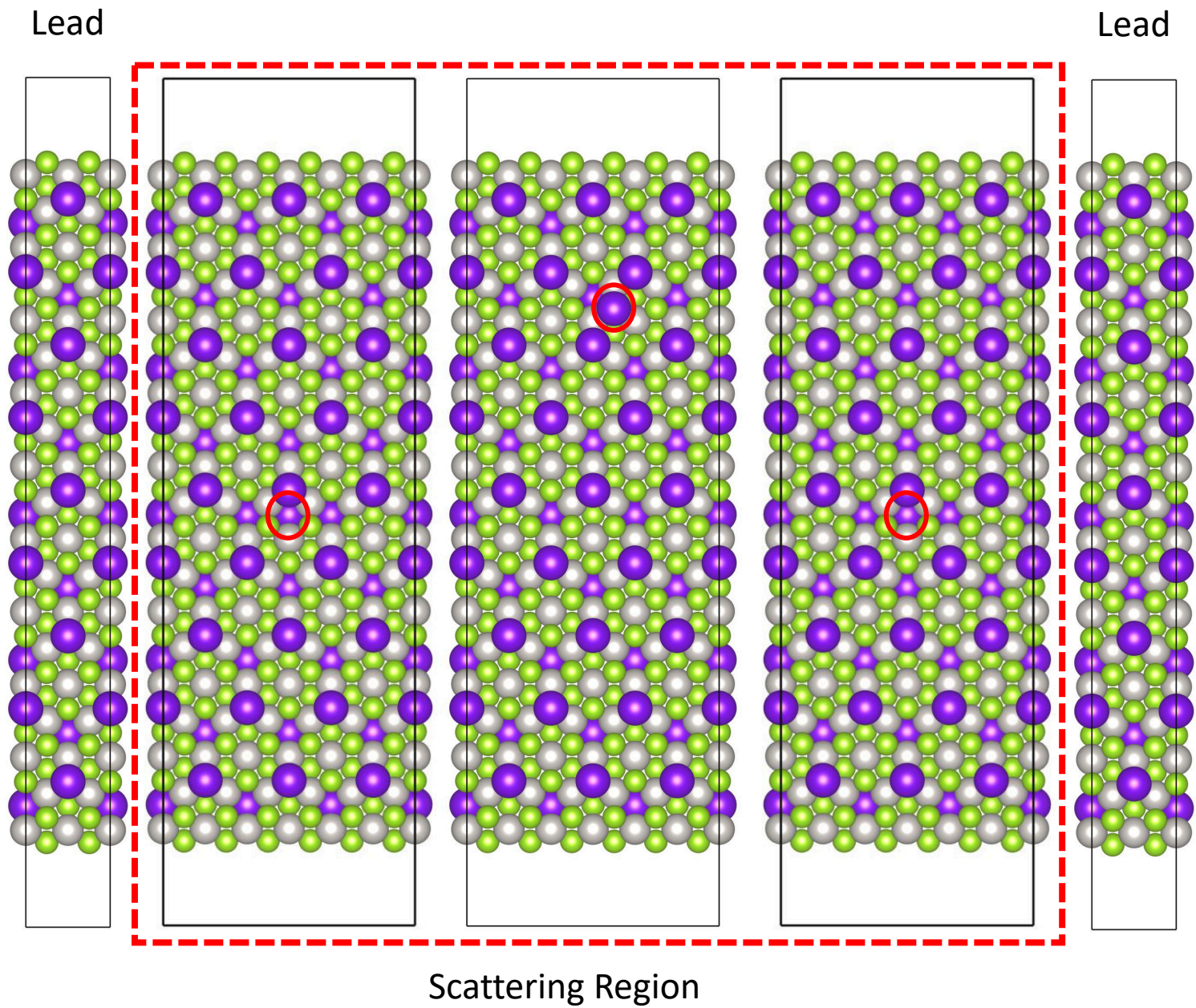
Random Substitutional Defect - Stoichiometry break



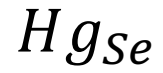
$Pt_2HgSe_3 / HgSe$



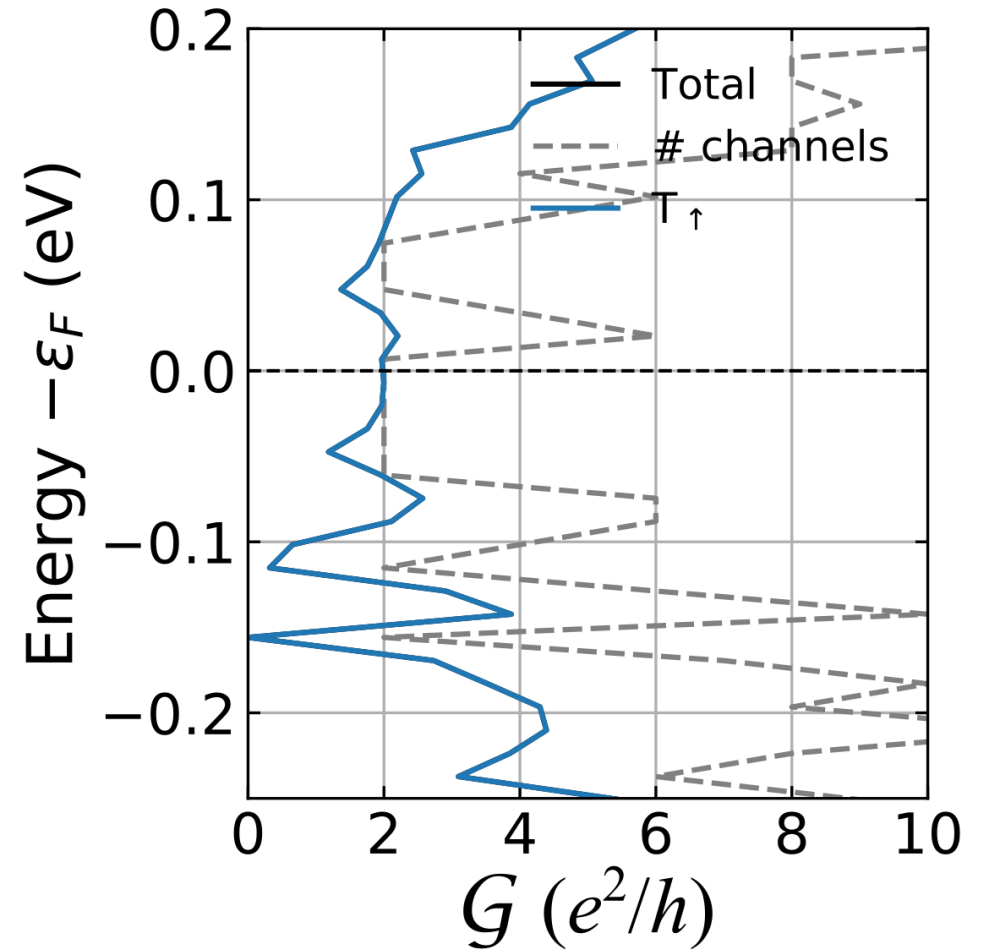
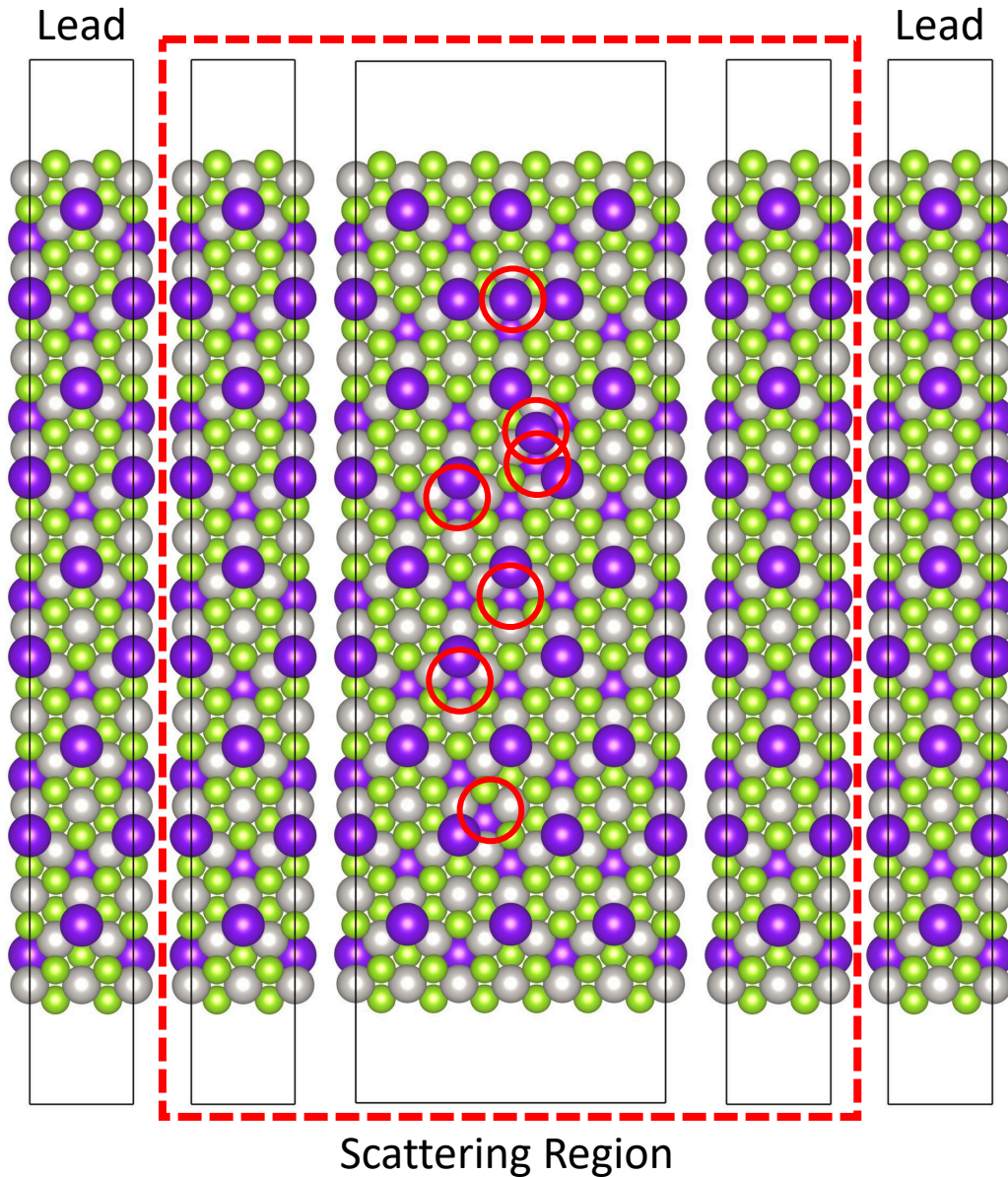
	Lead	Scattering
atoms	114	342



Random Substitutional Defect - Stoichiometry break



Width $\rightarrow 60 \text{ \AA}$



- By Increasing the ribbon width, one can recover some of the transport channels close to Fermi level
- Less influence from the edge states

Conclusion

***Based on ab initio calculations, we have studied the energetic stability and trivial > non-trivial topological phase transition in single-layer PtSe₂ mediated by substitutional Hg_{Se} atoms, Pt(Hg_xSe_{1-x})₂ alloys.**

**** We found an energetic preference for a random distribution of Hg with x= 25% (jacutingaite's stoichiometry), with respect to the PtSe₂ host ruled by the configurational entropy, for KT> 15meV and Random alloys with x=50%, PtHgSe , become more stable for KT>32meV**

***** The QSH phase against the random distribution of Hg_{Se} substitutional atoms has been verified for alloy concentration between 25% and 75%**

******. With percolation model we estimated a threshold concentration of about 9% for topological non-trivial>trivial transition in Pt(Hg_xSe_{1-x})₂ random alloys**

Collaborators



Bruno Focassio
(PhD-fapesp)



Rafael Freire
(Pos-Doc/fapesp)



Felipe David Lima
(CNPEM/ILUM)



Roberto Hiroki Miwa
(UFU-MG)

Thank you !

Financial



CNPEM
Brazilian Center for Research
in Energy and Materials

Vacancies centers is the simplest defect but can provide drive exotic effects as charge density waves in indium (In) nanowires,ferromagnetism on transition metal dichalcogenides(TMD) ,transitions Metal-Insulators in GeSbTe(IV-VI) , negative U in Si....etc

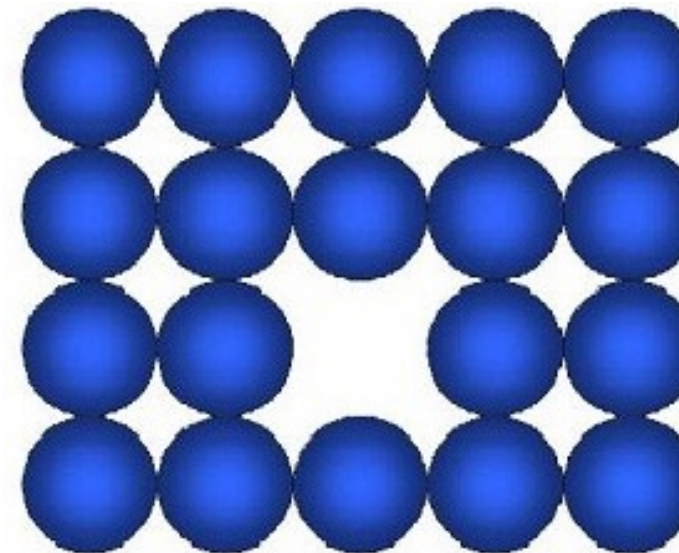
We investigate the trivial 2D semiconductor
PtSe₂ **Z₂=0**

NANO LETTERS

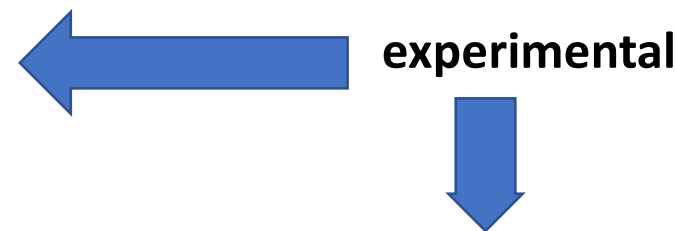
pubs.acs.org/NanoLett

Atomic-Level Dynamics of Point Vacancies and the Induced Stretched Defects in 2D Monolayer PtSe₂

Jun Chen,¹ Jiang Zhou,¹ Wenshuo Xu, Yi Wen, Yuanyue Liu,^{*} and Jamie H. Warner^{*}

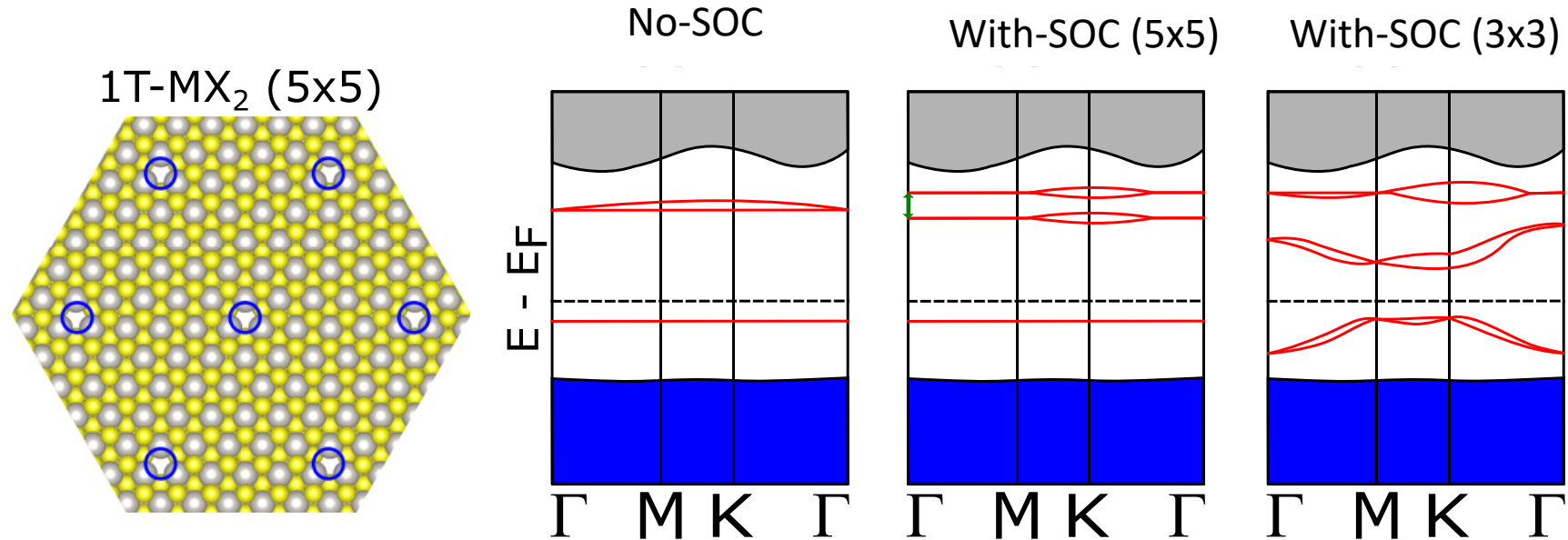


Letter



Se vacancy formation on PtSe₂ can controlled by electron radiation...recent advances on controlled Atomic positioning on surfaces by AFM/STM TIPS

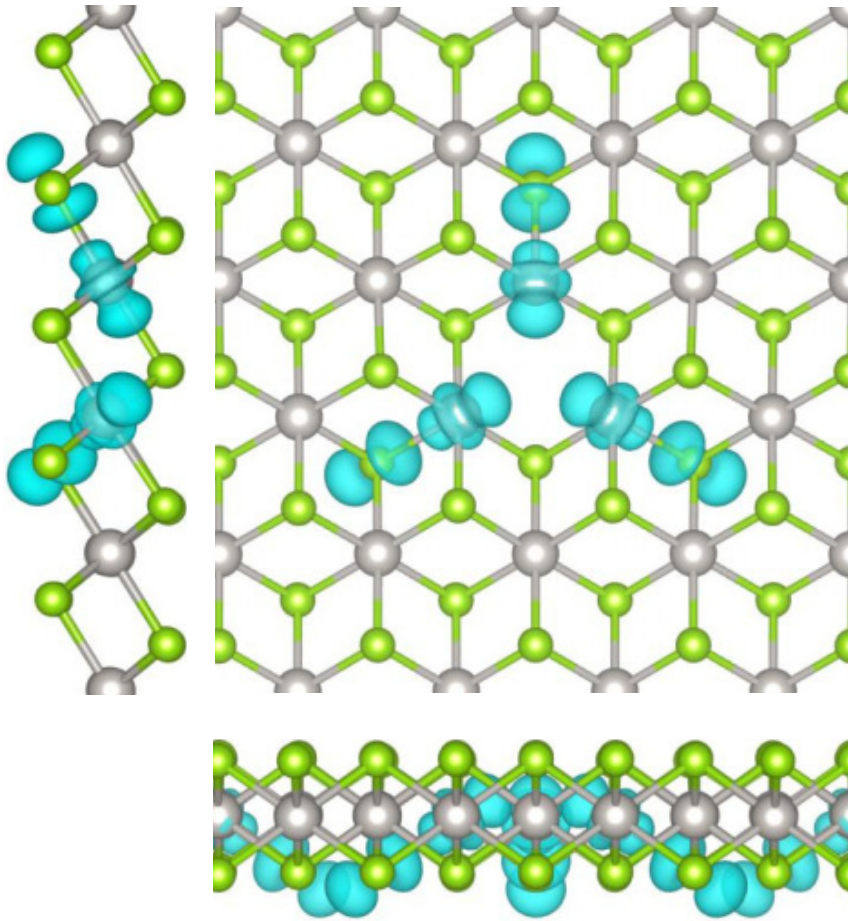
Chalcogens vacancies: universal schematic of band structure of each semiconducting phase, respectively, with and without spin-orbit corrections.



transition metal dichalcogenides.



1T-PtSe₂ (V_{Se})



Se vacancy introduces localized states in the host PtSe₂ bandgap

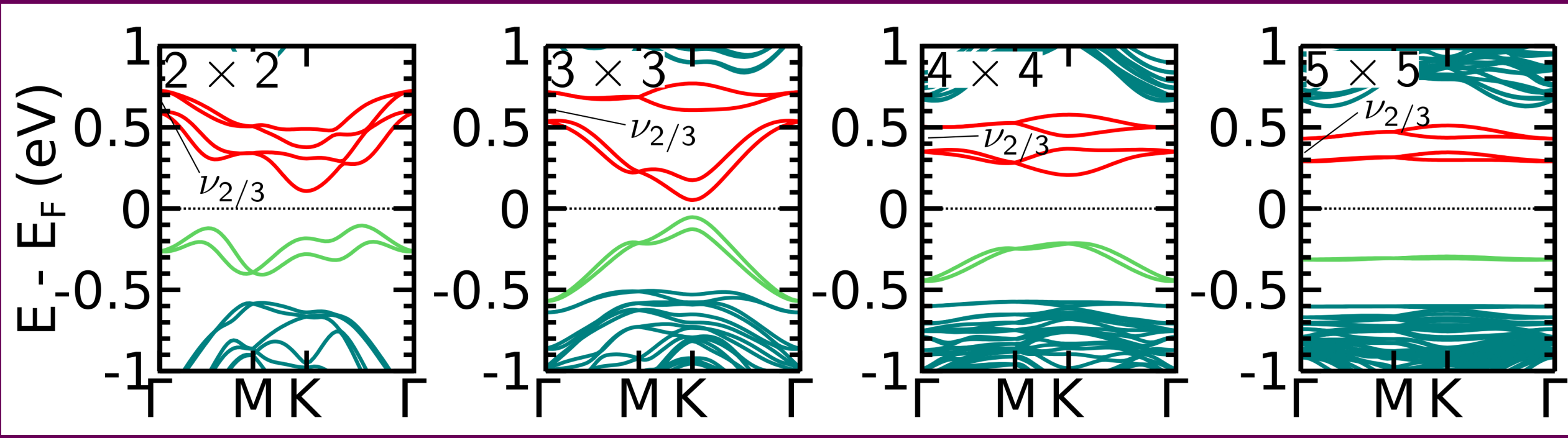
Three lone pairs arise in the Pt atoms neighboring the vacancy.

Increasing the vacancy density, those states can interact forming energy bands.

Orbitals with major contribution from Pt dxz/dyz with its interactions mediated by the host Se p orbitals

PtSe₂ is a trivial semiconductor with an energy gap of 1.2 eV.





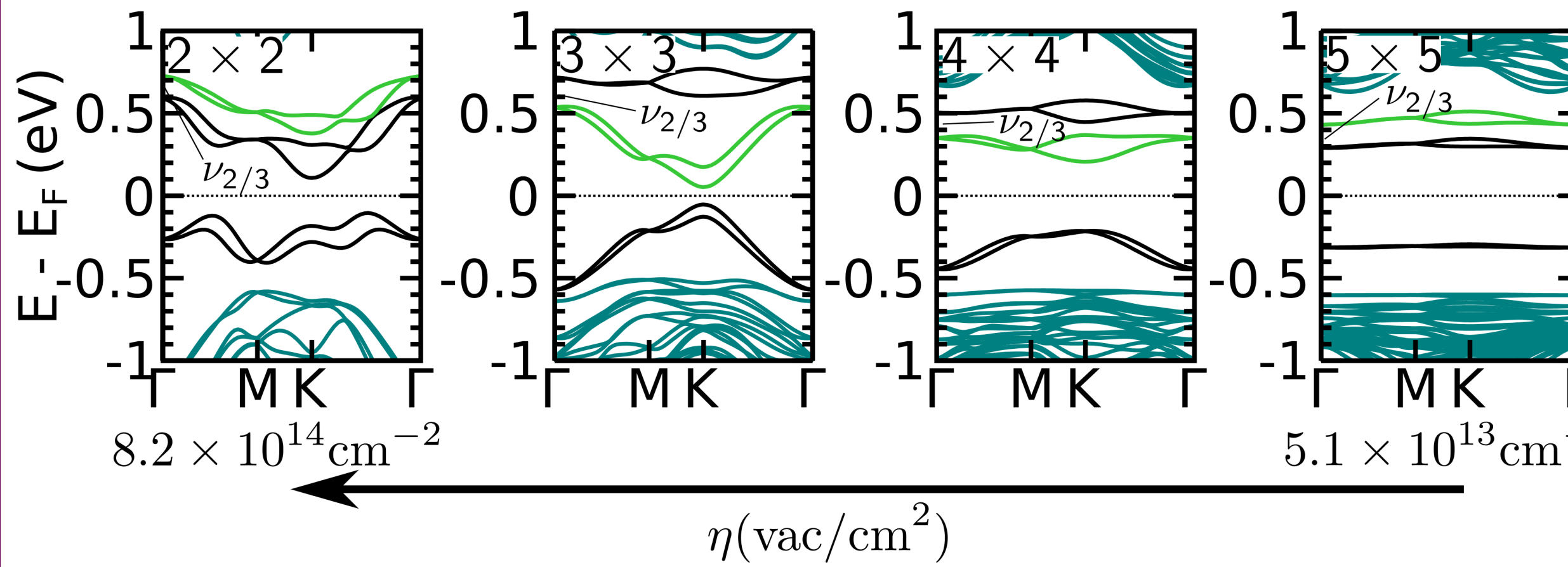


trivial

$Z_2=1$
Non-trivial

$Z_2=1$
Non-trivial

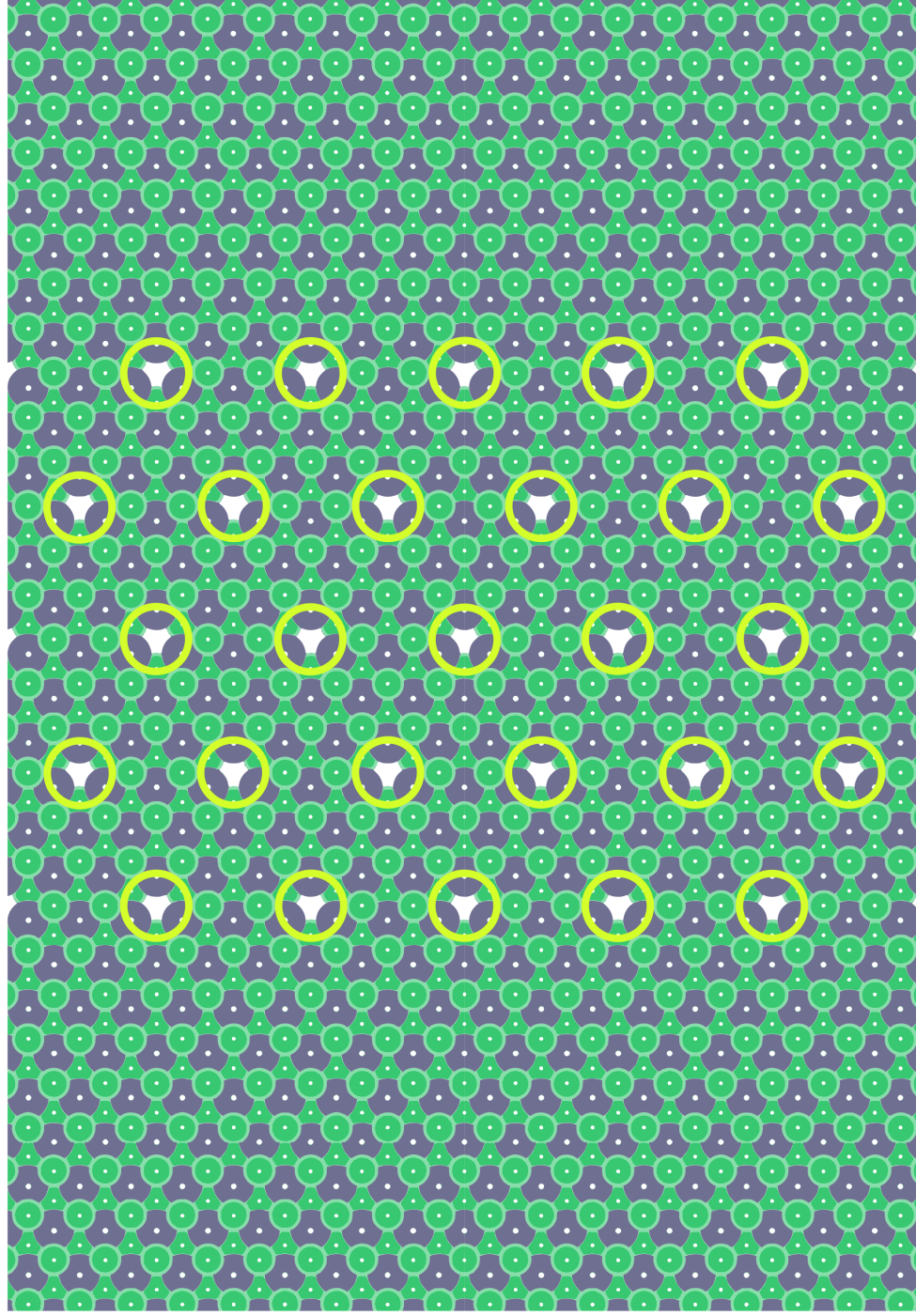
trivial

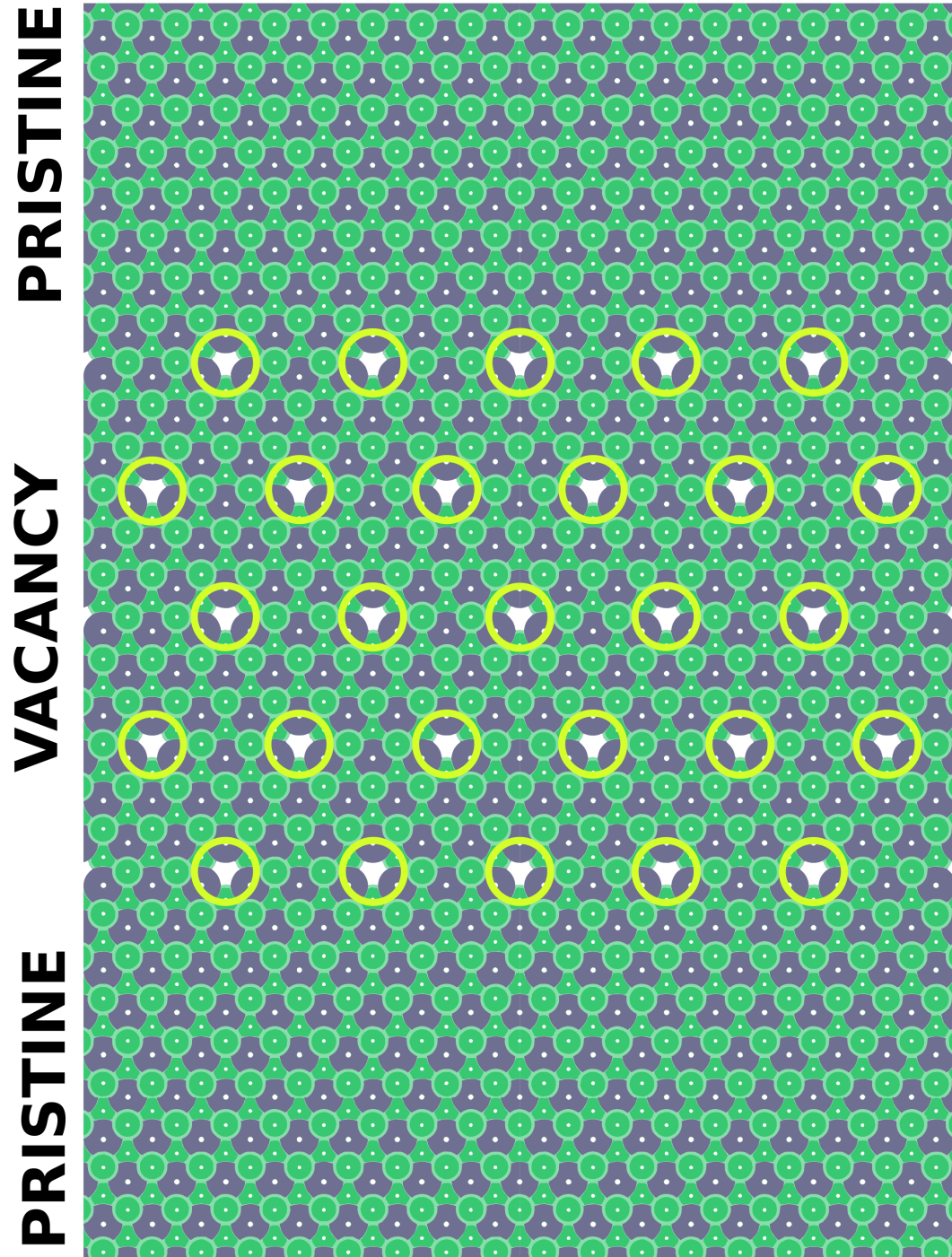


PRISTINE

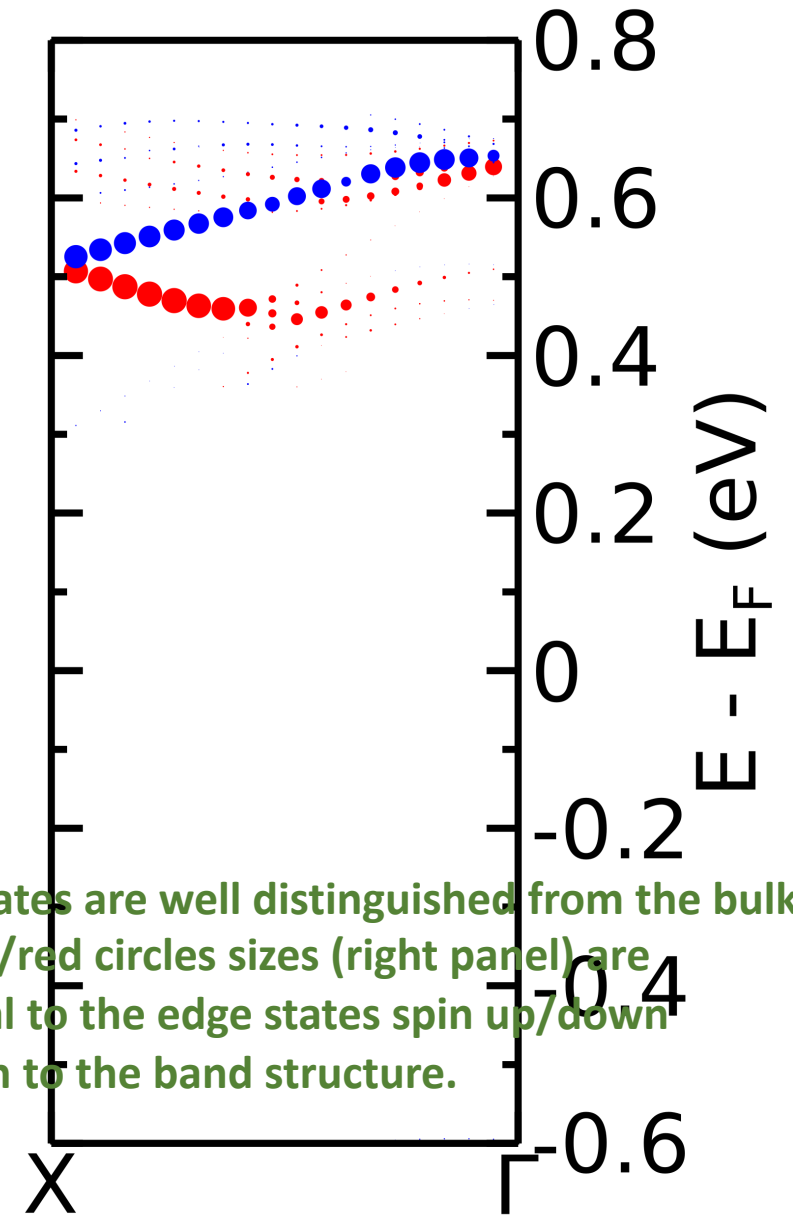

VACANCY

PRISTINE

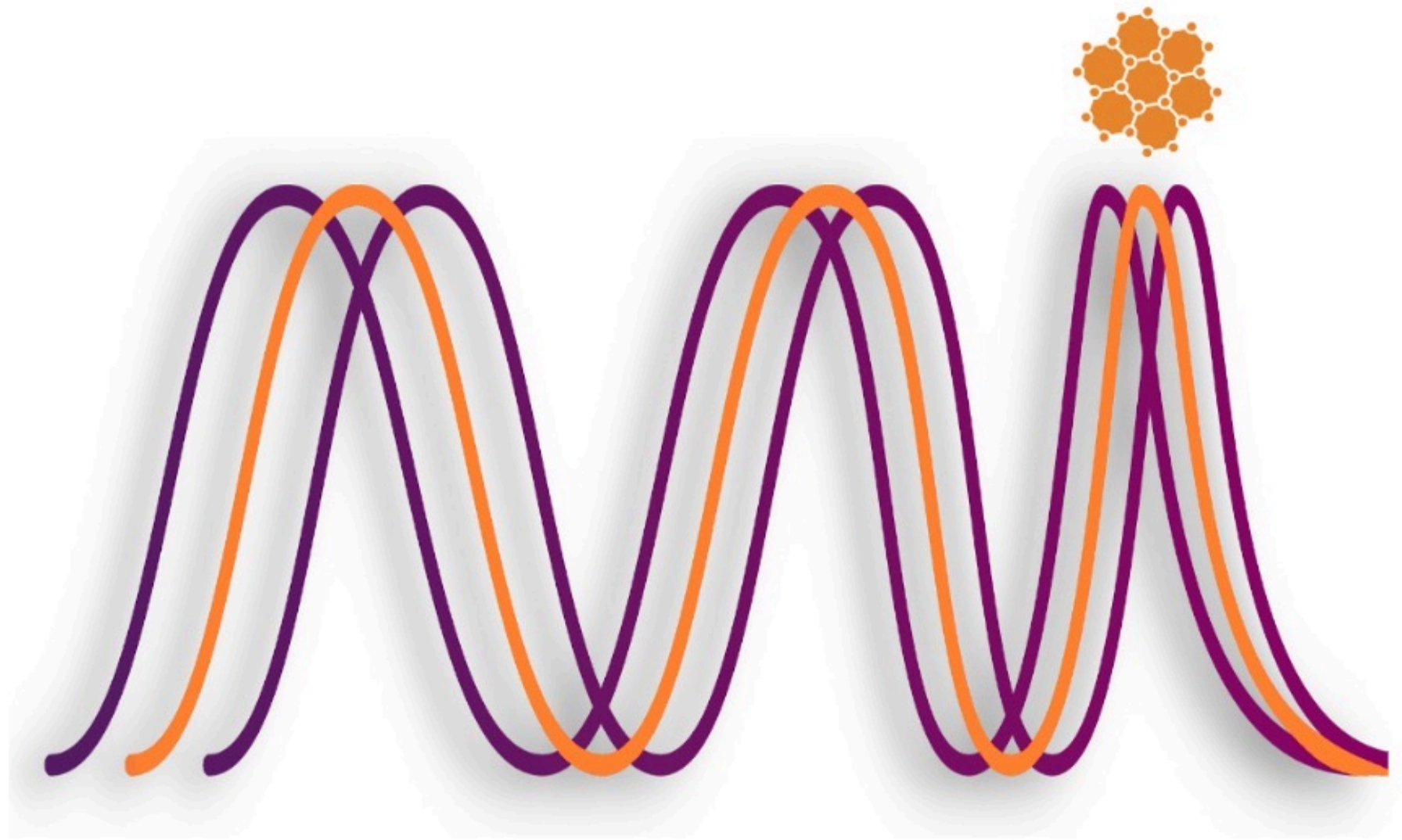




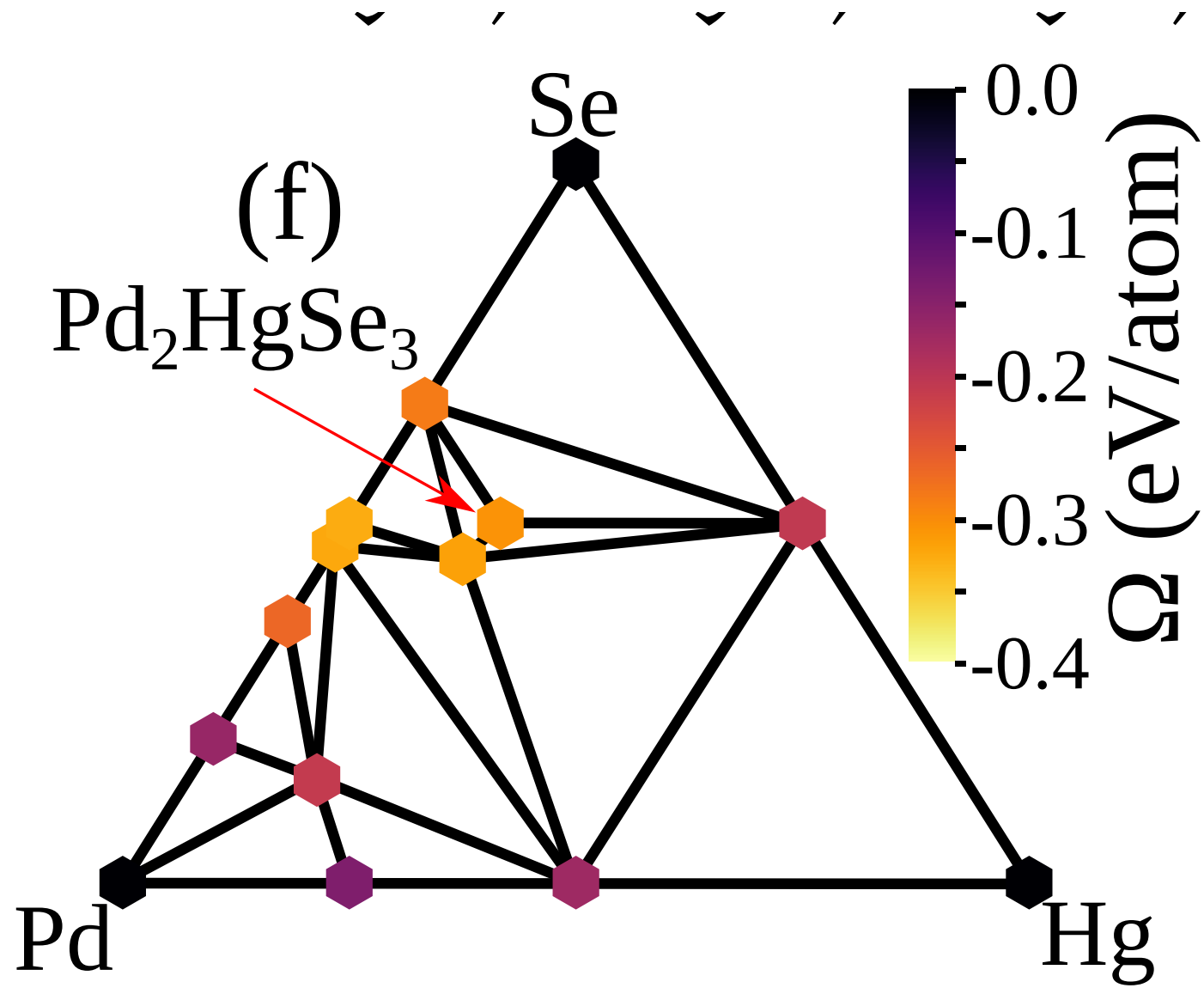
edge
states








The edge states are well distinguished from the bulk bands. Blue/red circles sizes (right panel) are proportional to the edge states spin up/down contribution to the band structure.



I N C T **M**aterials
Informatics



Amorphous Bi₂Se₃ structural, electronic, and topological nature from first principles

 Bruno Focassio ^{1,2,*} Gabriel R. Schleder ^{1,2,3} Felipe Crasto de Lima ^{2,4} Caio Lewenkopf ⁵ and Adalberto Fazzio ^{2,1,4,†}
¹Center for Natural and Human Sciences, Federal University of ABC (UFABC), 09210-580 Santo André, São Paulo, Brazil

²Brazilian Nanotechnology National Laboratory (LNNano), CNPEM, 13083-970 Campinas, São Paulo, Brazil

spin Bott index is defined as

$$P_{\pm} = \sum_n^{N_{\text{occ}}/2} |\phi_n^{\pm}\rangle \langle \phi_n^{\pm}|, \quad (5)$$

$$B_s = \frac{1}{2}(B_+ - B_-),$$

where $|\phi_n^{\pm}\rangle$ are the eigenstates of P_z with eigenvalues S_{\pm} . In the case of 2D systems, for each spin sector one then constructs the projected position operators

$$U_{\pm} = P_{\pm} e^{i2\pi X} P_{\pm} + (I - P_{\pm}), \quad (6)$$

$$V_{\pm} = P_{\pm} e^{i2\pi Y} P_{\pm} + (I - P_{\pm}), \quad (7)$$

where X and Y are diagonal matrices with the x and y components of the spatial coordinate of each orbital site rescaled

$$B_{\pm} = \frac{1}{2\pi} \text{Im}\{\text{Tr}[\log(V_{\pm} U_{\pm} V_{\pm}^{\dagger} U_{\pm}^{\dagger})]\}.$$

For a non-periodicity of the random alloy, we have computed a real space invariant : Spin Bott-index, which is equivalent to the spin-Chern number.

been explained in the literature [18,19,24,30,31]. First, one constructs the projector operator of the occupied states below

Given the method of calculating the Bott index, now we give a general construction of the spin Bott index. One begins by introducing a projected spin operator

$$P_z = P\hat{s}_zP, \quad (5)$$

where $\hat{s}_z = \frac{\hbar}{2}\sigma_z$ is the spin operator (σ_z is the Pauli matrix). For a spin-conserving model, \hat{s}_z commutes with the Hamiltonian H and P_z , the Hamiltonian as well as eigenvectors can be divided into spin-up and spin-down sectors. Thus, the eigenvalues of P_z consist of just two nonzero values $\pm\frac{\hbar}{2}$. For systems without spin conservation (for example, the Kane-Mele model with nonzero Rashba terms which will be discussed later), the \hat{s}_z and H no longer commute. The spectrum of P_z spreads toward zero. However, as long as the spin-mixing term is not too strong, the eigenvalues of P_z remain two isolated groups which are separated by zero. Since the rank of P_z is N_{occ} , the number of positive eigenvalues equals to the number of negative eigenvalues, which is one half of N_{occ} . The corresponding eigenvalue problem can be denoted as

$$P_z|\pm\phi_i\rangle = S_{\pm}|\pm\phi_i\rangle. \quad (6)$$

In this way, one can construct new projector operators

$$P_{\pm} = \sum_i^{N_{\text{occ}}/2} |\pm\phi_i\rangle\langle\pm\phi_i|, \quad (7)$$

which satisfy $P = P_+ \oplus P_-$, and projected position operators

$$U_{\pm} = P_{\pm}e^{i2\pi X}P_{\pm} + (I - P_{\pm}), \quad (8)$$

$$V_{\pm} = P_{\pm}e^{i2\pi Y}P_{\pm} + (I - P_{\pm}), \quad (9)$$

The Bott indices for two spin sectors are now given by [27–29,32]

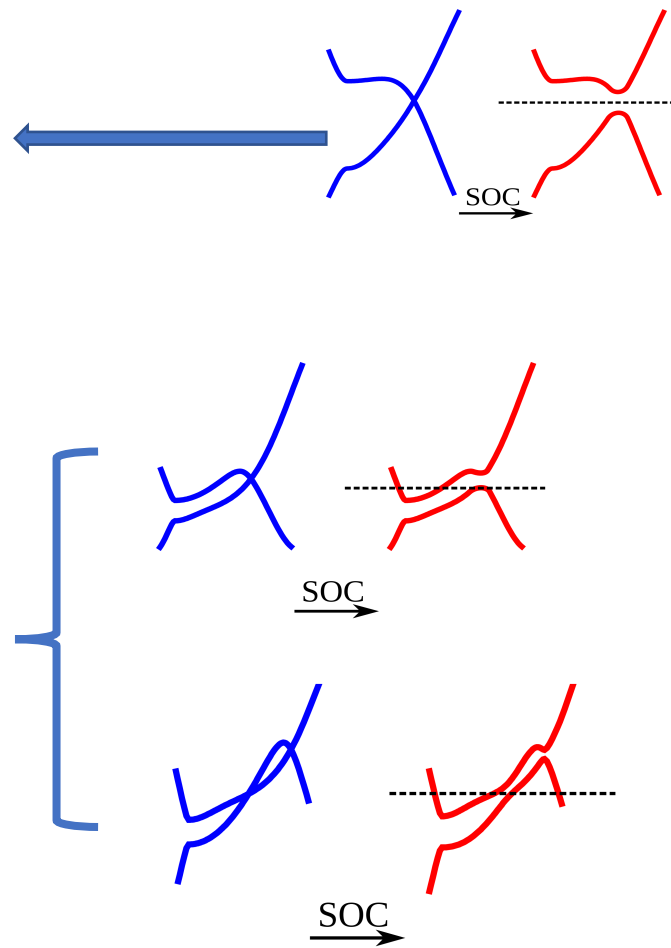
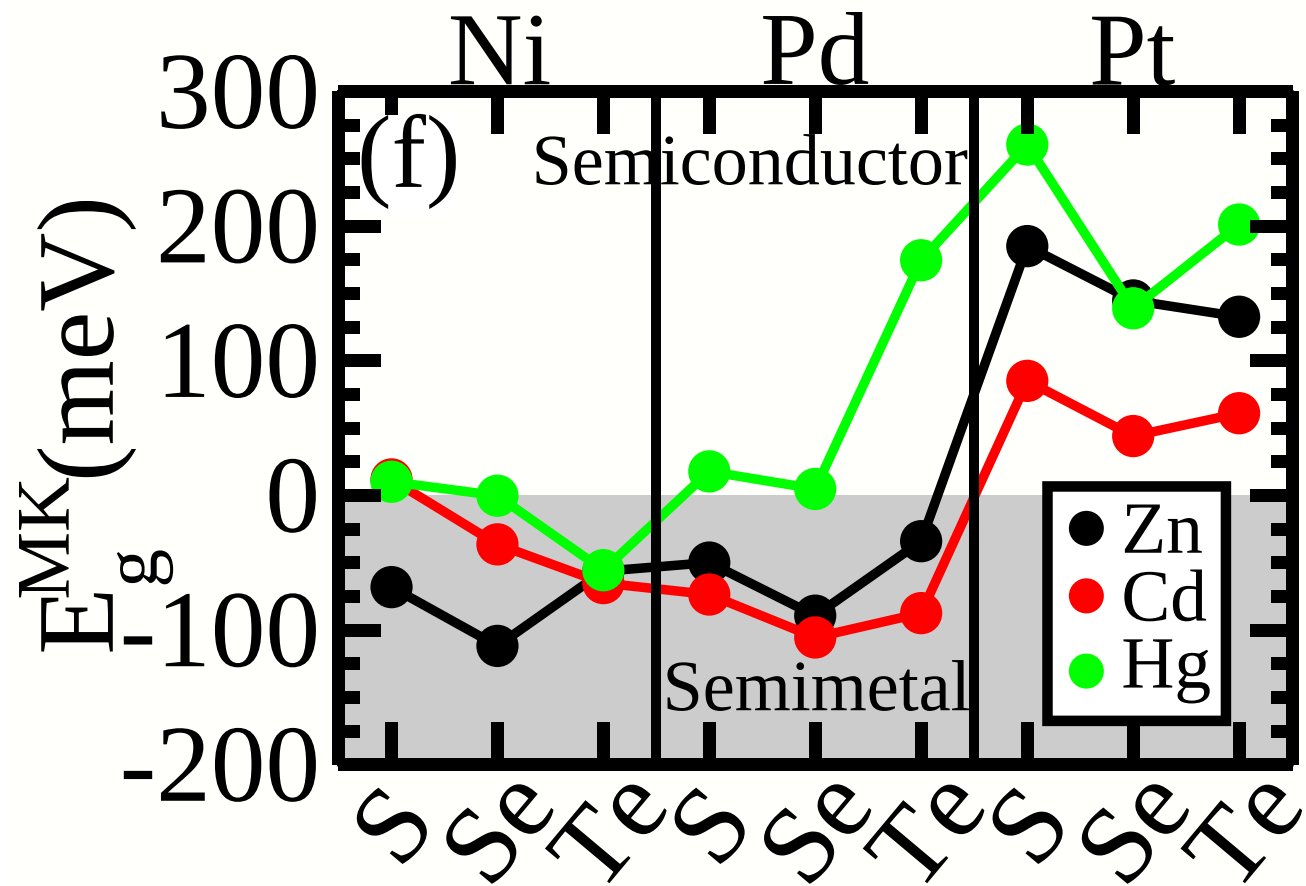
$$B_{\pm} = \frac{1}{2\pi} \text{Im}\{\text{tr}[\log(\tilde{V}_{\pm}\tilde{U}_{\pm}\tilde{V}_{\pm}^{\dagger}\tilde{U}_{\pm}^{\dagger})]\}. \quad (10)$$

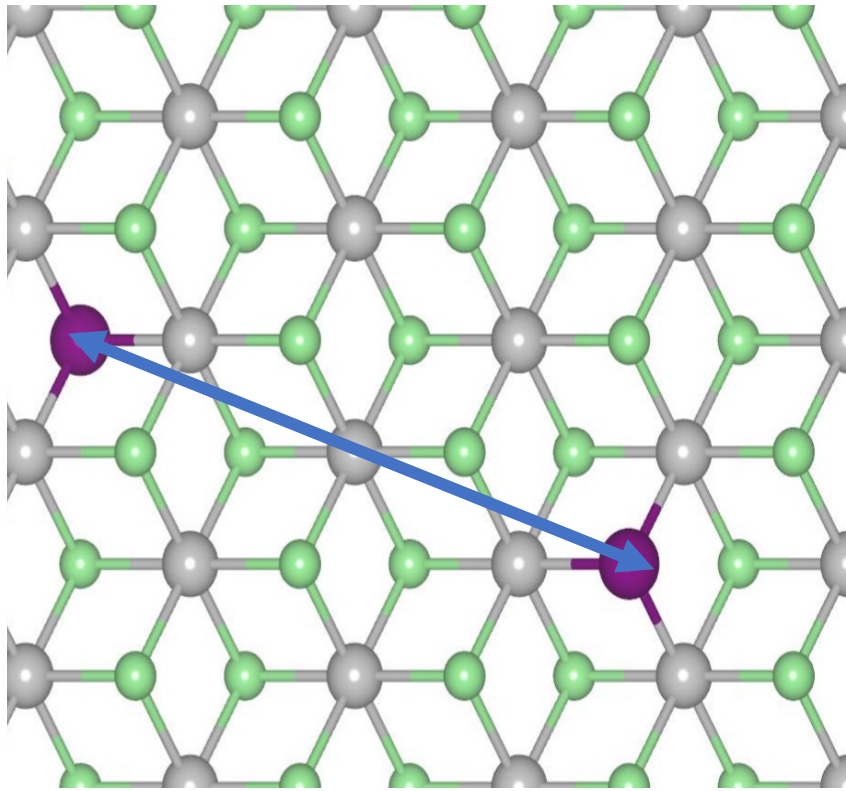
Finally, we define the spin Bott index as the half-difference between the Bott indices for the two spin sectors

$$B_s = \frac{1}{2}(B_+ - B_-). \quad (11)$$

Similar to the spin Chern number [8–10,25,26] the spin Bott index is a well-defined topological invariant. The spin Bott index is also directly related to the \mathbb{Z}_2 topological invariant. Its robustness is due to the existence of two spectral gaps: the insulating gap of the Hamiltonian and the spectral gap of the projected spin operator P_z . As long as the two gaps persist, the computational formalism of the spin Bott index can be applied. The spin Bott index is applicable to quasiperiodic and nonperiodic systems, which provides especially a useful tool to determine the electronic topology of those systems without periodicity.

FIG. 1. (a) Topological phase transition in the Haldane model. The parameters are $t = -1$ and $t_2 = 0.15e^{-i\pi/3}$. (b) Topological phase transition in the Kane-Mele model. The parameters are $t = 1$, $\lambda_{SO} = 0.3$, and $\lambda_R = 0.25$. The Bott B (spin Bott B_s) index is consistent with the Chern number (\mathbb{Z}_2 invariant) except around the phase transition point. This is because we use a relatively small supercell to calculate the Bott index. The small divergence would disappear if a larger supercell is used in the calculation of (spin) Bott index. The calculated (spin) Bott index with SVD shows a better performance than the one without SVD.





>The Hg wavefunctions are interacting with each other up to $\sim 1\text{nm}$, defining a localization length



>Spatial localized wave functions are topologically trivial:

$$c^{(s)} = c_+ - c_-$$

$$c_\sigma = \sum_n^{\text{occup}} \oint_C \vec{A}_n^{(\sigma)} \cdot d\vec{k}$$

$$\vec{A}_n^{(\sigma)} = i \langle n, \vec{k}, \sigma | \nabla_k | n, \vec{k}, \sigma \rangle$$

>fully localized wave functions are eigenfunction of the position operator:

$$\hat{x} = i \nabla_k$$

$$\therefore c_\sigma = \sum_n^{\text{occup}} x_n \oint_C dk = 0$$

